Squalene monooxygenase: a novel control point in cholesterol synthesis

Author:
Gill, Saloni

Publication Date:
2011

DOI:
https://doi.org/10.26190/unsworks/15149

School of Biotechnology and Biomolecular Sciences

SQUALENE MONOOXYGENASE: A NOVEL CONTROL POINT IN CHOLESTEROL SYNTHESIS

A thesis submitted in fulfilment of the requirements for the Degree of Doctorate of Philosophy

by

Saloni Gill

Submitted:

December 2011

ORIGINALITY STATEMENT

‘I hereby declare that this submission is my own work and to the best of my knowledge it contains no materials previously published or written by another person, or substantial proportions of material which have been accepted for the award of any other degree or diploma at UNSW or any other educational institution, except where due acknowledgement is made in the thesis. Any contribution made to the research by others, with whom I have worked at UNSW or elsewhere, is explicitly acknowledged in the thesis. I also declare that the intellectual content of this thesis is the product of my own work, except to the extent that assistance from others in the project's design and conception or in style, presentation and linguistic expression is acknowledged.’

Signed ……

Date …….

COPYRIGHT STATEMENT

Signed ……

Date ……

AUTHENTICITY STATEMENT

Signed ……

Date ……

ABSTRACT

Exquisite control of cholesterol synthesis is crucial for maintaining homeostasis of this vital yet toxic lipid. Squalene monooxygenase (SM) catalyzes the first oxygenation step in cholesterol synthesis, acting on squalene before cyclization into the basic steroid structure. Using a variety of CHO cell-lines, we found that cholesterol caused the accumulation of the substrate squalene, suggesting that SM may serve as a flux-controlling enzyme beyond 3-hydroxy-3-methylglutaryl-coenzyme A reductase (HMGR), the first rate-limiting enzyme in cholesterol synthesis. At the post-translational level, cholesterol induced the proteasomal degradation of SM, which was reversed by a proteasome inhibitor, eliminating squalene accumulation. The cholesterol accelerated polyubiquitination and proteasomal degradation mechanism for SM is unique from that of HMGR: it is not mediated by Insig, 24,25-dihydrolanosterol or side-chain oxysterols, but rather by cholesterol itself. Furthermore, this mechanism requires the N-terminal domain of SM, which is partially conserved in vertebrates, but not lower organisms. Importantly, the N-terminal domain conferred cholesterol-regulated turnover on heterologous fusion proteins, highlighting its importance as the regulatory domain of SM. This previously unrecognized mechanism underlies the cholesterol-dependent rate-limiting activity of SM, making it an important second control point in cholesterol synthesis.

Owing to its unique location in the cholesterol synthesis pathway, SM also participates in the synthesis of 24(*S*),25-epoxycholesterol (24,25EC), the only oxysterol to be produced in parallel with cholesterol. 24,25EC acutely regulates the levels of newly synthesized cholesterol. We generated an SM overexpressing stable cell line, and as part of its characterization, show that these cells synthesize relatively more 24,25EC than cholesterol compared to the wild-type cells. This could be attributed to a compensatory mechanism through which these stable cells control the amount of newly synthesized cholesterol. Like SM, 2,3-oxidosqualene cyclase (OSC) also participates in the synthesis of 24,25EC and cholesterol, and when partially inhibited, OSC produces more 24,25EC. Using this approach, we show that in cultured cells, increased 24,25EC levels helps overcome the ‘Statin

Rebound Effect', a phenomenon characterized by a burst in cholesterol synthesis due to the upregulation of the cholesterol synthesis pathway post-statin treatment.

LIST OF PUBLICATIONS

Gill S, Chow R, and Brown AJ. 2008. Sterol Regulators of Cholesterol Homeostasis and Beyond: The Oxysterol Hypothesis Revisited and Revised. Progress in Lipid Research, 47: 391-404.

Gill S, Stevenson J, Kristiana, I, and Brown, AJ. 2011. Cholesterol-Dependent Degradation of Squalene Monooxygenase, a Control Point in Cholesterol Synthesis Beyond HMG-CoA Reductase. Cell Metabolism, 13: 260-273.

Gill S, and Brown AJ. 2011. Exploiting a Physiological Regulator to Improve the Efficacy and Safety of Statins. Cardiovascular Drug Therapy, 25: 183-185.

Zerenturk, EJ, Kristiana, I, **Gill, S**, and Brown, AJ. 2011. The Endogenous Regulator 24(*S*),25-Epoxycholesterol Pares Back Cholesterol Synthesis at DHCR24 (Seladin-1). BBA-Molecular and Cell Biology of Lipids, in press.

PRESENTATIONS AND POSTERS

Oral Presentations

Gill S. A Novel Control Point in Cholesterol Synthesis. Presented at Australian Atherosclerosis Society Annual Scientific Meeting 2009, St Kilda, Melbourne, Australia, October 13-16 2009

Gill S. A Novel Control Point in Cholesterol Synthesis. Presented at Experimental Biology 2010, ASBMB Annual Scientific Meeting 2010, Anaheim, CA, America, April 24-28 2010

Poster Presentations

Gill S, Stevenson, J, Kristiana, I, and Brown, AJ. A Novel Control Point in Cholesterol Synthesis. Presented at Experimental Biology 2010, ASBMB Annual Scientific Meeting 2010, Anaheim, CA, America, April 24-28 2010

ACKNOWLEDGEMENTS

Every PhD student desires to have a research project that he/she can be proud of, and at the same time derive the satisfaction of doing work that is significant, even if it only uncovers a single piece in a huge complex puzzle. I would like to begin by thanking **A/Prof Andrew Brown** for giving me such an amazing project that I am and will always be immensely proud to have been a part of. Andrew, despite the high and lows, and occasions where none of the experiments really made any sense, I appreciate your positive attitude towards my work. My journey as a PhD student would not have been so amazing without your excellent supervision and great ideas. Once again, a BIG thank you!

I appreciate all the advice given by my committee members **Drs Ingrid Gelissen** and **Bruno Gaeta**. Ingrid I also thank you for always being helpful and providing us with reagents and/or antibodies when needed. Furthermore, your supervision during the ^{35}S pulse chase experiments is much appreciated. I would also like to thank **Dr Maaike Kockx** for her expertise and immense help during the ^{35}S pulse chase experiments, and other members at the Center for Cardiovascular Research (CVR, UNSW) for being accommodating and helpful each time I invaded their laboratory space. I would also like to thank **Dr Jenny Wong** for her preliminary results for SM, and **Dr Anne Galea** for her beautiful cover art for the SM Cell Metabolism paper and her useful suggestions during our lab meetings.

My project would certainly not be complete without the other two members of Team SM: **Ika Kristiana** and **Julian Stevenson**- looking back, it was great working with you guys! Ika, besides your beautiful and perfect western blots and TLCs for my project, it was wonderful getting to know you, and even though we've had our ups and downs, I truly cherish your friendship. From my first day in the lab, you've always been very helpful in every way. I also want to thank you for taking me around Sydney and making me feel comfortable when I was new to the city. We've had some great times together and enjoyed many plates of basil chicken and chocolate éclairs. Julian, I thank you for your expertise in Molecular Biology, and for all the countless constructs that you made for the SM project. I really admire your calm attitude even in the most stressful situations. Beyond science, I've

enjoyed the really random conversations that we've had, ranging from politics to movies to music and even nail polishes (sorry, I couldn't resist!).

I would also like to thank **Dr Laura Sharpe** for all her help and useful suggestions especially for my qRT-PCR and sequencing issues. Laura, its been fun getting to know you and your ever expanding stationary collection.

I would also like to thank **James Krycer** for all his suggestions and troubleshooting ideas. James, I really appreciate your help and expertise during my teaching period. I've enjoyed reading all your poems and random notes (or 'ramble' as you like to call it)- you have an interesting and different sense of humor.

I thank **Winnie Luu** for being a great and understanding friend and colleague. You are like a little sister to me. Thanks also for always being helpful and very accommodating each time we invaded your office space for our never-ending 'Team SM' meetings. I also really liked your cute notes (especially with Molly the sheep) and funny character drawings.

Eser Zerenturk, its been fun chatting with you about shoes, TV shows and other girlie stuff. Hope you get to travel a lot and maybe one day we bump into each other in some other part of the world, hopefully not wearing the same pair of boots again (just kidding!).

I would also like to thank **Drs Robin Du** and **Stephen** from A/Prof Robert Yang's lab for being helpful in supplying us with reagents each time we ran out. I also thank **John-Sebastian Eden** for being generous and sharing reagents whenever we needed any.

I would also like to thank all the **administrative staff at the BABS school** office for being extremely helpful on various occasions.

I am also very grateful to **Dr Susan Scharffenberg** for her guidance, encouragement, and support right from my very first day at university.

Behind the scenes, I've had invaluable family support at every step of my PhD. I'd like to begin by thanking my grandparents, especially my grandfather for being a constant source of blessings, encouragement, wisdom, and showing me the

importance of being a good and humble person. A big thank you to mom and dad for ALWAYS being there for me, and being incredibly patient and understanding whenever I gave you'll a hard time. You'll are the most amazing parents! Gaurav, you are definitely the best brother to have- I can see how proud you are of your little sister, and that makes me very happy. A big thank you to Abhinav for always supporting and believing in me. I truly appreciate every piece of advice you have ever given me, and your remarkable patience when listening to my problems. Lastly, woof woof to Buddy- I miss you so much! I feel privileged to have a rock-solid and amazing support system like you all ☺

TABLE OF CONTENTS

LIST OF FIGURES

LIST OF TABLES

ABBREVIATIONS

19HC	19-hydroxycholesterol
24,25DHL	24,25-dihydrolanosterol
24,25EC	24(*S*),25-Epoxycholesterol
24HC	24(S)-Hydroxycholesterol
25HC	25-Hydroxycholesterol
27HC	27-Hydroxyholesterol
7DHC	7-dehydrocholesterol
7KC	7-ketocholesterol
7αHC	7α-hydroxycholesterol
7βHC	7β-hydroxycholesterol
ABC	ATP-Binding Cassette
ABCA1	ATP-Binding Cassette Transporter A1
ABCG1	ATP-Binding Cassette Transporter G1
ACAT	Acyl-Coenzyme A:Cholesterol Acyltransferase acLDL
ApoAI	Apolipoprotein AI
ATP	Adenosine Triphosphate
BCA	Bicinchoninic Acid
bHLHZip	Basic Helix-Loop-Helix Leucine Zipper
BSA	Bovine Serum Albumin
CD	Methyl-β-Cyclodextrin
Cdc48	Cell Division Cycle 48
cDNA	Complementary DNA
CHO	Chinese Hamster Ovary
CPN	Compactin
CMV	Cytomegalovirus CNS
CNX/CRT	Calnexin Calreticulin
CVD	Cardiovascular Disease
DOS	2,3(*S*);22(*S*),23-Dioxidosqualene
ER	Endoplasmic Reticulum
ERAD	ER-associated Degradation

GFP	Green Fluorescent Protein
GGOH	Geranylgeraniol
GST	Glutathione S Transferase
HDL	High Density Lipoprotein
HMGR	3-hydroxy-3-methylglutaryl coenzyme A
Insig	Insulin-Induced Gene
LCAT	Lecithin-cholesterol acyltransferase
LDL	Low Density Lipoprotein
LXR	Liver X Receptor
MOS	2,3(*S*)-Monooxidosqualene
NADH	Nicotinamide Adenine Dinucleotide
NADPH	Nicotinamide Adenine Dinucleotide Phosphate
NPC1	Niemann Pick C Type 1
OSC	2,3-Oxidosqualene Cyclase
PDI	Protein Disulphide Isomerases
RCT	Reverse Cholesterol Transport
RING	Really Interesting New Gene
RXR	Retinoid X Receptor
S1P	Site 1 Protease
S2P	Site 2 Protease
Scap	SREBP-Cleavage Activating Protein
SM	Squalene Monooxygenase
SPF	Supernatant Protein Factor
SREBP	Sterol Regulatory Element Binding Protein

CHAPTER 1

GENERAL INTRODUCTION

1. GENERAL INTRODUCTION

In this chapter, an in-depth background of cholesterol homeostasis including the key regulatory steps and the proteins involved, is provided. Additionally, a brief historical characterization of Squalene monooxygenase (SM) and its role in cholesterol synthesis is discussed. The scope of this chapter also includes the role of oxysterols, in particular, 24(*S*),25-expocholesterol (24,25EC) in cholesterol homeostasis. Lastly, since the use of statin treatments has been an integral part of the project, an overview of the molecular basis of statin therapy and its implications on lowering cholesterol are provided.

1.1 Cholesterol

More than two centuries have passed since Poulletier de la Salle, studying bile and gallstones, first characterized cholesterol (or 'cholesterine' as it was originally named by Chevreul) (Chevreul, 1816; Fieser, 1959). The complicated structures of cholesterol (Figure 1.1) and bile acids were elucidated by Wieland and Windaus, for which they were awarded a Nobel Prize in 1928. Over the centuries, cholesterol has developed a 'bad' reputation for causing of a number of cardiovascular diseases. Nevertheless, the importance of this biological molecule and the various functions it performs in animal systems cannot be overlooked. Cholesterol is a structural component of all cell membranes, and is one of the most important regulators of lipid organization in membranes (Maxfield and Tabas, 2005). This property is required for the structural integrity of microdomains (lipid rafts) that participate in signal-transduction processes (Simons and Ikonen, 1997). It is also a precursor to steroid hormones such as estrogen, progesterone, corticosteroids, aldosterone, and testosterone (Hsu et al., 2006), bile acids (Norlin and Wikvall, 2007), and oxysterols [reviewed in (Gill et al., 2008)], compounds that carry out important biological functions. Within membranes, the cholesterol to polar lipid ratios affect stability, permeability, and protein mobility (Simons and Ikonen, 2000).

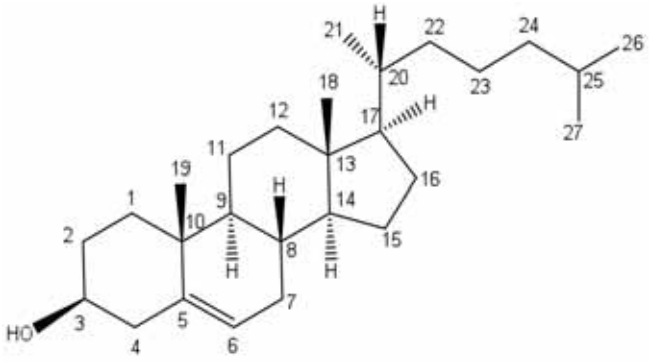

Figure 1.1 Structure of the cholesterol molecule

The cholesterol molecule consists of 4 fused hydrocarbon rings, a side-chain, and a hydroxyl (OH) group positioned at carbon three.

1.2 Cholesterol and Disease

Cholesterol was first isolated from gallstones, and since then, has been associated with disease. In fact, major breakthroughs in the field of lipid research have arisen from studying human models with defects in cholesterol metabolism. A classic example is the discovery of the low-density lipoprotein (LDL) receptor and the process of 'receptor mediated endocytosis' by Nobel laureates Drs. Micheal S. Brown and Joseph L. Goldstein (Brown and Goldstein, 1976; Brown and Goldstein, 1986). Brown and Goldstein began their venture into cholesterol research by investigating the underlying genetic defects of the LDL receptor that caused familial hypercholesterolemia (FH), a disease that produces high plasma cholesterol levels and myocardial infarctions in young people, and is transmitted as an autosomal dominant trait determined by a single gene (Goldstein and Brown, 2009).

Another major cholesterol-related disease is atherosclerosis, a chronic condition associated with the deposition of plasma lipoproteins including cholesterol on the interior of the arteries. A combination of proteoglycan binding and lipoprotein aggregation impedes the exit of lipoproteins from the arterial wall, thus causing the arterial walls to thicken and harden (Maxfield and Tabas, 2005). Over

time, this condition compromises blood flow, and leads to the onset of cardiovascular diseases such as acute myocardial infarction, ischemic stroke, and in some cases sudden death (Aikawa and Libby, 2004). At the cellular level, monocyte-derived macrophages are central in the initiation and progression of atherosclerosis. Macrophages express scavenger receptors that bind to and internalize modified forms of lipoproteins such as oxidized-LDL (Kunjathoor et al., 2002). These scavenger receptors are distinct from LDL receptors, and unlike LDL, oxidized-LDL is not subjected to feedback regulation (Brown and Goldstein, 1986; Pennings et al., 2006). The over-accumulation of different modified lipoproteins in macrophages transform them into foam cells, which eventually form the fatty streaks of the atherosclerotic plaques in the inner most layer of the arteries (Moore and Tabas, 2011).

Another example of cholesterol-associated human diseases is Niemann-Pick type C (NPC), which, at the cellular level is a result of improper trafficking of lipids such as cholesterol and glycosphingolipids to lysosome-like storage organelles (Mukherjee and Maxfield, 2004). Tangier disease is a very rare autosomal recessive disorder caused by defects in the cholesterol efflux protein ABCA1 (Section 1.6). This is associated with an acute deficiency in high-density lipoproteins (HDL) and reduced cholesterol efflux, especially from macrophages and other reticuloendothelial cells (Stefkova et al., 2004). This leads to cholesteryl ester accumulation in these cells, and is also associated with increased susceptibility to atherosclerosis. Therefore, due to the existence of a large number of cholesterol-related diseases, it is extremely necessary to have a detailed understanding of cholesterol homeostasis.

1.3 Cholesterol Homeostasis: An Overview

Cholesterol is synthesized in cells via a tightly regulated complex pathway. This ensures that cholesterol levels in cells are maintained at the physiological levels necessary for it to perform its various functions. The understanding of cholesterol regulation has come a long way from the initial recognition of cholesterol feedback

inhibition via 3-hydroxy-3-methylglutaryl coenzyme A reductase (HMGR), the first rate-limiting enzyme in the cholesterol synthesis pathway (Rodwell et al., 1976). The molecular mechanisms of how cells regulate their cholesterol levels has been greatly facilitated by the elucidation of the Sterol Regulatory Element Binding Protein (SREBP) pathway over the past two decades by the laboratory of Brown and Goldstein (Goldstein et al., 2006b). This in turn has further boosted extensive research into fully understanding how animal cells regulate their cholesterol levels- a question with significant scientific and clinical implications.

The harmony of cholesterol homeostasis largely depends on the sterol-sensing ability of certain membrane-embedded proteins. In the following sections, the processes of cholesterol uptake, synthesis, and efflux (Figure 1.2) will be discussed.

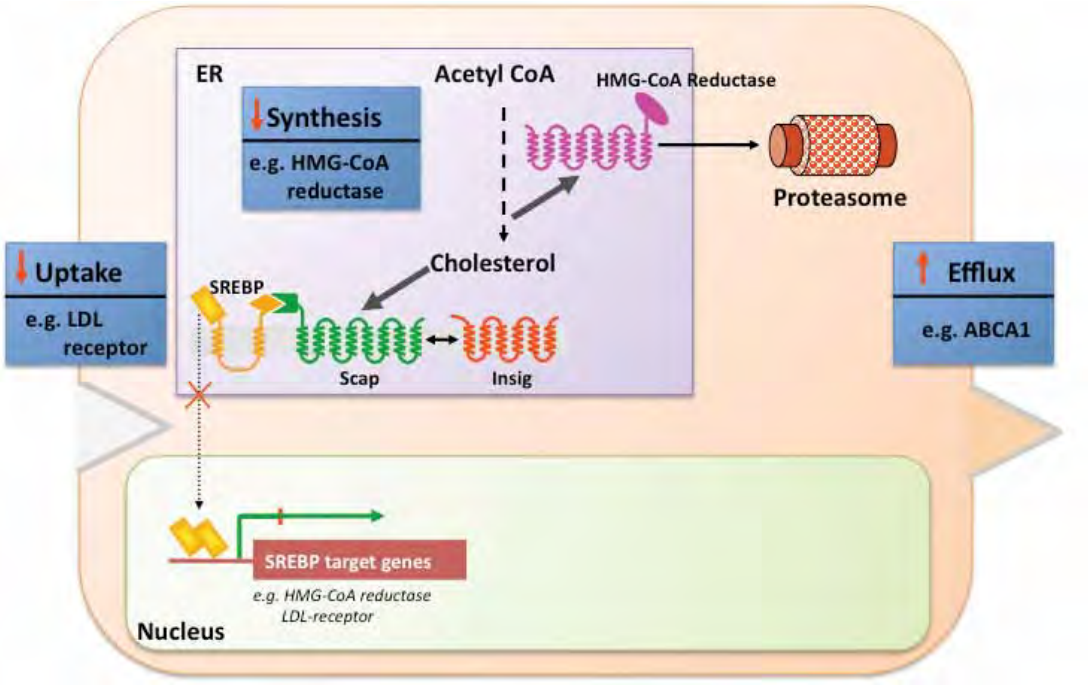

Figure 1.2 Cholesterol Homeostasis: A balance between cholesterol uptake, synthesis, and efflux

Cholesterol acts at multiple levels to regulate its amount within cells: At the transcriptional level, via inhibition of SREBP target genes, it blocks de novo synthesis (HMGR) and uptake (LDL receptor). Post-translationally, cholesterol indirectly induces proteasomal degradation of HMGR, and is effluxed from cells via ABCA1. (Figure modified from A.J. Brown)

1.3.1 Cholesterol Uptake and the Role of the LDL Receptor

Animal cells receive cholesterol from two sources: exogenously via receptor-mediated endocytosis from circulating plasma low-density lipoprotein (LDL), some of which is acquired from the diet; and endogenously through the cholesterol synthesis pathway. The major classes of plasma lipoproteins were discovered in the 1950s and 1960s, and since then, LDL has been established as the most abundant cholesterol-carrying lipoprotein in human plasma (Brown and Goldstein, 1986; Goldstein and Brown, 2009). Due to the extremely hydrophobic nature of cholesteryl esters, they are packaged into the core of the LDL molecule, which carries the esterified cholesterol into the cell. The cell surface contains LDL receptors that bind to the LDL and internalize it by receptor mediated endocytosis (Brown and Goldstein, 1986). The internalized lipoproteins are then taken to lysosomes where its cholesteryl esters are hydrolyzed to release free cholesterol. This free cholesterol exerts the following regulatory actions to prevent the over-accumulation of cholesterol in cells: firstly, via inhibition of the SREBP pathway (Section 1.3.2) it downregulates the expression of target genes involved in cholesterol synthesis (for example, HMGR) and uptake (LDL receptor), and secondly, it activates the cholesterol esterifying enzyme acyl-coA:cholesterol acyltransferase (ACAT), thus increasing cholesterol esterification (Goldstein and Brown, 1990).

1.3.2 Transcriptional Regulation: The SREBP Pathway

The year 1993 marked an important milestone towards our current understanding of cholesterol homeostasis, with the purification of the first member of the family of key transcription factors, the SREBPs, from nuclear extracts of cultured HeLa cells (Briggs et al., 1993). There are two SREBP genes which encode three isoforms (~1150 amino acids each): SREBP-2 controls the expression of genes predominantly involved in cholesterol homeostasis, including sterol synthesizing enzymes and the LDL receptor; SREBP-1c controls the expression of genes mostly involved in the synthesis of fatty acids, phospholipids, and triglycerides; and SREBP-1a regulates the gene targets of both SREBP-1c and SREBP-2 (Horton et al., 2002b). As a

group, SREBPs transcriptionally regulate more than 30 different genes involved in lipid metabolism (Horton et al., 2003; Sakakura et al., 2001). Despite having different gene targets, the proteolytic activation of all three SREBP isoforms occurs via a common mechanism, and is modulated by cholesterol (Rawson et al., 1999).

SREBPs are positioned in the endoplasmic reticulum in a hairpin-like fashion such that the N and C termini extend into the cytosol (Figure 1.3). Each SREBP isoform has a similar structure, consisting of three distinct regions: (1) an NH_2-terminal domain of 480 amino acids, which belongs to the family of basic helix-loop-helix leucine zipper transcription factors; (2) a middle hydrophobic region of 80 amino acids containing two transmembrane domains; and (3) a COOH-terminal regulatory domain of 590 amino acids which is involved in the sterol regulation of this protein (Sakai et al., 1997).

1.3.2.1 Proteolytic Activation

In the endoplasmic reticulum (ER), SREBPs are bound to an SREBP-cleavage activating protein (Scap) (Hua et al., 1996; Rawson et al., 1999). The COOH-terminal of Scap contains WD repeat (tryptophan-aspartate repeat) sequences, a motif which promotes the binding of Scap to SREBP (Kuwabara and Labouesse, 2002). Scap monitors cholesterol levels in the ER through its sterol-sensing domain (Hua et al., 1996). When cholesterol levels are insufficient in the ER, Scap escorts SREBP to the Golgi in COPII vesicles (Espenshade et al., 2002). To activate nuclear gene expression, the N-terminus of SREBP is sequentially cleaved by the action of Site-1 and Site-2 Proteases (S1P and S2P) (Espenshade, 2006). The now soluble SREBP transcription factor enters the nucleus and activates the target genes required for cholesterol synthesis and uptake (Figure 1.3).

Under sterol-replete conditions in the cell, the SREBP-Scap complex is held back in the ER by the retention protein, Insig (Insulin-induced gene) (Yang et al., 2002). There are two Insig isoforms, Insig-1 and Insig-2, and binding to either inhibits the vesicular transport of the SREBP-Scap complex to the Golgi (Yabe et al., 2002). Cholesterol acts by causing a conformational change in Scap, facilitating the binding of the SREBP-Scap complex to Insig (Brown et al., 2002). Recently it

has been shown that cholesterol binds loop 1 of Scap (a 245-amino acid sequence that projects into the ER lumen), and this leads to a conformational change in loop 6 of Scap, blocking its binding to COPII vesicles (Motamed et al., 2011). Collectively, this work provides compelling mechanistic evidence that cholesterol can indeed regulate its own synthesis and uptake at the level of SREBP activation.

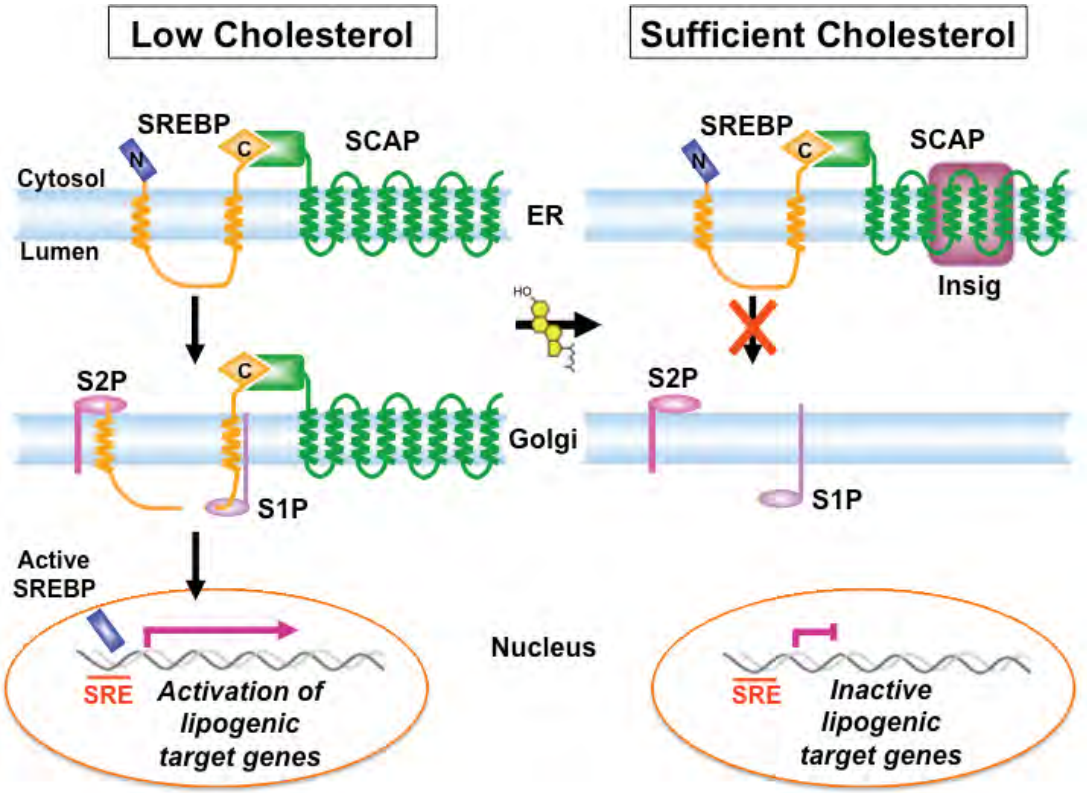

Figure 1.3 The SREBP pathway

(A) Low cholesterol levels in the ER are sensed by SCAP, and it escorts SREBP into the Golgi for proteolytic activation to release the active SREBP transcription factor. This is then delivered into the nucleus for binding to the sterol response element (SRE) in the promoter of target genes. **(B)** When SCAP senses high cholesterol levels, the SREBP-SCAP complex is held back in the ER by Insig. This prevents proteolytic activation of SREBP. [Figure modified from (Brown, 2007)].

1.3.3 The Sterol-Sensing Domain

As mentioned in the previous section, Scap, which acts as a cholesterol sensor in the ER, contains a sterol-sensing domain. Sterol-sensing domains are conserved intramembrane amino acid sequences that are essential for sterol interactions and homeostasis (Radhakrishnan et al., 2004). These domains consist of 180 amino acids that form five membrane-spanning helices with short intervening loops. Originally observed in Scap (Hua et al., 1996), other proteins that contain the sterol-sensing domain include: the cholesterol biosynthetic enzymes HMGR and 7-dehydrocholestertol reductase, and NPC1, a protein involved in sterol trafficking (Kuwabara and Labouesse, 2002).

1.3.4 Cholesterol Synthesis

All animal cells produce cholesterol, with relative production rates varying by cell type and organ function. The two carbon substrate acetate (acetic acid) initiates the pathway, with over 30 different enzymes involved in synthesizing cholesterol, as well as non-sterol precursors essential for normal cell function (Figure 1.4). These include the isoprenoids ubiquinone and hemeA, that are involved in aerobic cellular respiration, dolichol, which is required for co-translational modifications of proteins (such as N-glycosylation), and the farneysl and geranylgeranyl groups that attach to various proteins, increasing their membrane association (Goldstein and Brown, 1990). Furthermore, some of the cholesterol biosynthetic enzymes are also involved in the production of 24(*S*),25-epoxycholesterol (24,25EC), the only oxysterol to be synthesized in parallel with cholesterol (Section 1.8.3). Here, the roles of two key enzymes will be discussed in detail.

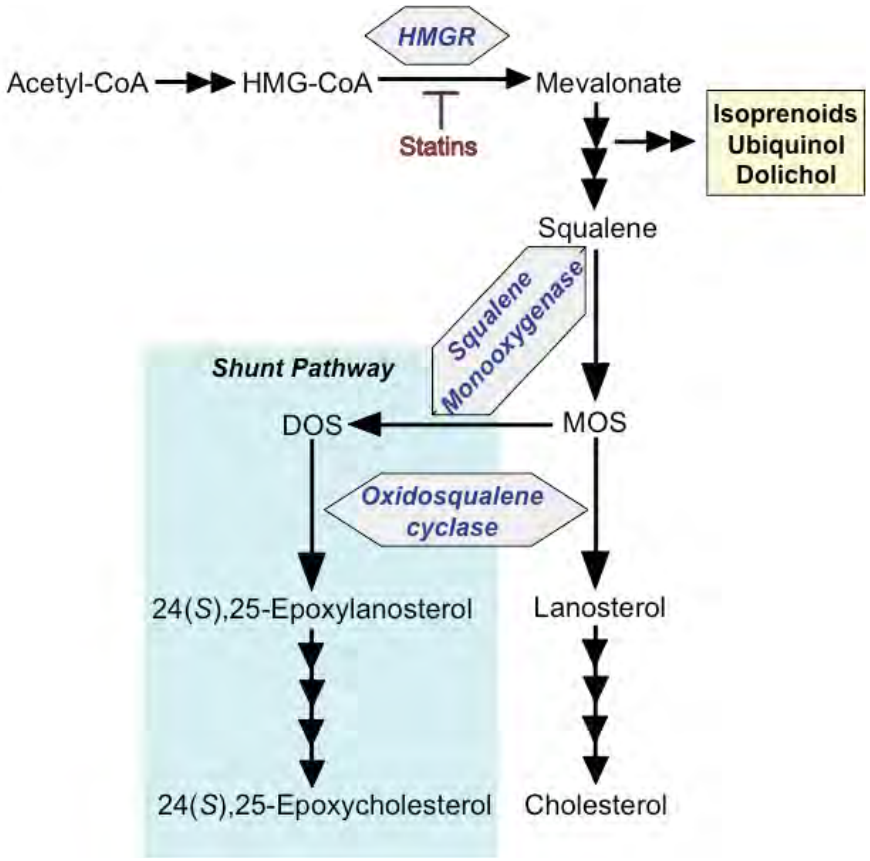

Figure 1.4 The Cholesterol Synthesis Pathway

A simple schematic of the cholesterol synthesis pathway depicting key enzymes that are further discussed in this chapter. HMGR: 3-hydroxy-3-methylglutaryl coenzyme A reductase; MOS: 2,3(*S*)-monooxidosqualene; DOS: 2,3(*S*);22,23-dioxidosqualene.

1.3.4.1 3-Hydroxy-3-methylglutaryl coenzyme A reductase

3-Hydroxy-3-methylglutaryl coenzyme A reductase (HMGR) catalyzes the first rate-limiting step in the cholesterol synthesis pathway (Rodwell et al., 1976), converting HMG-CoA into mevalonate (Figure 1.4). In addition to being a precursor for cholesterol, mevalonate is also required for the synthesis of non-sterol products such as ubiquinone (commonly known as coenzyme Q_{10}), dolichol, heme, and the isoprenylated proteins farnesyl and geranylgeranyl pyrophosphate (Goldstein and Brown, 1990).

A multivalent regulatory system controls expression levels of HMGR in order to protect cells from build-up of excess cholesterol. At the transcriptional level, cholesterol regulates *HMGCR* mRNA levels via the SREBP pathway (Horton et al., 2002a). Next, at the translational level, a mevalonate-derived non-sterol product whose identity remains unknown to date, has been shown to inhibit the translation of HMGR mRNA (Nakanishi et al., 1988). Finally at the post-translational level, certain sterols as well as non-sterols induce the proteasomal degradation of HMGR (discussed in detail in section 1.5.1), which reduces the half-life of this protein from ~11-12 hr to less than 1 hr (Ravid et al., 2000; Sever et al., 2003b).

In extensively studied mammalian species such as humans, hamster, rat and mouse, HMGR is localized to the ER. Its eight membrane-spanning N-terminal domain separated by short hydrophilic loops is embedded in the ER membrane, whereas the C-terminal domain extends into the cytosolic region and is responsible for the catalytic activity of the enzyme (Liscum et al., 1985; Roitelman et al., 1992) (Figure 1.5). The membrane domain of HMGR contains the five consecutive membrane-spanning sterol-sensing domain (Section 1.3.3). In addition to providing membrane anchorage, the N-terminal domain of HMGR is required for sterol-dependent degradation via the proteasome (Section 1.5.1). Two key observations that shaped this finding are: a truncated version of the protein missing the N-terminal membrane domain was not subjected to degradation in the presence of sterols (Gil et al., 1985); and that the N-terminal membrane domain fused to either β-galactosidase, luciferase or green fluorescent protein (GFP) demonstrated sterol-accelerated degradation similar to the wild-type full length enzyme (Jo and DeBose-Boyd, 2010a; Skalnik et al., 1988). Interestingly, the membrane region of HMGR is the most highly conserved region of the enzyme among mammalian species (Luskey and Stevens, 1985). This supports the idea of the membrane domain being a functionally important part of the enzyme.

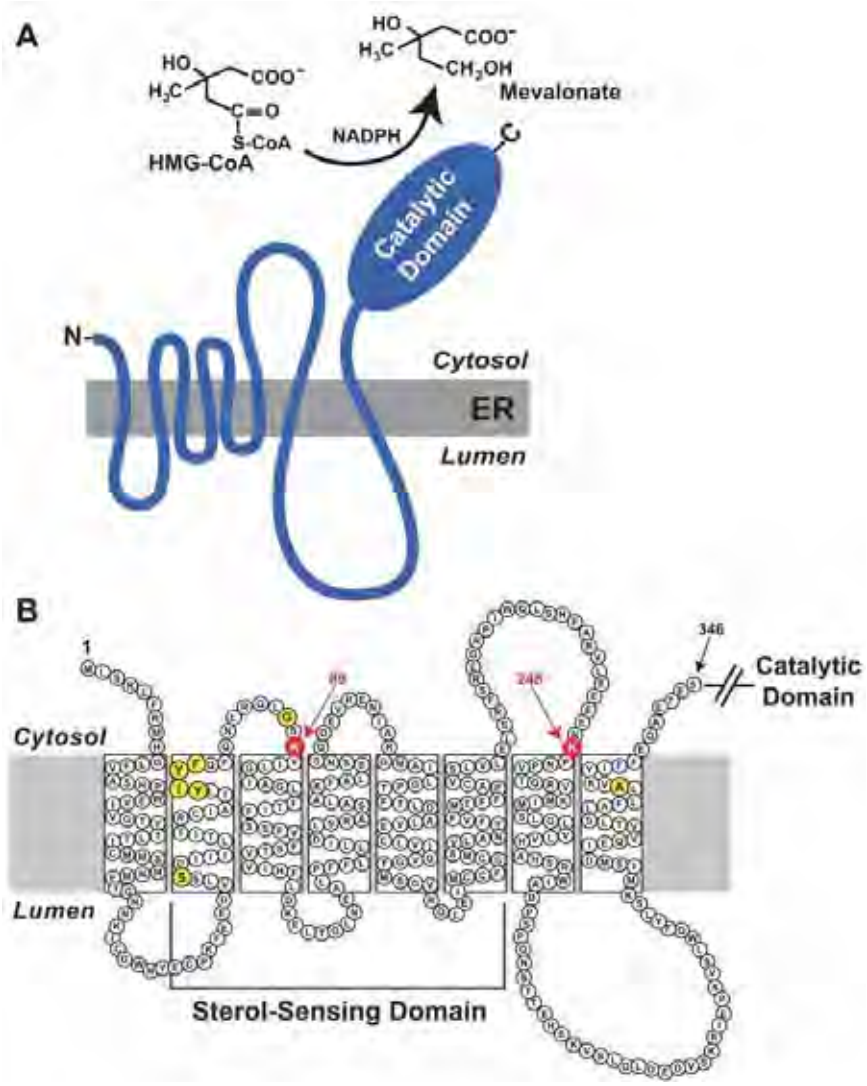

Figure 1.5 The N- and C-terminal domain structures of HMGR

(A) HMGR consists of two distinct domains: a hydrophobic N-terminal domain with eight membrane-spanning segments that plays a key role in sterol-accelerated degradation of the enzyme; and a hydrophilic C-terminal domain that directs enzymatic activity. **(B)** Amino acid sequence and topology of the membrane domain of HMGR. The lysine residues that are required for Insig-mediated, sterol-induced ubiquitination of HMG CoA reductase are enlarged, highlighted in red, and denoted by arrows. Sequences required for sterol-regulated binding of HMGR to Insigs (YIYF, Ser-60, Gly-87, and Ala-333) are enlarged and highlighted in yellow. [Figure and legend reproduced from (Jo and DeBose-Boyd, 2010b)].

1.3.4.2 Squalene Monooxygenase

In 1957, Bloch and Tchen presented evidence for the first oxygenation step in the process of cholesterol synthesis by showing that molecular oxygen is incorporated into the isoprenoid squalene to form the 3β-hydroxyl group of the steroid structure (Tchen and Bloch, 1957). Initially, it was believed that squalene was converted into lanosterol in a one step reaction, the first sterol product in the cholesterol synthesis pathway. In 1966, a stepwise mechanism was put forward independently by the laboratories of Corey and Van Tamelen, with 2,3(*S*)-monooxidosqualene (MOS) being identified as an intermediate in the process of squalene to lanosterol conversion (Corey et al., 1966; Van Tamelen, 1966). This put the spotlight on SM (then known as squalene epoxidase, EC 1.14.99.7) as the enzyme that catalyzes the epoxidation of squalene into MOS, the first oxygenation step in the cholesterol synthesis pathway. Konrad Bloch's laboratory extensively characterized this enzyme using mostly rat liver microsomes (Ono and Bloch, 1975; Tai and Bloch, 1972; Yamamoto and Bloch, 1970). His laboratory showed that SM is bound to the ER in cells, and is associated with NADPH-cytochrome P450 reductase, its electron transfer partner (Ono and Bloch, 1975). In addition to molecular oxygen, SM requires the cofactor flavin adenine dinucleotide (FAD), and supernatant protein factor (SPF). SPF (47 kDa) stimulated the activity of SM in rat liver homogenates by ~ 4 to 10 fold, and has been shown to facilitate the intermembrane transport of squalene (Ferguson and Bloch, 1977; Fuks-Holmberg and Bloch, 1983; Saat and Bloch, 1976). Studies have used *in vitro* assay systems to show that the cytosolic fraction, which contains the SPF and anionic phospholipids, can be replaced by a non-ionic detergent such as Triton X-100 (Ono and Bloch, 1975; Tai and Bloch, 1972).

Although SM was first identified in the early 1970s, its low expression levels in most tissues including the liver, made it a difficult task to purify SM in its active form, due to which, studies were carried out using subcellular fractions from HepG2 cells [for example, (Hidaka et al., 1990)]. The first mammalian (rat) SM sequence was reported in 1995, (Sakakibara et al., 1995), followed by mouse (Kosuga et al., 1995) and then human (Laden et al., 2000). The sequence homology between

mammalian and yeast (*Candida albicans*) SM is only 32% (Favre and Ryder, 1997; Laden et al., 2000). Interestingly, the yeast sequence lacks the N-terminal region, which is characteristic of mammalian SM (Laden et al., 2000). Also, fungal SM does not require SPF for its activity, and NADH is its electron transfer partner instead of NADPH. To date, the membrane topology of SM has not been fully elucidated, however, there is evidence for vertebrate SM having one possible transmembrane domain at the N-terminal region, which is absent in yeast (Sakakibara et al., 1995).

SM catalyzes a second reaction converting MOS into 2,3(*S*);22,23-dioxidosqualene (DOS), a step that initiates the shunt pathway which eventually leads to the synthesis of 24,25EC (Section 1.8.3).

1.4 Cholesterol efflux via LXR activation

The liver X receptors (LXR) are nuclear receptors that act as cholesterol sensors in controlling transcription of genes involved in cholesterol homeostasis and particularly in reverse cholesterol transport (RCT). These receptors function as a 'safety valve' that limits free cholesterol in tissues that have high cholesterol flux (Cummins and Mangelsdorf, 2006). The LXR receptors function by forming a heterodimer with the retinoid X receptors. The identification of oxysterols as physiological ligands for LXRs initiated extensive research to elucidate their physiological functions (Janowski et al., 1996; Lehmann et al., 1997b). Some potent activators of LXR include 20(S)-hydroxycholesterol, 22(R)-hydroxycholesterol, 24(S)-hydroxycholesterol, and 24,25EC (Janowski et al., 1996; Lehmann et al., 1997b). The two LXR gene targets that play an important role in cholesterol efflux from cells are the ATP-binding cassette proteins, ABCA1 and ABCG1. ABCA1 exports free cholesterol and phospholipids from cells to lipid-depleted high density lipoprotein (HDL) apolipoproteins, the most common being apoA1 (Oram et al., 2003). Similarly, ABCG1 promotes the export of free cholesterol to HDL and other lipoproteins (Kennedy et al., 2005; Wang et al., 2004), thus contributing to cholesterol homeostasis.

1.5 Feedback Control of Cholesterol Synthesis

Feedback control by cholesterol was first observed by Schoenheimer and Breusch (Schoenheimer and Breusch, 1933). In these landmark metabolic studies, it was found that mice synthesized less cholesterol when placed on a cholesterol containing diet. Two decades later, the concept of feedback regulation of cholesterol by cholesterol itself, and related sterols was further developed by Gould and Taylor, and Tomkins and colleagues (Gould et al., 1952; Tomkins et al., 1953). Since then, the complex feedback inhibition system of cholesterol synthesis has been under the spotlight, mostly due to its impact on drug discovery for hypercholesterolemia and cardiovascular diseases.

Feedback regulation of cholesterol synthesis is achieved through the donwregulation of the SREBP-2 pathway (Section 1.3.2) in the presence of a sufficient amount of sterols. This in turn inhibits the activation of the LDL receptor, thus blocking cholesterol uptake (Section 1.6), and the SREBP-2 target enzymes involved in cholesterol synthesis. Additionally, HMGR is also subjected to post-translational regulation mediated by sterols as well as non-sterols, which leads to its degradation (Section 1.6.1).

There is another proposed model for feedback inhibition of cholesterol synthesis known as ‘convergent feedback inhibition’ (Goldstein et al., 2006a; Gong et al., 2006). This model highlights the indispensable role of Insig in maintaining appropriate cholesterol levels in the cell via the SREBP-2 pathway. When there is sufficient cholesterol in the cell, Scap binds to Insig-1 and stabilizes it, leading to a reserve of a stable Insig-1/Scap-SREBP complex. When cells are cholesterol-depleted, the Scap-SREBP complex dissociates from Insig-1, binds to COPII proteins and is transported into the Golgi where SREBP is processed to its active nuclear form. On the other hand, Insig-1 is ubiquitinated and degraded via the ubiquitin-proteasome pathway (Gong et al., 2006). The activated nuclear SREBP upregulates expression of its target genes involved in synthesis and uptake, and also *Insig-1*. This increases the amount of Insig-1 synthesis, but the protein rapidly degrades unless sufficient cholesterol accumulates to bind to Scap, allowing Scap to

stabilize Insig-1. Therefore, according to this process, the blocking of SREBP processing requires the convergence of 2 molecules: newly derived cholesterol (either from synthesis or uptake) and newly synthesized Insig-1 (Gong et al., 2006). The exact significance of this convergent mechanism is not fully known as yet, however, it is postulated to be a 'failsafe mechanism' to ensure that in addition to cholesterol, the cells have sufficient time to synthesize and accumulate vital isoprenoids, before the pathway is shutdown by cholesterol itself (Goldstein et al., 2006a).

Another process through which certain ER proteins are regulated via feedback inhibition is proteasomal degradation, also known as endoplasmic reticulum-associated degradation (ERAD).

1.6 ER-associated Degradation (ERAD) Pathway

The ERAD pathway was originally thought to degrade and eliminate only misfolded/damaged, mutated, or unassembled members of multiprotein complexes from the ER. However, as exemplified by HMGR, this process is also required for the regulated turnover of ER proteins. ERAD substrates are selected by a quality control system within the ER lumen and are eventually degraded by the cytoplasmic ubiquitin-proteasome system. In the yeast *Saccharomyces cerevisiae*, three distinct ERAD pathways (ERAD-C: cytosolic; ERAD-L: lumenal; ERAD-M: membrane-bound) have been determined depending on the location of the substrate (Ahner and Brodsky, 2004). Even though these three pathways have not been fully defined in mammalian cells, these cells could potentially contain more misfolded/mutated proteins that could easily fit into one of the three above mentioned yeast ERAD pathways.

The pathway begins by the detection of misfolded or unassembled proteins. A few examples of substrate detection methods include- N-linked glycan processing by ER lumenal chaperone proteins such as calnexin/calreticulin (CNX/CRT) (Hebert et al., 1997), and disulfide linkages between ERAD substrates and protein disulphide isomerases (PDI) (Molinari et al., 2002) (illustrated in Figure 1.6). The selected

ERAD substrates are then targeted to the cytoplasm since the ubiquitination enzymes are present in this compartment. This process is termed as retrotranslocation because it often involves a protein complex, called Sec61, which functions as a channel (also called the retrotranslocon) necessary for the transport of the ERAD substrates (Vembar and Brodsky, 2008). Substrate translocation into the cytoplasm might be initiated in part by the cell-division-cycle-48 (Cdc48) complex (Jentsch and Rumpf, 2007). The energy for this process is derived from ATP hydrolysis by a Cdc48, which is an AAA+ATPase, and is coupled to retrotranslocation. In this manner, substrates are targeted either to the retrotranslocon and/or to E3-ubiquitin ligases. For ERAD substrates that are located in the ER membranes, ubiquitination precedes or can occur together with retrotranslocation (Vembar and Brodsky, 2008).

Most ERAD substrates are ubiquitinated prior to degradation. Protein ubiquitination requires the action of E1-ubiquitin activating enzyme, E2-ubiquitin conjugating enzymes, E3-ubiquitin ligases, and most importantly, the specificity of the substrate is determined by the E3 ubiquitin ligases (Deshaies and Joazeiro, 2009). Ubiquitin (76 amino acids) covalently attaches to the ε-amino groups of lysines in substrate proteins forming an isopeptide bond (Vembar and Brodsky, 2008). Ubiquitination is initiated by the formation of a high-energy thioester linkage between a cysteine residue in the active site of the E1-ubiquitin-activating enzyme and the C-terminal glycine of ubiquitin (Vembar and Brodsky, 2008). The resulting activated ubiquitin is then passed to E2-ubiquitin conjugating enzyme, forming another thioester linkage. The E3-ubiquitin ligase catalyzes the transfer and attachment of ubiquitin from the E2-conjugating enzyme to the selected substrate. Following successive additions of ubiquitin molecules to lysine residues of the previously attached ubiquitin, a polyubiquitin chain is formed. At least a tetra-ubiquitin chain is required before the ERAD substrate is degraded (Vembar and Brodsky, 2008).

The polyubiquitinated substrate is then extracted from the ER membranes, and is recognized by specific ubiquitin receptors in the 19S capping complexes of the 26S proteasome. The polypeptide chain is fed into the central chamber of the

20S core region that contains the proteolytically active sites. Before terminal digestion, ubiquitin is cleaved by deubiquitinating enzymes and is recycled.

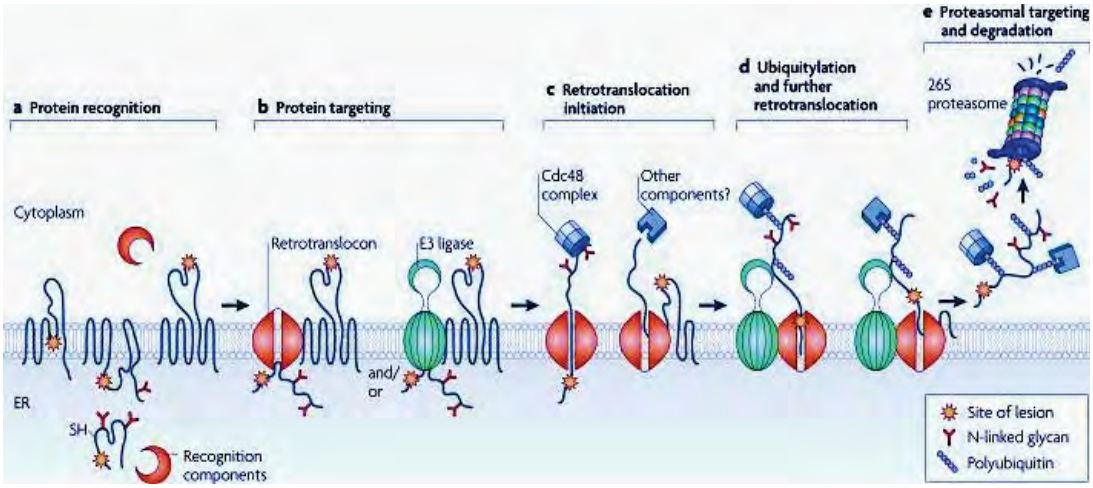

Figure 1.6 A step-by-step illustration of the ERAD pathway

(A) *Protein recognition*: Misfolded proteins containing cytoplasmic, intramembrane or endoplasmic reticulum (ER)-luminal lesions are recognized by cytoplasmic and luminal chaperones and associated factors, such as (Hsp70)-family members, calnexin and calreticulin, and protein disulphide isomerases. **(B)** *Protein targeting*: ERAD substrates are targeted to the retrotranslocon) and/or to E3 ligases. **(C)** *Retrotranslocation initiation*: Substrate retrotranslocation into the cytoplasm might be initiated in part by Cdc48 complex; other components, such as molecular chaperones or the proteasome, might also be required for this step. The energy derived from ATP hydrolysis by Cdc48, which is an AAA+ATPase, is coupled to retrotranslocation. **(D)** *Ubiquitination and further retrotranslocation*: As proteins exit the retrotranslocon they are polyubiquitinated by E3 ubiquitin ligases. This promotes further retrotranslocation and is aided by cytoplasmic ubiquitin-binding protein complexes. **(E)** *Proteasomal targeting and degradation*: Once a polyubiquitinated substrate is displaced into the cytoplasm, it is recognized by receptors in the 19S cap of the 26S proteasome. De-ubiquitinating enzymes (not shown) remove the polyubiquitin tag, and peptide *N*-glycanase (not shown) might also be required for efficient degradation. The substrate is then threaded into the 20S catalytic core of the proteasome where it is broken down into peptide fragments. Ubiquitin that is generated by this process can be recycled for subsequent rounds of modification. Figure and legend reproduced from (Vembar and Brodsky, 2008).

1.6.1 Proteasomal Degradation of HMGR

The complex yet fascinating sterol-accelerated degradation mechanism of mammalian HMGR and the machinery involved have been well elucidated by DeBose-Boyd and colleagues [reviewed in (DeBose-Boyd, 2008 ; Jo and DeBose-Boyd, 2010)]. The extensive work done on unraveling the proteasomal degradation of the yeast homolog Hmg2 has assisted in better understanding of the mammalian system (Hampton and Bhakta, 1997).

The degradation signals for mammalian HMGR include: 24,25-dihydrolanosterol, and the oxysterols 25-hydroxycholesterol, 27-hydroxycholesterol, and 24,25EC (Song et al., 2005b). Insigs play an essential role in the sterol-regulated degradation process of HMGR, binding to the YIYF tetrapeptide sequence of HMGR (Lee et al., 2007; Sever et al., 2003b). A key study showed that when HMGR was overexpressed in CHO cells, sterol-dependent degradation of the enzyme was abolished (Sever et al., 2003b). This was restored when Insig-1 was co-transfected along with HMGR in the study. Furthermore, RNA interference (RNAi)-mediated knockdown of Insig-1 and Insig-2, or mutation of genes encoding both isoforms abolishes sterol-mediated ubiquitination and degradation of HMGR (Lee et al., 2005; Sever et al., 2004; Sever et al., 2003b).

Insigs are associated with a membrane-bound E3-ubiquitin ligase called gp78 (Song et al., 2005a). The N-terminal region of gp78 is associated with Insigs. The C-terminal region projects into the cytosol and contains a RING (Really Interesting New Gene) finger domain that is required for its activity. It also contains binding sites for the AAA-ATPase VCP/p97 and the ubiquitin-conjugating enzyme Ubc7 (Kostova et al., 2007). Insig acts like a bridge and mediates the binding of gp78 to the membrane domain of HMGR in the presence of sterols (Figure 1.7). This step initiates the degradation process of HMGR. It is interesting to note that RNAi-mediated knockdown of gp78 blunts sterol induced ubiquitination and degradation of endogenous HMGR (Song et al., 2005a). The lysine residues at positions 89 and 248 in the membrane domain of HMGR participate in the ubiquitination of the enzyme (Song and DeBose-Boyd, 2004b). Ubiquitin molecules from the E2-Ubc7 complex are transferred onto these lysine residues. This

ubiquitinates HMGR and in turn ‘marks’ it to be recognized by the gp78-associated VCP/p97 complex. Along with its cofactors, this complex then extracts the ubiquitinated HMGR from the ER membrane and delivers it to the proteasome for degradation via an unknown mechanism (Jo and DeBose-Boyd, 2010). It was postulated that geranylgeraniol (GGOH) enhances degradation of mammalian HMGR by mediating the extraction of the ubiquitinated enzyme from the ER, and facilitating its delivery to the proteasomes for degradation (Sever et al., 2003a). Similarly, in yeast, a phosphorylated derivative of GGOH, GG-pyrophosphate has been shown to stimulate the degradation of Hmg2p (Garza et al., 2009). Geranylgeranylated proteins include the Rab family of proteins that carry out various aspects of vesicular transport (Seabra et al., 2002). Therefore, there is a possibility that GGOH converts into GG-pyrophosphate, incorporates into a protein, and mediates vesicular transport of ubiquitinated HMGR from the ER membrane to a specific subdomain or organelle in the ER where it is then degraded (Jo and DeBose-Boyd, 2010).

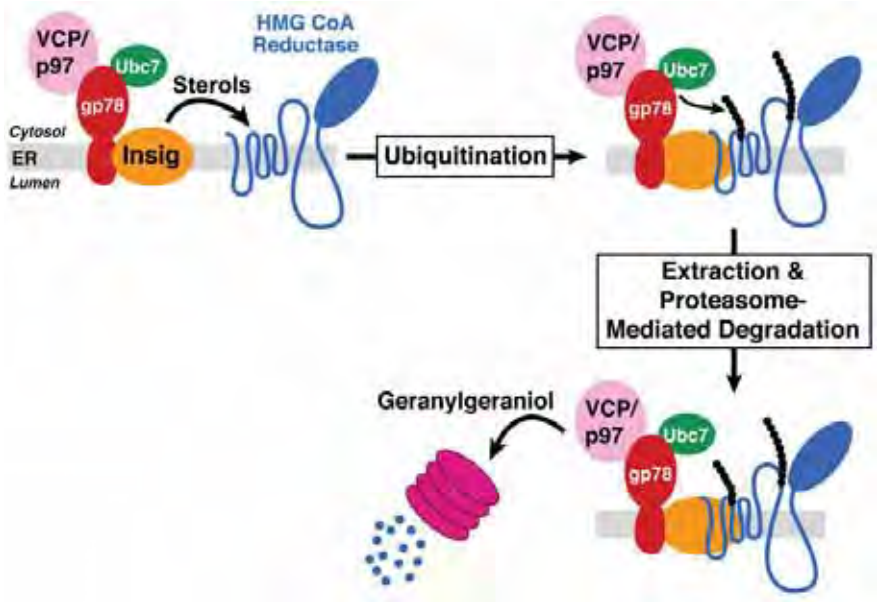

Figure 1.7 Current model for ER-associated degradation (ERAD) of HMGR

Accumulation of certain sterols and/or oxysterols stimulates binding of Insigs to the membrane domain of HMGR. Some of the Insig molecules are associated with gp78, a membrane-anchored ubiquitin ligase that associates with the ubiquitin conjugating enzymes Ubc7 and VCP/p97. Ubc7 and gp78 combine to initiate the polyubiquitination of two cytosolic lysine residues (89 and 248) in the membrane domain of HMGR. This ubiquitination triggers extraction of HMGR from ER membranes through the action of VCP/p97 and its associated cofactors; this step appears to be enhanced by the isoprenoid geranylgeraniol through an undefined mechanism. Once extracted, HMGR is delivered to proteasomes for degradation. [Figure reproduced from (Jo and DeBose-Boyd, 2010)].

1.7 Squalene Monooxygenase: A Neglected Rate-Limiting Enzyme

Since the early 1970s, there were reports of [^{14}C]-squalene being the most abundant cholesterol precursor to accumulate in the kidney slices of rats and dogs within 1 hr of being incubated with [^{14}C]-mevalonate (Hellstrom et al., 1973; Raskin and Siperstein, 1974). Specifically, in dog kidney slices, of the total non-saponifiable lipids produced from [^{14}C]-mevalonate, 56% was present as [^{14}C]-squalene, 5% as [^{14}C]-lanosterol, and only 3% as [^{14}C]-cholesterol (Raskin and Siperstein, 1974). A few years later, Gonzalez and colleagues provided evidence that in human renal cancer cells exogenous cholesterol not only decreased the activity of HMGR, but also inhibited the conversion of mevalonate to cholesterol, resulting in the accumulation of squalene (Gonzalez et al., 1979). They postulated that in addition to HMGR, SM could be another major regulatory step in cholesterol synthesis (Gonzalez et al., 1979). Similar squalene accumulation was documented in human fibroblasts in the presence of LDL-cholesterol and [^{3}H]-mevalonate (Brown and Goldstein, 1980). Chinese hamster ovary (CHO) cells grown in full serum exhibited an increase in squalene accumulation as compared to the control cells grown under lipoprotein-deficient conditions (Eilenberg and Shechter, 1984). In HepG2 cells, the cholesterol synthesis inhibitor L-654969 that blocks HMGR, increased SM activity by 2 fold (Hidaka et al., 1990). On the other hand, LDL-cholesterol decreased SM activity by 70% after a 18 hr treatment (Hidaka et al., 1990). Together, Hidaka and colleagues presented evidence that SM is subject to feedback regulation mediated by endogenous and exogenous sterols (Hidaka et al., 1990). Furthermore, the regulatory mechanism of SM was thought to be due to the change in the amount of its protein levels, either caused by the change in protein synthesis rate, or degradation (Hidaka et al., 1990). Furthermore, the concept that SM may be a largely overlooked regulatory enzyme in cholesterol synthesis is suggested by its much lower specific activity in liver cells compared to that of HMGR (Hidaka et al., 1990). Despite the compelling evidence, the sterol-mediated rate-limiting activity of this enzyme has not been fully explored.

1.7.1 Therapeutic Role

SM has been extensively explored as a target for anti-fungal drug treatment and has proven to be very lucrative in this respect. The drug Terbinafine, a treatment for athlete's foot, is a potent non-competitive inhibitor of SM in various fungal species and causes the inhibition of ergosterol synthesis (Ryder, 1992). A modified version of Terbinafine called NB-598, a highly potent and specific inhibitor of vertebrate SM was developed as a treatment for hypercholesterolemia. In HepG2 cells, NB-598 inhibited cholesterol synthesis from [^{14}C]-acetate in a dose-dependent manner, which lead to the accumulation of [^{14}C]-squalene (Horie et al., 1990). In dogs, oral doses of NB-598 reduced serum cholesterol levels, and had no effect on the levels of free fatty acids, phospholipids, and triacylglycerol, strengthening its role as a specific SM drug target (Hidaka et al., 1991).

Interestingly, a number of naturally occurring compounds have been shown to inhibit SM activity *in vitro*. A few examples include garlic extracts such as selenocystine and S-allylcysteine were shown to inhibit cholesterol biosynthesis in cultured hepatocytes (Gupta and Porter, 2001), resveratrol found in red wine is suggested to inhibit human SM and may decrease endogenous cholesterol synthesis (Laden and Porter, 2001; Soleas et al., 1997). The cholesterol lowering effect of gallate esters from green tea has been attributed to the potent inhibition of SM (Abe et al., 2000). However, due to the commercial success of statins as potent LDL-cholesterol lowering agents and their beneficial pleiotropic effects, the regulatory role of SM in cholesterol synthesis has not received sufficient interest.

1.8 Oxysterols

The existence of oxysterols was recognized by Lifschütz who regarded "oxycholesterol" as a single chemical entity, a monohydroxylated derivative of cholesterol (Smith, 1981). Currently, a number of different oxysterols are known, however, they often have very different origins and biological activities. Figure 1.8

depicts the structures of some of the more common oxysterols and indicates how they are derived.

Oxysterols were first identified as autoxidation products of cholesterol. These are mainly oxidized by the addition of a hydroxyl or keto group to the B-ring of the sterol, particularly at the 7th position. Studies of non-enzymatically derived oxysterols were mostly conducted by applying high concentrations of free oxysterol to cultured cells. However, since non-enzymatically derived oxysterols are mostly esterified within the cell, and presumably sequestered out of harm's way (Brown and Jessup, 1999), such studies probably have overestimated their biological activities. Several cytochrome P450 enzymes participate in the conversion of cholesterol into particular hydroxycholesterols. For example, CYP7A1 produces 7α-hydroxycholesterol (also generated non-enzymatically) as the first committed step in the classical bile acid pathway. CYP46 is a microsomal enzyme present particularly in neurons and produces 24(*S*)-hydroxycholesterol (24HC), also called cerebrosterol because of its relative abundance in the brain (Björkhem, 2007). Enzymatically derived oxysterols such as 24HC, 25-hydroxycholesterol (25HC), 27-hydroxycholesterol (27HC), and 24,25EC are known to be potential physiological regulators and participate in cholesterol homeostasis (Gill et al., 2008).

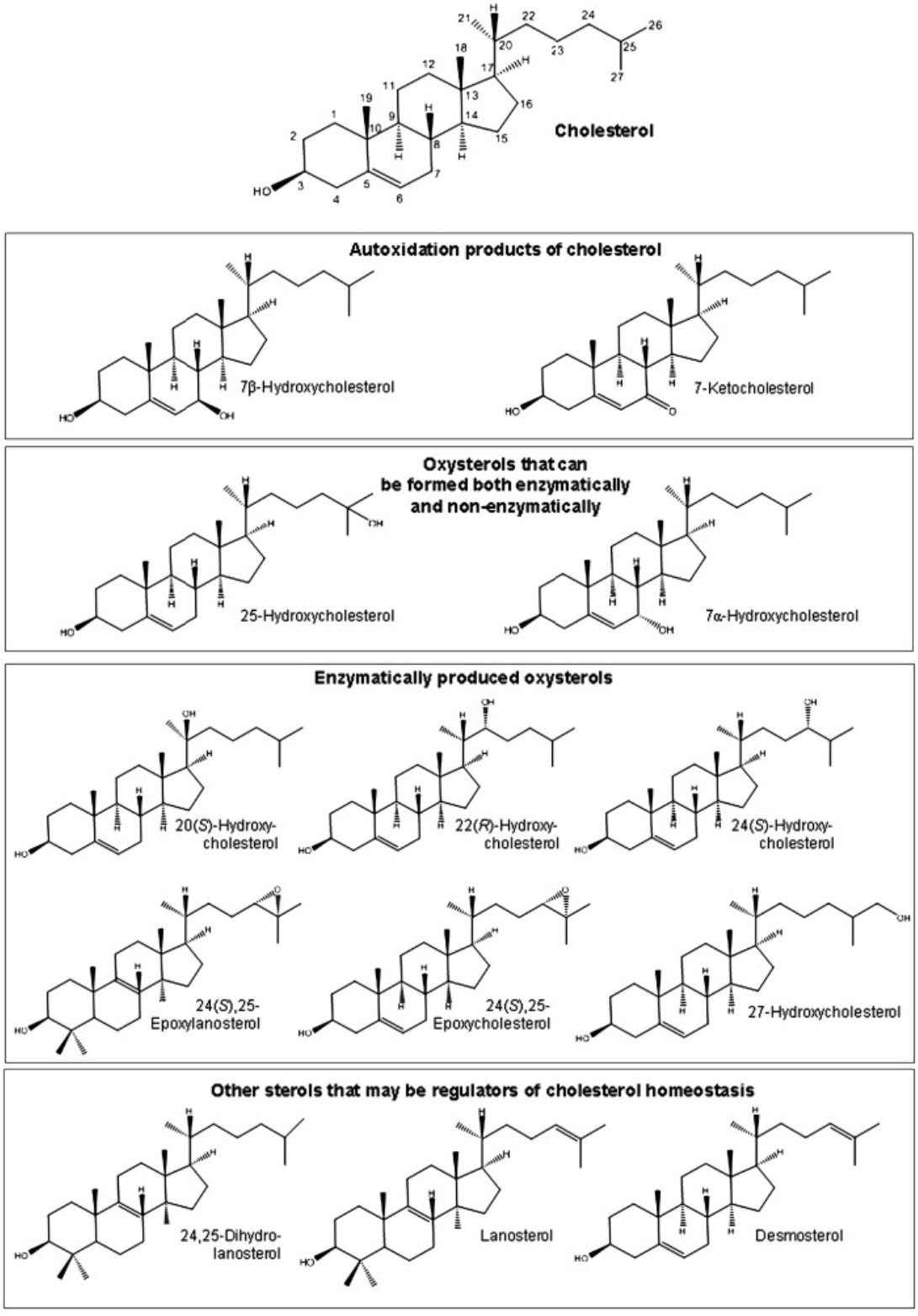

Figure 1.8 Structures of some common oxysterols and how they are derived

Figure from (Gill et al., 2008)

1.8.1 The Oxysterol Hypothesis: Revisited and Revised

Background

The arrival of the Oxysterol Hypothesis came half a century after feedback control by cholesterol was first observed by Schoenheimer and Breusch (Schoenheimer and Breusch, 1933). By the time the Oxysterol Hypothesis was published in 1978 (Kandutsch et al., 1978), many details regarding cholesterol homeostasis and metabolism had already been elucidated (Table 1) (Gould et al., 1952; Tomkins et al., 1953). Although it was clear that activity of the LDL receptor and HMGR were regulated by LDL-cholesterol, the molecular basis by which cells sense cholesterol and use this information to regulate those proteins remained a mystery.

Formulation of The Oxysterol Hypothesis

Kandutsch and colleagues first demonstrated the possibility that oxysterols served as regulators of cholesterol synthesis in 1973 (Kandutsch and Chen, 1973). Using a variety of cell culture models, they found that purified cholesterol was unable to inhibit cholesterol synthesis, therefore, they did not support the assumptions at the time that cholesterol acted directly as a regulatory molecule. They showed that cholesterol synthesis could be inhibited by impure cholesterol, which they attributed to trace amounts of contaminating oxysterols (Kandutsch et al., 1978). This and subsequent studies over the next five years by their own and other groups seemed to confirm that the inhibitory potency of some oxysterols was orders of magnitude higher than that of cholesterol itself. Furthermore, Kandutsch and colleagues discovered a cytosolic protein, dubbed the oxysterol binding protein, which displayed a number of properties consistent with it being responsible for regulating the transcriptional responses of oxysterols. For example, the oxysterol binding protein bound to a wide variety of oxysterols with affinities that were generally proportional to their potencies in suppressing HMGR activities (Taylor et al., 1984). However, in gene silencing experiments, inhibition of cholesterol synthesis by oxysterols was found to be independent of the oxysterol binding protein (Adams et al., 2004; Nishimura et al., 2005). Attention shifted away from the oxysterol

binding protein when the SREBP transcription factors were identified as the key regulators of cholesterol homeostasis (Section 1.3.2).

The Oxysterol Hypothesis was criticized for a number of reasons. For example, researchers challenged the method used to deliver oxysterols and cholesterol to the cell cultures. Experiments by Kandutsch and coworkers were conducted by dissolving sterols in ethanol and adding them to protein containing aqueous culture media. In such conditions, cholesterol forms an amorphous suspension and thus has poor access to the interior of the cell. Also, the physiological relevance of the high concentrations at which the oxysterols were used in *in vitro* studies was questioned.

A Revised Hypothesis

In light of the developments made in the field of cholesterol research, we proposed a revised Oxysterol Hypothesis which argues that while cholesterol is central to achieving its own balance, oxysterols play an important role in smoothing this regulation in the short term (Gill et al., 2008). In the absence of such a regulator, cellular cholesterol homeostatic responses become erratic and exaggerated. Furthermore, we proposed that an oxysterol like 24,25EC, formed in parallel with cholesterol, has a special role in smoothing cholesterol responses in all cholesterogenic cells when cholesterol synthesis is active (Figure 1.9). Other regulatory sterols produced in the cholesterol biosynthetic pathway such as desmosterol, 24,25-dihydrolanosterol, and 24(*S*),25-epoxylanosterol would also be predicted to be important when cholesterol synthesis is active. When cholesterol accumulates so that the cholesterol biosynthetic pathway is shut down, other oxysterols are produced from the excessive cholesterol to serve as auxiliary regulators. These tend to be produced in a tissue specific way, such as 24HC in neurons (Björkhem and Diczfalusy, 2004), and 27HC in macrophages and arterial endothelium (Javitt, 2002). Therefore, oxysterols do play an important role in cholesterol homeostasis, even if it is a lesser role than that originally envisaged by Kandutsch and colleagues more than 30 years ago. The Oxysterol Hypothesis will certainly continue to evolve in order to accommodate new findings from various areas of oxysterol research.

Table 1.1 Major discoveries that shaped the Oxysterol Hypothesis[#]

Year	Milestone
1769	Characterization of cholesterol by Poulletier de la Salle
1816	Named as ‘cholesterine’ by Chevreul
1906	Identification of ‘oxycholesterol’ (oxysterols) by Lifschütz
1927–8	Nobel Prizes awarded to Windaus and Wieland for elucidation of the structure of cholesterol and bile acids respectively
1933	Feedback control by cholesterol first observed
1953	Feedback regulation of cholesterol synthesis by other cholesterol-like compounds noted; 24(*S*)-hydroxycholesterol (cerebrosterol) discovered in human brain
1956	27-Hydroxycholesterol discovered to be produced from cholesterol by liver mitochondria
1964	Nobel Prize awarded to Bloch and Lynen for elucidating the cholesterol and fatty acid biosynthetic pathways
1973	Possible role of oxysterols as cholesterol synthesis mediators
1978	The Oxysterol Hypothesis formulated
1981	24(*S*),25-Epoxycholesterol discovered in human liver
1985	Nobel Prize awarded to Brown and Goldstein for their discoveries concerning the regulation of cholesterol metabolism, including discovery of the LDL receptor
1993	Certain oxysterols suppress activation of SREBP (master regulators of cholesterol homeostasis)
1994	Evidence that 27-hydroxycholesterol provides a mechanism for cholesterol elimination from macrophages
1996	Evidence that 24(*S*)-hydroxycholesterol provides a mechanism for cholesterol elimination from the brain
1997	Certain oxysterols proposed as natural ligands for the liver X receptors

Year	Milestone
2005	Certain oxysterols, and some sterol intermediates of cholesterol, accelerate degradation of HMGR
2007	Evidence that certain oxysterols are important ligands for LXR *in vivo*; Identification of Insig as the oxysterol sensing protein in the ER
2008	Evidence that an endogenous oxysterol [24(*S*),25-epoxycholesterol] plays an acute role in smoothing cholesterol homeostatic responses

[#] The references for this table are given in Appendices Table A1

1.8.2 Role of Oxysterols in the SREBP Pathway

Cholesterol and oxysterols both block SREBP processing by inducing Scap binding to Insig, it was postulated that there was another ER membrane protein that mediates the effect of oxysterols (Adams et al., 2004). The identity of this oxysterol sensing protein has only been discovered recently, and turns out to be Insig itself. There are two important points to note from these studies (Adams et al., 2004; Radhakrishnan et al., 2007). Firstly, the sterol binding properties of Scap and Insig are reciprocal. Scap recognizes the tetracyclic steroid nucleus and the 3β-hydroxyl group of cholesterol. It binds equally well to sterols lacking a side-chain but cannot bind to sterols with a polar group on the side-chain. By contrast, Insig binding absolutely requires a polar group on the side-chain. Secondly, cholesterol and oxysterols have the same net effect in diminishing SREBP activation but operate via two different yet converging mechanisms: cholesterol via binding to Scap and oxysterols via binding to Insig.

1.8.3 24(*S*),25-Epoxycholesterol

Nelson and colleagues first discovered 24(*S*),25-Epoxycholesterol (24,25EC) in 1981 (Nelson et al., 1981b). It was detected in the human liver, and found to decrease HMGR activity (Spencer et al., 1985). It is one of the most potent known

oxysterol activators of LXR (Janowski et al., 1999), can inhibit SREBP processing (Janowski et al., 2001; Rowe et al., 2003), and can lead to the degradation of HMGR (Song and DeBose-Boyd, 2004a). All of these findings establish 24,25EC as a natural regulator of cholesterol homeostasis.

When compared with other oxysterols, 24,25EC has a unique origin. Rather than being derived from cholesterol, this oxysterol is produced in a shunt of the same mevalonate pathway that produces cholesterol (Figure 1.4). The enzyme 2,3-Oxidosqualene cyclase (OSC) not only cyclizes the conversion of MOS into lanosterol, the first sterol in the pathway, but also catalyzes the cyclization of DOS to 24(*S*),25-epoxylanosterol, which is then converted into 24,25EC in an alternative oxysterol synthesis pathway (Figure 1.4). Like most genes in cholesterol synthesis pathway, OSC is also regulated by SREBP-2 (Horton et al., 2002a; Horton et al., 2003). The shared nature of this pathway has important implications. Firstly, all cells that can produce cholesterol should be able to synthesize 24,25EC. Our laboratory has shown that human brain cells can produce 24,25EC with likely consequences for brain cholesterol homeostasis (Wong et al., 2007a). Secondly, the fact that 24,25EC is produced in parallel means that it is subject to the same feedback control that inhibits cholesterol synthesis (Wong et al., 2007a).

Interestingly, levels of endogenous 24,25EC can be artificially elevated by partially inhibiting the above described step catalyzed by OSC (Beyea et al., 2007; Dollis and Schuber, 1994; Mark et al., 1996; Rowe et al., 2003; Wong et al., 2004, 2007a). This is because DOS has a lower K_m for OSC than does MOS (Boutaud et al., 1992), and therefore, when partially inhibited, synthesis of 24,25EC is favored over cholesterol. Thus, this approach has the potential confounding effect of reducing cholesterol synthesis.

It has been previously shown by our laboratory that 24,25EC acutely regulates newly synthesized cholesterol levels, thus contributing to cholesterol homeostasis (Wong et al., 2008). This characteristic makes OSC an attractive target for cholesterol-lowering drugs. However, high dose OSC inhibitors caused early-stage cataracts in hamsters and dogs (Funk and Landes, 2005). Nevertheless, low

doses of these inhibitors that only partially inhibit OSC could possibly minimize the adverse effects of these pharmacological inhibitors in humans.

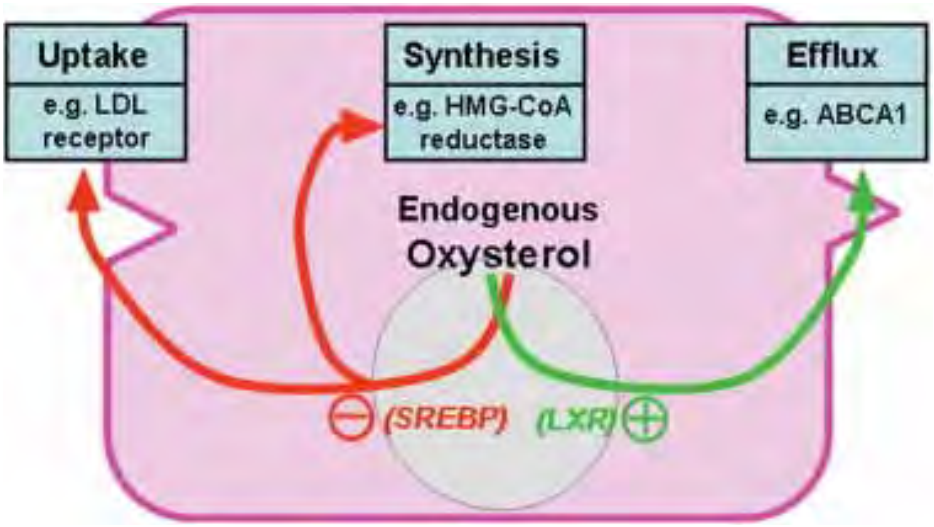

Figure 1.9 Regulatory role of 24,25EC in cholesterol homeostasis

24,25EC acts on multiple levels: decreasing cholesterol uptake and synthesis via SREBP, while stimulating cholesterol efflux via LXR. Not shown here is that endogenous oxysterols may also accelerate the degradation of HMGR. [Figure courtesy of A.J. Brown (Gill et al., 2008)]

1.8.4 Metabolism of Oxysterols

Oxysterols are metabolized for deactivation and eventual elimination from the body. By virtue of their increased polarity relative to cholesterol, oxysterols tend to efflux more readily from cells, although there are exceptions to this rule as seen with the impaired efflux from macrophages of 7-ketocholesterol (also called 7-oxocholesterol) (Gelissen et al., 1996). There is some evidence that ABC transporters may be involved in the transport of oxysterols from or into cells [ABCA1 for 25HC (Tam et al., 2006) and ABCG1 for 7β-hydroxycholesterol (Engel et al., 2007), and 7-ketocholesterol (Terasaka et al., 2007)].

Esterification may be one mechanism whereby oxysterols are sequestered in an inactive form. Many oxysterols measured in tissues (Brown and Jessup, 1999) or plasma (Dzeletovic et al., 1995) are predominantly esterified, suggesting

that they are good substrates for ACAT (acyl-CoA cholesterol acyl transferase) in cells and LCAT (lecithincholesterol acyl transferase) in the circulation. Other deactivation mechanisms involve biochemical modifications of the sterol itself. Ring-oxygenated sterols like 7-ketocholesterol can be metabolized by CYP27A1 to form 27-hydroxylated derivatives and further to water-soluble metabolites (Brown et al., 2000; Lee et al., 2006; Lyons and Brown, 2001).

1.9 Statins

HMGR inhibitors, collectively referred to as statins, have revolutionized the treatment of hypercholesterolemia and cardiovascular disease because of their superior ability to reduce levels of LDL-cholesterol. The first member of these competitive HMGR inhibitors was compactin (also known as ML-236B and mevastatin), isolated from the fungus *Penicillium citrinum* by Endo and colleagues (Endo et al., 1976). Statins inhibit HMGR competitively by occupying its catalytic portion, thus blocking access of the substrate to the active site. This inhibitory action of statins is due to their structural homology to HMG-CoA, the natural substrate for HMGR (Istvan, 2002; Istvan and Deisenhofer, 2001). The potency of different statins reflects the number of bonding interactions they have with HMGR (Istvan and Deisenhofer, 2001).

Statins act by targeting HMGR in hepatocytes, thereby blocking cholesterol synthesis. When the intracellular availability of cholesterol decreases, the SREBP-2 pathway is activated, leading to the upregulation of target gene expression, including the LDL receptor (Goldstein et al., 2006b; Horton et al., 2002b). In this manner, the cholesterol-lowering effect of statins is facilitated by the activation of the cell surface LDL receptors, leading to an increase in the hepatic uptake of circulating LDL-cholesterol.

In addition to their cholesterol-lowering properties, statins exert actions other than those for which they were specifically developed, which have been called pleiotropic effects (Liao and Laufs, 2004). Most of the pleiotropic effects of statins

are due to the inhibition of isoprenoid synthesis occurring as part of the mevalonate pathway. Inhibition of HMGR blocks the synthesis of mevalonate, which is the precursor for isoprenoid synthesis (Goldstein and Brown, 1990). Some of the pleiotropic effects include stabilization of atherosclerotic plaques, decreasing LDL oxidation, improving endothelial function, and reducing inflammation and inhibiting the thrombogenic response (Liao and Laufs, 2004).

1.9.1 Station Rebound Phenomenon and Side-effects

The side-effects attributed to statins limit patient compliance and reduce the ability to meet clinical targets of LDL-cholesterol lowering (McGinnis et al., 2007). Moreover, there is increasing evidence that taking statins intermittently may cause more harm than not taking statins at all. This has been termed the "Statin Rebound Phenomenon" and has been especially observed after an acute vascular event, when statin discontinuation results in a worse outcome than in patients who never received statins (Daskalopoulou, 2009). Evidence has also been presented for the existence of a rebound inflammatory effect after statin cessation (measured as C-reactive protein) (Sposito et al., 2009). The statin rebound effect is caused by the exquisite nature of feedback control, and can be reproduced in cultured cells (Wong et al., 2007a). The inhibitory effect of statin on cholesterol synthesis leads to a compensatory increase in the expression of several key cholesterol biosynthetic enzymes, including HMGR, the target of statins. Hence, removal of the statin results in a concentration-dependent surge in cholesterol synthesis (Wong et al., 2007a). Accordingly in normal subjects, stopping statins caused a rebound of serum cholesterol levels, monocyte HMGR activity and sterol synthesis (Stone et al., 1989).

A common side-effect of statin therapy is myopathy (muscle pain), but in rare cases rhabdomyolysis, which is the breakdown of skeletal muscle causing damage to the kidney, and sometimes complete renal failure (Graham et al., 2004). In 2001, cerivastatin was withdrawn from the global markets following the death of 31 patients suffering from acute renal failure caused by rhabdomyolysis (Furberg and Pitt, 2001). Another adverse effect of statins is the inhibition of coenzyme Q_{10}

synthesis (also known as ubiquinone). Coenzyme Q_{10} participates in mitochondrial energy production. Taking an oral dose of coenzyme Q_{10} has been shown to improve the condition of patients with myalgia associated with statin therapy (Folkers et al., 1990; Langsjoen and Langsjoen, 2003; Rundek et al., 2004).

Overall, statins are comparatively safe but like any other drug, they are not exempt from adverse reactions. Importantly, with statin use, dose and potency all on the rise, the number of adverse reactions can be expected to also increase (Brown, 2010). This is recognized as an important area of investigation, with numerous trials underway to ameliorate the side-effects of statins (particularly those involving coenzyme Q_{10} and muscle-related side-effects). Also, there is a need to develop alternatives to statin therapy, one possibility being combination therapies (Gill and Brown, 2011).

1.10 Hypothesis and Aims

As discussed in this chapter, elaborate homeostatic mechanisms exquisitely control cholesterol levels within the cell at the transcriptional and post-transcriptional levels. Extensive research on HMGR has highlighted its importance as a crucial control point in cholesterol synthesis. Over the years, evidence for another rate-limiting enzyme in cholesterol synthesis has emerged. SM has been suggested as a second rate-limiting enzyme in cholesterol synthesis after HMGR. Nevertheless, the precise regulatory role played by SM, and the molecular mechanisms behind it, have not been explored.

Research done in our laboratory has confirmed and extended previous findings of squalene accumulating in various cell-types upon treatment with cholesterol and/or LDL. Therefore, **we hypothesized that cholesterol regulates its own synthesis in part by feeding back and inhibiting the activity of SM at a post-transcriptional level, causing squalene to accumulate in cells.** Also, based on the well-elucidated feedback mechanism of HMGR, and the fact that SM is also an ER protein, we hypothesized that SM is degraded via the ERAD pathway in a cholesterol-dependent manner. The aims of this thesis are:

a. **To investigate the role of cholesterol in the post-transcriptional regulation of SM** (Chapters 3 and 4)
b. **To elucidate the cholesterol-mediated ubiquitination and proteasomal degradation mechanism of SM** (Chapter 5)
c. **To identify the regulatory domain of SM involved in the cholesterol-dependent regulation of the enzyme** (Chapter 5)

SM and OSC participate in cholesterol as well as 24,25EC synthesis. Manipulations of these enzyme levels can lead to a shift in the balance of cholesterol and 24,25EC synthesis. Additionally, 24,25EC acutely controls the level of newly synthesized cholesterol in cultured cells (Wong et al., 2008). In Chapter 6, we extend these findings to investigate **the modulating effect of artificially raised 24,25EC levels on newly synthesized cholesterol levels in a 'statin rebound**

effect' setting. Also, we aimed to characterize SM overexpressing stable cell-line that has higher levels of 24,24EC.

CHAPTER 2

GENERAL MATERIALS AND METHODS

2. GENERAL MATERIALS AND METHODS

2.1 Materials List

Table 2.1 List of all common materials and reagents and their sources

Materials/ Reagents	Source (Company)
[1-^{14}C] Acetic Acid Sodium Salt (specific radioactivity: 56 mCi/mmol)	GE Healthcare Bio-Sciences, NSW (now Perkin Elmer, Waltham, MA)
[2-^{14}C]-mevalonolactone (mevalonate) (specific radioactivity: 40-60 mCi/mmol)	Perkin Elmer, Waltham, MA
[^{35}S]-Protein Labeling Mix [EXPRE^{35}S^{35}S Protein Labeling Mix (specific radioactivity: >1000 Ci/mmol)]	Perkin Elmer, Waltham, MA
7-dehydrocholesterol	Steraloids, Newport, RI, USA
24,25-dihydrolanosterol	Steraloids, Newport, RI, USA
7α-hydroxycholesterol	Steraloids, Newport, RI, USA
7β-hydroxycholesterol	Steraloids, Newport, RI, USA
7-ketocholesterol	Steraloids, Newport, RI, USA
19-hydroxycholesterol	Steraloids, Newport, RI, USA
24(*S*)-Hydroxycholesterol	Sigma-Aldrich, NSW
24(*S*),25-Epoxycholesterol	Steraloids, Inc., Newport, Rhode Island, USA
25-Hydroxycholesterol	Steraloids, Newport, RI, USA
27-Hydroxyholesterol	Steraloids, Newport, RI, USA
40% Arcylamide/Bis Solution (37.5:1)	Bio-Rad Laboratories, NSW
Agar	Sigma-Aldrich, NSW
AGFA Developer Solution and Rapid Fixer Solution	AGFA Healthcare Australia, VIC
Amersham Hyperfilm ECL	GE Healthcare Bio-Sciences,

Materials/ Reagents	Source (Company)
Ampicillin	Sigma-Aldrich, NSW
Amplex Red Cholesterol Assay Kit	Invitrogen Australia Pty Ltd., VIC
β- mercaptoethanol	Sigma-Aldrich, NSW
Bicinchoninic Acid Assay Kit	Pierce, Rockford, Illinois, USA
BigDye v3.1	Applied Biosystems, VIC
Bovine Serum Albumin (BSA)	Sigma-Aldrich, NSW
Butylated Hydroxytoluene	Sigma-Aldrich, NSW
Cholesterol	Steraloids, Newport, RI, USA
Chloroquine	Sigma-Aldrich, NSW
Compactin/Mevastatin	Sigma-Aldrich, NSW
Cycloheximide	Sigma-Aldrich, NSW
Cysteine	Sigma-Aldrich, NSW
Deoxycholate, sodium salt	Sigma-Aldrich, NSW
Desmosterol	Sigma-Aldrich, NSW
Developer	AGFA, Morstel, Belgium
DH5α *E. coli*	Invitrogen Australia Pty Ltd., VIC
Diethyl Ether	Ajax FineChem, NSW
Dimethyl Sulfoxide(DMSO)	Ajax FineChem, NSW
Dulbecco's Modified Eagle's Medium High or Low Glucose	Invitrogen Australia Pty Ltd., VIC
Dulbecco's Modified Eagle's Medium: Ham's F-12 (1:1)	JRH Biosciences, VIC and Invitrogen Australia Pty Ltd., VIC
Dulbecco's Phosphate Buffered Saline (PBS)	Sigma-Aldrich, NSW
Dynabeads	Invitrogen Australia Pty Ltd., NSW

Materials/ Reagents	Source (Company)
Ethanol	Ajax FineChem, NSW
Fatty Acid-Free BSA Fraction V	Sigma-Aldrich, NSW
Fetal bovine Serum	Invitrogen Australia Pty Ltd., VIC
Fixer	AGFA, Morstel, Belgium
Glacial Acetic Acid	May and Baker Australia Pty Ltd, VIC
GlutaMAX	Invitrogen Australia Pty Ltd., VIC
Glutathione sepharose	GE Healthcare, Rydalmere, NSW
Glycine	Sigma-Aldrich, NSW
GR144000X (squalene monooxygenase inhibitor)	Gift from Glaxo-SmithKline
GW534511X	Glaxo-SmithKline
HEPES	Acros Organics, New Jersey, USA
Hexane	APS FineChem, NSW
HiSpeed Plasmid Maxi Kit	Qiagen, Doncaster, VIC
Hyperfilm ECL	GE Healthcare, Rydalmere, NSW
iQ SyBr Green Supermix	Bio-Rad Laboratories, NSW
Isopropanol	Ajax FineChem, NSW
L-Glutamine	Invitrogen Australia Pty Ltd., VIC
Lactacystin	Sigma-Aldrich, NSW
Lanosterol	Steraloids, Newport, RI, USA
Lathosterol	Steraloids, Newport, RI, USA
LDL (d=1.019-1.063 g/ml) was isolated by standard ultracentrifugation techniques from the plasma of healthy male volunteers	(Brown et al., 1996)

Materials/ Reagents	Source (Company)
Lipofectamine LTX	Invitrogen Australia Pty Ltd., VIC
LB broth	Sigma-Aldrich, NSW
Methanol AR	Ajax FineChem, NSW
Methionine	Sigma-Aldrich, NSW
Methyl-β-Cyclodextrin (MeβCD)	Sigma-Aldrich, NSW
Mevalonate	Sigma-Aldrich, NSW
N-Acetyl-Leu-Leu-Norleu-al (ALLN)	Sigma-Aldrich, NSW
N,N,N',N'-Tetramethylethylenediamine (TEMED)	Sigma-Aldrich, NSW
Newborn Calf Serum	Invitrogen Australia Pty Ltd., VIC
Oligonucleotide Primers	Synthesized by Sigma-Genosys, Sigma-Aldrich, NSW
Opti-MEM I Reduced-Serum Medium	Invitrogen Australia Pty Ltd., VIC
pcDNA4.1-Myc-His TOPO TA Cloning Kit	Invitrogen Australia Pty Ltd., VIC
Penicillin/Streptomycin	Invitrogen Australia Pty Ltd., VIC
Peroxidase-conjugated AffiniPure Donkey Anti-Mouse IgG	Jackson ImmunoResearch Laboratories (West Grove, PA)
Peroxidase-conjugated AffiniPure Donkey Anti-Rabbit IgG	Jackson ImmunoResearch Laboratories (West Grove, PA)
Ponceau S solution	Sigma-Aldrich, NSW

Materials/ Reagents	Source (Company)
Precision Plus Protein Kaleidoscope standards	Bio-Rad Laboratories, NSW
Protease Inhibitor Cocktail	Sigma-Aldrich, NSW
Restriction Endonucleases	New England BioLabs, Inc., Ipswich, Massachusetts, USA
SensiMix dT	Quantace Ltd., London, UK (now Bioline, NSW)
Silica Gel 60 F_{254} TLC Plates	Merck, Australia, VIC
Skim Milk Powder	Diploma, Bonlac Foods, Melbourne, VIC
S.O.C Medium	Invitrogen Australia Pty Ltd., VIC
Sodium Chloride	Ajax FineChem, NSW
Sodium Dodecyl Sulfate (SDS)	Sigma-Aldrich, NSW
Sodium Oleate	Sigma-Aldrich, NSW
SuperScript III First Strand cDNA	Invitrogen Australia Pty Ltd., VIC
Tris-Base	Sigma-Aldrich, NSW
Tris-HCI	Sigma-Aldrich, NSW
Triton X-100	Sigma-Aldrich, NSW
TrypLE (Trypsin)	Invitrogen Australia Pty Ltd., VIC
Tween-20	Sigma-Aldrich, NSW
Z-Leu-Leu-Leu-al (MG132)	Sigma-Aldrich, NSW
Zaragozic acid A trisodium salt	Sigma-Aldrich, NSW

2.1.1 Cell lines

Chinese Hamster Ovary-7 (CHO-7), SRD-1, SRD-13A, and HEK293 cells were generous gifts of Drs. Michael S. Brown and Joseph L. Goldstein (UT Southwestern Medical Center, Dallas, TX). SRD-15 cells were generously donated by Dr Russell DeBose-Boyd (UT Southwestern Medical Center, Dallas, TX). HepG2 cells and primary human fibroblasts were kind gifts from the Centre for Vascular Research (UNSW, Sydney, NSW, Australia). BE(2)C cells were generously donated by Dr Louise Lutze-Mann (UNSW, Sydney, NSW, Australia). The OSC overexpressing stable cell line was prepared by Dr Jenny Wong (Wong et al., 2008).

2.1.2 Plasmids

The HA-tagged ubiquitin plasmid, pMT123, encoding 8 tandem HA-ubiquitins (Treier et al., 1994), was a gift from Dr Dirk Bohmann (University of Rochester Medical Center, Rochester, NY). pCMV-SM-V5 was prepared by Dr Jenny Wong (unpublished data). The following plasmids were prepared by Julian Stevenson according to methods described in (Gill et al., 2011): pTK-SMΔ(W_2-K_{100})-V5 (plasmid encoding SM missing the first 99 amino acids driven by a TK promoter), pCMV-SMΔ(W_2-K_{100})-V5 (plasmid encoding SM missing the first 99 amino acids driven by a CMV promoter), pTK-SM-V5-GAr (contains a 30 amino-acid repeat from Epstein-Barr virus nuclear antigen-1 after the V5-His tag), pTK-GAr-SM-V5-GAr (contains an additional copy of the repeat after the initiating methionine), pTK-SM-N100-GFP-V5 (encodes the first 100 amino-acids of human followed by a linker 'AGSGA', the enhanced green fluorescent protein and the V5-His tag), pTK-SM-N100-GST-V5 [instead includes a glutathione S-transferase (GST) fusion].

2.1.3 Sterol Complexing to Methyl-β-Cyclodextrin

Sterols and oxysterols complexed with methyl-β-cyclodextrin were prepared as described (Brown et al., 2002). Sterol/CD complexes were diluted without addition of further cyclodextrin, so a constant molar ratio of ~0.1 sterol to methyl-β-cyclodextrin was used.

2.2 General Methods

2.2.1 Cell Culture

Cell culture was performed in a Laminar Flow Biological Safety Cabinet (Gelaire, Australia). All cells were maintained in a monolayer at 37°C in 5% CO_2. Cells were seeded at the following densities: 1×10^5 cells/well in triplicate in 12-well plates for quantitative Real-Time PCR (qRT-PCR); 2×10^6 cells/6 cm dish for Immunoprecipitation; 4×10^6 cells/10 cm dish for cell Glutathione Sepharose (GST) Pulldown; 2×10^5 cells/well in 6-well plates for all other experiments including Thin-Layer Chromatography (TLC) and Immunoblot analysis. CHO-7, SRD-1, and SRD-15 cells were maintained in medium A, HepG2 cells in medium D, and BE(2)C, HEK293, and fibroblasts in medium G. SRD-13A cells were maintained in medium C supplemented with 5 μg/ml cholesterol, 1 mM mevalonate, and 20 μM sodium oleate. Please refer to Table 2.2 for the exact contents of each media.

Unless otherwise stated, cells were statin pretreated overnight (16 hr) to deplete sterols through incubation in medium containing LPDS, the HMGR inhibitor compactin (5 μM), and a low level of mevalonate (50 μM) that allows synthesis of essential non-sterol isoprenoids but not of cholesterol (Hartman et al., 2010). After statin pretreatment, cells were washed once with PBS, which was sufficient to remove any residual compactin. For treatment, the media was refreshed to include test agents (added in ethanol or dimethylsulfoxide to refreshed media) as described in the figure legends for the times indicated, followed by cell harvesting for the assays described below. Within an experiment, the final concentrations of solvent were kept constant between conditions and did not exceed 0.28 % (v/v).

Table 2.2 Cell Culture Media

Medium*	Contents and Supplements
A	DMEM/F12** supplemented with 5% LPDS***
B	Medium A containing 5 μM compactin, and 50 μM mevalonate
C	DMEM/F12 supplemented with 5% NCS
D	DMEM low glucose supplemented with 10% FBS
E	DMEM low glucose supplemented with 5% LPDS
F	Medium E containing 5 μM compactin, and 50 μM mevalonate
G	DMEM high glucose supplemented with 10% FBS
H	DMEM high glucose supplemented with 5% LPDS
I	Medium H containing 5 μM compactin, and 50 μM mevalonate

* All media containing penicillin (100 U/ml), streptomycin (100 μg/ml), and L-glutamine (2 mM)

** DMEM/F12 cell culture media was reconstituted from powered stock, and sterilized through a 0.22 μm filter before use.

***Lipoprotein-Deficient Serum (LPDS) was prepared from heat inactivated NCS as described previously (Goldstein et al., 1983).

DMEM/F-12: Dulbecco's modified Eagle's medium: Ham's F-12 [1:1 (v/v)]
FBS: fetal calf serum
NCS: newborn calf serum
LPDS: lipoprotein-deficient serum
BSA: bovine serum albumin

2.2.2 The Bicinchoninic Acid (BCA) Protein Assay

Protein concentrations were determined by using BCA protein assay kit (Pierce, Rockford, IL). Duplicate aliquots (5 μl) of cell lysates were transferred to a 96-well microplate. To each well, 200 μl of BCA reagent [a mixture (50:1) of BCA reagent A (BCA solution) and reagent B ($CuSO_4 \cdot 5H_2O$)] was added and incubated at 37^{o}C for 30 min. The absorbance was then measured at 562 nm using a SPECTRAmax 340PC microplate spectrophotometer (Molecular Devices, CA, USA). Protein concentrations were determined using a standard curve generated from BSA.

2.2.3 Transfection

CHO cells in 6-well plates and 10 cm dishes were grown in medium A (without antibiotics) and transfected the following day using Lipofectamine LTX reagent (Invitrogen) according to the manufacturer's instructions, using a ratio of 1 μg of DNA: 4 μl of transfection reagent. DNA was equalized with empty vector between different conditions. Following 24 hr transfection, cells were statin pretreated overnight, and then treated as indicated in the respective figure legends.

2.2.4 Western Blotting

During harvest, after rinsing once with 1X PBS, cells were lyzed in 100 μl 10% (w/v) SDS with 5 μl protease inhibitor cocktail. Lysates were passed through 18G needles, and were vortexed vigorously for 20 min at room temperature. After equalizing protein concentrations using the BCA assay (Section 2.2.2), samples (usually 40 μg of protein) were analyzed by 10% SDS-PAGE, and transferred onto nitrocellulose membrane. The membrane was then incubated in blocking solution [5% (w/v) skim milk, 0.1% (v/v) Tween-20 in 1X PBS] for 1 hr. After incubating the membrane in the appropriate primary antibody (1 hr or overnight at 4^{o}C) and secondary antibody (1 hr), it was washed thrice for 10 min in 1X PBST [0.1% (v/v) Tween-20 in 1X PBS]. After the washes, the membrane was incubated in enhanced chemiluminescent (ECL) substrate for 1 min, followed by exposure to Hyperfilm ECL, and processing with developer and fixer. The antibodies used and the immunoblotting specifications are listed in Table 2.3. The diluent was either 5% BSA or 5% skim milk made up in 1X PBST.

Table 2.3 Specifications of the antibodies used

Antibody	Company	Primary dilution and diluent	Secondary dilution and diluent
Anti-V5	Invitrogen	1:10 000 5% skim milk	1:20 000 (mouse) 5% skim milk
Anti-Myc	Invitrogen	1: 10 000 5% skim milk	1:20 000 (mouse) 5% skim milk
Anti-SM	Protein Tech	1:5 000 5% BSA	1:20 000 (rabbit) 5% skim milk
Anti-HA	Covance	1:10 000 5% BSA	1:20 000 (mouse) 5% BSA
Anti-α-tubulin	Sigma-Aldrich	1:200 000 5% BSA	1:20 000 (rabbit) 5% BSA

The observed protein bands migrated according to their calculated molecular weight: 64 kDa for SM, 78 kDa for OSC, and 50 kDa for α-tubulin. Digital images were scanned with a resolution of 1 200 dpi in greyscale (Hewlett-Packard). The relative intensities of bands were quantified by densitometry using ImageJ Software (1.36b).

2.2.5 Lipid Extraction and Thin Layer Chromatography

Following statin pretreatment, cells were metabolically labeled with 1 µCi/well [^{14}C]-acetate or [^{14}C]-mevalonate added to the existing media for the last 2 or 4 hr of treatment, as indicated in the respective figure legends. Cells were washed once with PBS, lyzed in 500 µl 0.1 M NaOH, and rinsed with 1.25 ml H_2O. Protein concentrations were measured using the BCA assay method (Section 2.2.2). Lysates were saponified with 500 µl 20% KOH (w/v) in methanol, butylated hydroxytoluene (1 µl, 20 mM), and EDTA (20 µl, 20 mM) at 70ºC for 1 hr. After cooling, the lipids were extracted with 2 ml hexane and evaporated to dryness. Extracts were re-dissolved in 60 µl hexane, and aliquots corresponding to equivalent amounts of

protein separated on Silica Gel 60 F_{254} plates (Merck, Whitehouse Station, NJ) with a mobile phase of hexane: diethyl ether: glacial acetic acid (60:40:1, v/v/v). Bands corresponding to cholesterol, 24(*S*),25-epoxycholesterol, MOS, and squalene were visualized using the FLA-5100 phosphorimager (Fujifilm, Tokyo, Japan). The relative intensities of bands were quantified using Sciencelab ImageGauge 4.0 Software (Fujifilm).

2.2.5.1 Argentation TLC (Chapter 6)

Cells were then lysed in 500 µl 0.1 M NaOH and protein concentrations measured using the BCA assay. Lysates were saponified with 1 ml ethanol, 500 µl 75% (w/v) KOH in H_2O, 1 µl 20 mM butylated hydroxyltoluene, and 20 µl 20 mM EDTA at 70ºC for 1 h. After cooling, non-saponifiable lipids were extracted into 2.5 ml hexane and evaporated to dryness. Lipid extracts were re-dissolved in 60 µl hexane, and aliquots corresponding to equivalent amounts of protein were separated by Arg-TLC using 4% (w/v) silver-coated Silica Gel 60 F_{254} plates with a mobile phase of heptane:ethyl acetate (2:1, v/v), run four times. Bands corresponding to cholesterol and desmosterol were visualized using the FLA-5100 phosphorimager (Fujifilm, Tokyo, Japan). The relative intensities of bands were quantified using Sciencelab ImageGauge 4.0 Software (Fujifilm).

2.2.6 Quantitative Real-Time PCR

Gene expression levels for *SQLE* and *HMGCR* were determined using quantitative Real-Time PCR (qRT-PCR). The extracted RNA was reverse transcribed into cDNA. qRT-PCR was performed using SYBR green to determine amplification of specific gene products.

2.2.6.1 RNA Extraction

Cells seeded in 12-well plates were washed twice using cold 1X PBS and harvested for isolating total RNA. Cells were lyzed using 500 µl of TRIzol reagent, transferred into 1.5ml microfuge tubes, and 50 µl 1-Bromo-3-chloro-propane was added. Samples were vigorously shaken and left for 7-10 min at room temperature. Following centrifugation (16 000 x g, 4°C, 20 min), the top aqueous layer

containing total RNA (clear) was transferred into a separate 1.5 ml microfuge tube. To precipitate the RNA, an equal volume of isopropanol was added to each sample, mixed by inversion and stored overnight at -20°C. The next day, samples were centrifuged (16 000 x g, 4°C, 20 min) to pellet the RNA. The supernatant (isopropanol) was discarded and the RNA pellet was washed with 500 µl of 70% (v/v) ethanol. Samples were then centrifuged (16 000 x g, 4°C, 5 min) again, the supernatant was removed, and the RNA pellet was air-dried for 10-15 min. The RNA pellets were then resuspended in 15-20 µl of DEPC nuclease-free water. The total RNA concentrations were measured using the Nanodrop ND-100 Spectrophotometer, Biolab.

2.2.6.2 Reverse-Transcriptase Polymerase Chain Reaction

To reverse transcribe the RNA into cDNA using the SuperScript III reverse transcriptase kit, 1 µg RNA was prepared in 10 µl DEPC water, and 1 µl 50 µM oligo dT primer and 1 µl 10 mM dNTP mix were added to the PCR tubes. This mixture was heated at 65^{o}C for 5 min to remove secondary structures, and then immediately transferred onto ice.

To these reactions, 2 µl 10x RT buffer, 2 µl 0.1M DTT, 4 µl of 50 mM $MgCl_2$, 1 µl RNase OUT, and 1 µl SuperScript III RT enzyme were added. These reactions were then incubated at 42°C for 50 min for the process of reverse transcription, and then heated at 72°C for 15 min to deactivate the enzyme. For each experiment, one reaction was left without SuperScript III RT enzyme to serve as a negative control. After completion, the cDNA samples were then used as template for PCR amplification.

2.2.6.3 Quantitative Real-Time PCR

Primers used for amplification are listed below in Table 2.4. Each amplification mixture contained 1 µl cDNA and 19 µl of reaction mixture containing the following: 10 µl 2x SensiMix dT, 0.4 µl SYBR Green, 0.4 µl 10 µM forward gene-specific primer, 0.4 µl 10 µM reverse gene-specific primer. And 7.8 µl Sterile water. Reactions were carried out in Corbett Rotorgene 3000, using the following thermocycling parameters: 95°C for 10 min, 32 cycles of 95°C for 15 seconds, and a primer temperature of 56°C for 60 seconds.

Melting curve analysis using Rotor Gene 6 was performed to confirm production of a single product for each reaction. Gene expression levels were determined by normalizing mRNA levels of the gene of interest to the mRNA levels of the housekeeping gene, porphobilinogen deaminase (*Pbgd*) (Kielar et al., 2001). Values were expressed relative to the vehicle-treated control, which was set to 1.

Table 2.4 Primer sequences for quantitative real-time PCR analysis

Gene	Direction	Primer Sequence (5'-3')	Reference
SQLE **(hamster)**	Forward	TCTGATACACGGCTACATAG	(Gill et al., 2011)
	Reverse	ACTTGCCATGGTGGAAAGCAA	
HMGCR **(hamster)**	Forward	CTGGTGATGGGAGCTTGCTGTG	(Du et al., 2006)
	Reverse	AATCACAAGCACGAGGAAGACG	
Pbgd **(mouse)**	Forward	AGATTCTTGATACTGCACTC	(Wong et al., 2006)
	Reverse	TGAAAGACAACAGCATCACA	

2.2.7 Cholesterol Mass Determination

Cells were washed with cold 1X PBS, harvested in RIPA buffer (50 mM NaCl, 1.0% IGEPAL CA-630, 0.5% sodium deoxycholate, 0.1% SDS, 200 mM Tris, pH 8.0) and passed through an 18G needle 20 times. Total cellular cholesterol content was determined using the Amplex Red Cholesterol assay kit (Invitrogen), according to the manufacturer's instructions (with an Fmax microplate spectrofluorometer (Molecular Devices, CA), excitation λ = 544 nm, emission λ = 590 nm), and expressed relative to protein (measured by the BCA assay, Section 2.2.2).

2.2.8 Ubiquitination assays for Human SM

Following transfection and treatment (as indicated in the figure legends), CHO-7 cells were harvested by washing twice with cold 1X PBS. Cells were then scraped in 1X PBS, transferred to a 50 ml tube, and centrifuged at 1000 g for 5 min. After

discarding the supernatant, the pellet (lysate) was resuspended in 500 µl RIPA buffer (described above) supplemented with N-ethylmaleimide (10 mM), protease inhibitor cocktail and ALLN (25 µg/ml), and lyzed by passing through an 18G needle 50-60 times.

2.2.8.1 Immunoprecipitation

Lysates were immunoprecipitated with monoclonal anti-V5-conjugated Dynabeads (Invitrogen), according to the manufacturer's instructions, with some modifications. Dynabeads (80 µl/500 µg protein) were prepared by washing three times (5 min each) with RIPA buffer. Fresh RIPA buffer (250 µl) was then added to the tube containing the beads, followed by 2 µg anti-V5 antibody (2 µg), and the antibody-beads mixture was allowed to rotate overnight at 4^{o}C. The next day, the microfuge tubes were placed on the magnetic stand and the supernatant (RIPA buffer) was removed. Lysates with equal cell protein (standardized using the BCA assay) were added to the antibody-beads mixture. These were then rotated for 4 h at 4^{o}C. The supernatant was then collected and stored for analyze the efficiency of the IP, and the pellets (antibody-beads-protein of interest) mixture were washed three times for 30 min each. After the final wash, supernatant was discarded, the pellets were resuspended in 50 µl modified loading buffer (2 volumes RIPA buffer + 2 volumes 10% SDS + 1 volume fresh 5X Laemmli Buffer/β-mercaptoethanol), and boiled for 5-10 min at 95^{o}C. Pellets were subjected to 7.5% SDS-PAGE, followed by immunoblot analysis with anti-V5 (for SM) and anti-HA (for ubiquitin) antibodies.

2.2.8.2 GST Pulldown Assay

Pull-down of the N100-GST fusion protein was achieved using glutathione sepharose beads. The beads (80 µl/500 µg protein) were prepared by adding 500 µl RIPA buffer, rotating for 2 min, and then centrifuging at 16 000 g for 1 min. This was repeated 3 times. After the final wash, the supernatant was replaced with the lysates with equal cell protein (standardized using the BCA assay). These were then rotated overnight at 4^{o}C. The next day, samples were centrifuged at 16 000 g for 5 min, and the supernatant was collected for analysis of the pulldown. The pellets (GST beads-protein of interest) were then resuspended in 1 ml RIPA buffer and allowed to rotate at 4^{o}C for 1 hr after which they were centrifuged at 16 000 g for 5

min. This step was repeated twice, however, pellets were allowed to rotate for 30 min instead. After the final wash, the supernatant was discarded, the pellets were resuspended in 50 μl modified loading buffer (2 volumes RIPA buffer + 2 volumes 10% SDS + 1 volume fresh 5X Laemmli Buffer/β-mercaptoethanol), and boiled for 10 min at 95^{o}C with occasional vortexing. Pellets were subjected to 7.5% SDS-PAGE, followed by Immunoblot analysis with anti-V5 (for SM) and anti-HA (for ubiquitin) antibodies.

2.2.9 Metabolic Labeling of N100-GST with [^{35}S]-Methionine/Cysteine

CHO-7 cells were transiently transfected as indicated in the figure legend. After statin pretreatment, cells were labeled in methionine-free medium (Invitrogen) supplemented with 5 μM compactin and 50 μM mevalonate containing 250 μCi/ml [^{35}S]-Protein Labeling Mix (Perkin Elmer) for 3 hr, then washed and chased in medium B containing 2 mM methionine and cysteine with or without Chol/CD, for 0-8 h. [^{35}S]-labeled N100-GST was pulled down from lysates with equal cell protein using glutathione sepharose beads, and pellets were subjected to 4-20% or 10% SDS-PAGE. Bands were visualized by phosphorimaging, and their relative intensities were quantified using Sciencelab ImageGauge 4.0 Software (Fujifilm).

2.2.10 Generation of pCMV-SM-Myc Construct

2.2.10.1 Subcloning

Subcloning was performed by amplifying the vector (pCMV-myc) and insert (human *SQLE*) by setting up the following reaction (total volume 25 μl):
1 ng DNA, 5 μl 5X iProof High Fidelity Buffer, 1 μl 10 mM dNTPs, 0.5 μl DMSO, 1.25 μl 10 μM forward primer, 1.25 μl 10 μM reverse primer, and 0.5U iProof enzyme. The cycling conditions were 98^{o}C for 30 seconds, followed by 98^{o}C for 10 seconds, 53^{o}C for 30 seconds, and 72^{o}C for 2.5 minutes, then a final extension at 72^{o}C for 10 minutes. The a small amount of the PCR products were visualized on a agarose gel using ethidium bromide, and compared to 100 bp and 1 kb markers. The remainder PCR products were purified using PCR Purification Kit (Qiagen) according to manufacturers instructions, and DNA concentration was determined by

NanoDrop.

Restriction digests were performed at 37^{o}C for 1-4 hr. The reaction contained ~ 1 μg DNA, 2 μl 10X NEB reaction buffer, 2 μg BSA, and 5 U restriction enzyme (BamH1 and Not1) in a total volume of 20 μl. Following digestion, gel extraction was performed to get rid of observed non-specific products using the Gel Extraction Kit (Qiagen) according to manufacturers instructions. DNA concentrations were determined by NanoDrop.

Ligation reactions were setup using ~ 50 ng DNA, and the vector: insert ratios used were 1:3 and 1:5. A vector only control was also prepared. The reaction was setup using 2 μl 10X ligase buffer, and 2.5 U T4 ligase. Ligations were done overnight at 4^{o}C.

2.2.10.2 Transformation

The ligation product was transformed into DH5α (competent *E.coli* cells) by mixing 5 μl ligation product with 25 μl of the competent cells. The mixture was then incubated on ice for 30 min, followed by heat shocking at 37^{o}C for 20 seconds, and then back on ice for 2 min. To this mixture, 475 μl SOC medium was added, and the microfuge tube containing the cells was put on an orbital shaker for 1 hr at 37^{o}C. This was then streaked onto Luria-Bertani (LB) containing 100 μg/ml ampicillin agar plates, and the plates were incubated overnight at 37^{0}C. The next day, one colony was selected to grow in 3 ml Lb/amp broth overnight at 37^{o}C on the orbital shaker. The following day, plasmid DNA was purified using Plasmid Mini Prep Kit (Qiagen) according to manufacturer's instructions. After determining the DNA concentration by NanoDrop, another restriction digest was done to confirm that the gene of interest (human *SQLE*) was correctly inserted into the vector, and sequencing was also performed.

2.2.10.3 Sequencing

Sequencing reactions were setup containing the following (final volume 20 μl):
~200-300 μg DNA, 3.2 pmoles primer, 4 μl 5X BigDye v3.1 sequencing buffer, 1 μl BigDye v3.1, and 1 μl DMSO. The sequencing reaction consisted of a cycle of 96^{o}C for 10 seconds, 50^{o}C for 5 seconds, 60^{o}C for 4 min, repeated for 25 cycles. 5 μl 125

mM EDTA and 60 µl absolute ethanol were added to clean up the product, and the mixture was incubated for 45 min at room temperature. After centrifuging the mixture at 16 200 g for 20 min at 4^{o}C, the supernatant was discarded, 250 µl 70% ethanol was added, and the mixture was centrifuged at 16 200 g again for 10 min. The pellet was then air-dried, and sequencing was performed by The Ramaciotti Centre for Gene Function Analysis, UNSW (Sydney, Australia). After checking the sequence for appropriate in-frame insertion of the gene (human *SQLE*), the plasmid was transformed into DH5α (Section 2.2.10.2), and was maxi-prepped using Qiagen's HiSpeed Maxi Kit according to manufacturer's instructions. Concentration of the purified plasmid DNA was determined using Biolab NanoDrop ND 1000.

2.2.10.3 Generation of SM Overexpressing Cells

CHO-7 cells were transfected with pCMV-SM-myc (1 µg) for 24 hr using Lipofectamine LTX transfection reagent (4 µl/well in a 6 well plate) and stable transfectants were selected for zeocin (500 µg/ml) resistance. Pure clones were obtained by limiting dilution, and were screened for SM-myc expression by Western blotting. The SM overexpressing stable cells were characterized by qRT-PCR (SM expression levels) and TLC (cholesterol, squalene, and 24,25EC synthesis).

2.2.11 Data Presentation

Unless otherwise indicated, values are normalized to the vehicle-treated control condition. Quantitative data are presented as averages and all error bars are SEM. The data are representative of at least n=2 separate experiments, unless otherwise stated in the figure legends.

CHAPTER 3

CHOLESTEROL-DEPENDENT ACCUMULATION OF SQUALENE

3. CHOLESTEROL-DEPENDENT ACCUMULATION OF SQUALENE

3.1 INTRODUCTION

Cholesterol is a vital lipid in animals, but can be toxic in excess. Consequently, elaborate homeostatic mechanisms have evolved, with exquisite control of cholesterol levels occurring at multiple points within the cell (Goldstein et al., 2006a). Research into the regulation of cholesterol synthesis has centered on 3-hydroxy-3-methylglutaryl-coenzyme A reductase (HMGR). It catalyzes a major 'rate-limiting' step or control point in cholesterol synthesis (Rodwell et al., 1976), yielding mevalonate, and is the target of the statin class of drugs to treat hypercholesterolemia. In contrast, relatively little is known about the regulatory role and control of other enzymes in the pathway, besides most being known SREBP-2 target genes (Horton et al., 2003).

One such enzyme is squalene monooxygenase (SM), formerly squalene epoxidase (EC 1.14.99.7). SM is a microsomal flavin monooxygenase (Yamamoto and Bloch, 1970) that catalyzes the first oxygenation step in cholesterol synthesis, the conversion of squalene to the non-sterol precursor for lanosterol, 2,3(*S*)-monooxidosqualene (MOS). SM is important clinically as the target of fungicides such as terbinafine (Chugh et al., 2003). In addition, a number of natural compounds proposed to reduce serum cholesterol levels in humans also inhibit this enzyme, such as polyphenols in green tea, resveratrol in wine, and garlic extract (Abe et al., 2000; Gupta and Porter, 2001).

Although not widely appreciated, SM has been proposed to be a second rate-limiting enzyme in cholesterol synthesis (Gonzalez et al., 1979; Hidaka et al., 1990). The precursor squalene accumulates when Chinese hamster ovary (CHO) cells (Eilenberg and Shechter, 1984), human fibroblasts (Brown and Goldstein, 1980), rat hepatoma cells and renal carcinoma cells (Gonzalez et al., 1979) are incubated with radiolabeled mevalonate and exogenous sterols. Similar accumulation has also been observed using rat and dog kidney slices (Raskin and Siperstein, 1974).

Like HMGR, SM is also an SREBP-2 target, and its expression is modulated by sterols at the transcriptional level, increasing under lipid depleted conditions (Hidaka et al., 1990). We hypothesized that in addition to regulating SM at a transcriptional level, cholesterol also plays a role in the post-transcriptional regulation of SM, causing squalene to accumulate. In this chapter, the specific aims are as follows:

a. **To document the cholesterol-dependent accumulation of squalene in various cell-types**
b. **To determine whether the cholesterol mediated accumulation of squalene occurs at the post-transcriptional level**

The evidence provided here strengthens the argument that SM is a second rate-limiting enzyme in the cholesterol synthesis pathway.

3.2 MATERIALS AND METHODS

Detailed lists of materials and methods are given in Chapter 2. The specific reagents and materials used for this chapter are given below.

3.2.1 Materials

TRIzol Reagent, and SuperScript III First Strand cDNA Synthesis Kit were purchased from Invitrogen (Carlsbad, CA). [1-^{14}C]-acetic acid sodium salt (specific radioactivity: 56 mCi/mmol) was purchased from GE Healthcare (Chalfont St. Giles, UK). Butylated hydroxytoluene, compactin (also called mevastatin), Dulbecco's phosphate buffered saline (PBS), methyl-β-cyclodextrin, mevalonate, primers, protease inhibitor cocktail, squalene synthase inhibitor (SSi), and sodium dodecyl sulphate (SDS), were obtained from Sigma (St. Louis, MO). The squalene epoxidase inhibitor, GR144000X (squalene monooxygenase inhibitor, SMi) was kindly donated by Glaxo-Smith Kline (Middlesex, UK). SYBR Green SensiMix dT was from Quantace (Norwood, MA).

3.2.2 Methods

3.2.2.1 Cell Culture

All cells were maintained in monolayer at 37°C in 5% CO_2. Cells were seeded at the following densities: 1×10^5 cells/well in triplicate in 12-well plates for quantitative Real-Time PCR, and 2×10^5 cells/well in 6-well plates for Thin Layer Chromatography. CHO-7 and SRD-1 cells were maintained in medium A, HepG2 cells in medium D, and BE(2)C, HEK293, and fibroblasts in medium G. Unless otherwise stated, cells were statin pretreated in media containing 5 μM statin (compactin) and 50 μM mevalonate overnight (CHO-7 and SRD-1cells in medium B, HepG2 cells in medium F, and BE(2)C, HEK293, and fibroblasts in medium I). Cells were then treated with test agents (added in ethanol or dimethylsulfoxide to refreshed media) as indicated in the figure legends. Within an experiment, the final concentrations of solvents were kept constant between conditions and did not exceed 0.28 % (v/v).

3.2.2.2 Lipid Extraction and Thin Layer Chromatography

Following statin pretreatment, cells were metabolically labeled with 1 µCi/well [^{14}C]-acetate added to the existing media for the last 2 or 4 hr of treatment, as indicated in the respective figure legends. Cells were washed once with PBS, lyzed in 500 µl 0.1 M NaOH, and rinsed with 1.25 ml H_2O. Protein concentrations were measured using the BCA assay method (Chapter 2, Section 2.2.2). Lysates were saponified with 500 µl 20% KOH (w/v) in methanol, butylated hydroxytoluene (1 µl, 20 mM), and EDTA (20 µl, 20 mM) at 70ºC for 1 hr. After cooling, the lipids were extracted with 2 ml hexane and evaporated to dryness. Extracts were re-dissolved in 60 µl hexane, and aliquots corresponding to equivalent amounts of protein separated on Silica Gel 60 F_{254} plates (Merck, Whitehouse Station, NJ) with a mobile phase of hexane: diethyl ether: glacial acetic acid (60:40:1, v/v/v). Bands corresponding to cholesterol and squalene (with relative R_f values of ~0.4 and ~0.9, respectively) were visualized using the FLA-5100 phosphorimager (Fujifilm, Tokyo, Japan). The relative intensities of bands were quantified using Sciencelab ImageGauge 4.0 Software (Fujifilm).

3.2.2.3 Quantitative Real-Time PCR

As described in Chapter 2 (Section 2.2.6), RNA was harvested in triplicate using TRIzol reagent, reverse transcribed to yield cDNA using the SuperScript III First Strand cDNA Synthesis kit (Invitrogen), and mRNA levels determined relative to the housekeeping gene by quantitative real-time PCR using SYBR Green and a Corbett Rotorgene 3000. Primers were directed against SM (*SQLE*) and HMGR (*HMGCR*), with porphobilinogen deaminase (*Pbgd*) as the housekeeping gene (refer to Chapter 2, Table 2.4). Values were expressed relative to the vehicle-treated control, which was set to 1.

3.3 RESULTS

3.3.1 Cholesterol treatment causes squalene to accumulate

A key observation that highlights the rate-limiting activity of SM is squalene accumulation when cholesterol levels are high (Brown and Goldstein, 1980; Eilenberg and Shechter, 1984; Gonzalez et al., 1979). These experiments were conducted using radiolabeled mevalonate, consequently bypassing HMGR. We labeled CHO-7 cells for 4 hr with [^{14}C]-acetate which feeds into the beginning of the cholesterol biosynthetic pathway. CHO-7 cells were chosen because they can be maintained in lipoprotein-deficient serum (LPDS) (Click and Balian, 1985), which offers considerable flexibility in manipulating cholesterol levels. Importantly, we found that treatment of CHO-7 cells with sterols and [^{14}C]-acetate also led to the accumulation of [^{14}C]-squalene (Figure 1A). This band was validated to be squalene since it was absent upon inhibition of squalene synthase (Figure 3.1A, lane 1), and accumulated when SM was inhibited (Figure 3.1A, lane 2). The most striking squalene accumulation resulted from addition of cholesterol complexed with methyl-β-cyclodextrin (Chol/CD) (Figure 3.1A, lane 5), followed by low-density lipoprotein (LDL) (Figure 3.1A, lane 4), and then the oxysterol 25-hydroxycholesterol (25HC) (Figure 3.1A, lane 6). Thus in this system, cholesterol treatment induces squalene accumulation, raising the possibility of a rate-limiting step after HMGR, involving SM.

Experiments examining cholesterol homeostasis commonly use statin pretreatment, which reduces cellular cholesterol status and increases the expression of cholesterogenic genes such as HMGR [For example (Wong et al., 2008)]. Under these conditions, HMGR activity may be increased sufficiently such that it is no longer rate-limiting, producing a bottleneck downstream at SM. To address this possibility, we tested the above conditions with and without statin pretreatment. Squalene accumulation was also observed without statin pretreatment (Figure 3.1B), that is, whether or not HMGR was first inhibited.

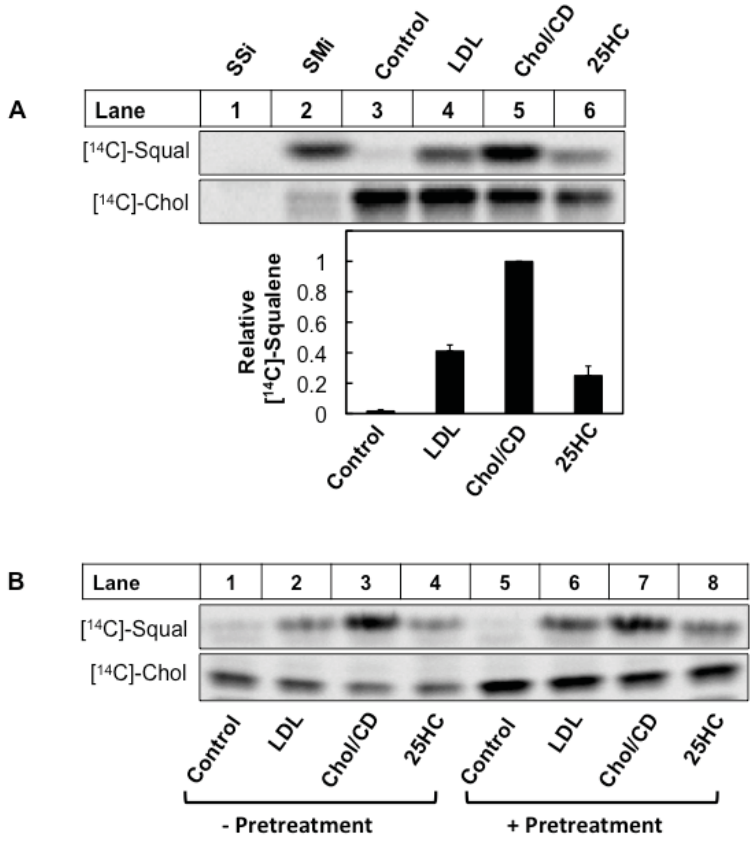

Figure 3.1 Sterol induced squalene accumulation in CHO-7 cells

(A) CHO-7 cells were statin pretreated overnight in medium B and the next day were treated and labeled with [^{14}C]-acetate in medium A with the following test agents for 4 hr: squalene synthase inhibitor (SSi, 150 μM), SM inhibitor (SMi, 10 μM), LDL (50 μg/ml), cholesterol complexed with methyl-β-cyclodextrin (Chol/CD, 20 μg/ml), or 25-hydroxycholesterol (25HC, 1 μg/ml). [^{14}C]-Squalene accumulation was expressed relative to the maximal condition (Chol/CD), which was set to 1 (n=5, +SEM). **(B)** CHO-7 cells were statin pretreated or not as indicated and then treated in medium A with 50 μg/ml LDL, 20 μg/ml Chol/CD, or 1 μg/ml 25HC and labeled with [^{14}C]-acetate for 4 hr. Bands corresponding to cholesterol and squalene were visualized by phosphorimaging and the image shown is representative of at least 2 separate experiments.

Furthermore, acute cholesterol treatments (Chol/CD and LDL) were repeated for CHO-7 cells maintained in full serum without statin pretreatment (Figure 3.2A and B). Squalene accumulated markedly when cells were grown in full serum (Figure 3.2A and B, lane 4), albeit to a lesser extent than seen for LPDS (Figure 3.2A and B, lane 2).

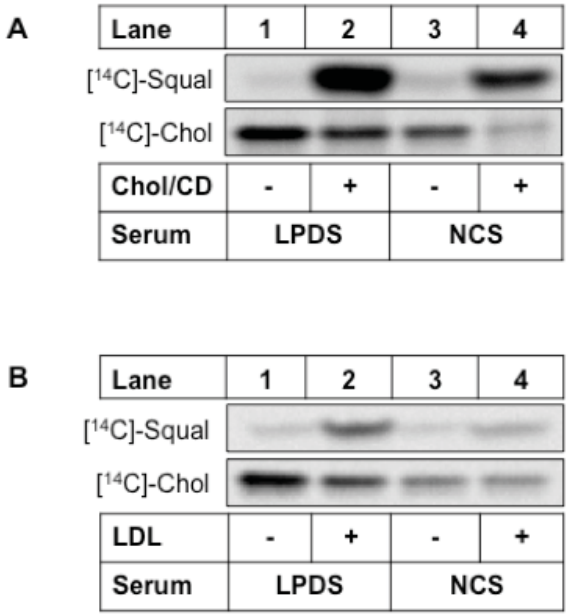

Figure 3.2 Squalene accumulates in a cholesterol dependent manner in CHO-7 cells grown in full serum

After 16 hr of growth in either LPDS (medium A) or NCS (medium C) without statin pretreatment, CHO-7 cells were labeled with [^{14}C]-acetate, and treated for 4 hr with or without **(A)** Chol/CD (20 μg/ml) or **(B)** LDL (50 μg/ml), and assayed for [^{14}C]-cholesterol and [^{14}C]-squalene accumulation. Representative phosphorimages are shown for n=2 experiments for each.

Moreover, if cholesterol treatment were to inactivate HMGR faster than SM, then accumulation of squalene (occurring after HMGR) would not be observed. However, cholesterol treatment caused squalene to accumulate under a variety of culturing conditions (Figures 3.1 and 3.2), suggesting that altered activity of earlier enzymes in the pathway, such as HMGR, is insufficient to explain the squalene accumulation.

Additionally, this effect is not restricted to CHO-7 cells (Figure 3.3): a cholesterol-dependent increase in squalene accumulation was also seen in human cell-lines of hepatic (HepG2), neuronal (BE(2)C), and renal origin (HEK293), as well as in primary human fibroblasts (Fb).

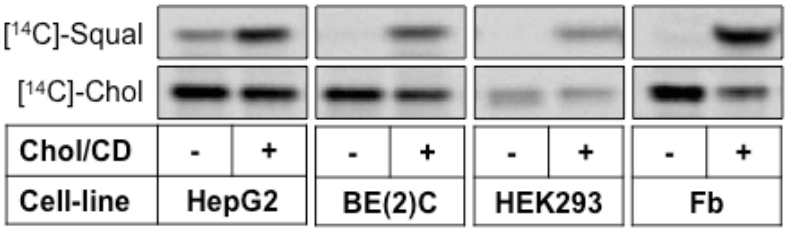

Figure 3.3 Cholesterol-dependent squalene accumulation is observed in cells of human origin

After overnight statin pretreatment, cells in medium E (HepG2) or medium H [BE(2)C, HEK293, and fibroblasts (Fb)] were labeled with [^{14}C]-acetate, and treated with or without Chol/CD (20 μg/ml) for 4 hr, and assayed for [^{14}C]-cholesterol and [^{14}C]-squalene accumulation. Representative phosphorimages are shown for n=2 experiments.

3.3.2 Cholesterol-dependent squalene accumulation over time

When examined over time, cholesterol treatment led to the progressive accumulation of squalene and decreased *de novo* cholesterol synthesis (Figure 3.4), most notably after 4 hr (lane 5), but also as early as 2 hr (lane 3). In the absence of exogenous cholesterol, the levels of newly synthesized cholesterol were relatively constant at all time points, with no observed squalene. These results suggest that SM becomes rate-limiting due to an acute cholesterol-dependent regulatory mechanism.

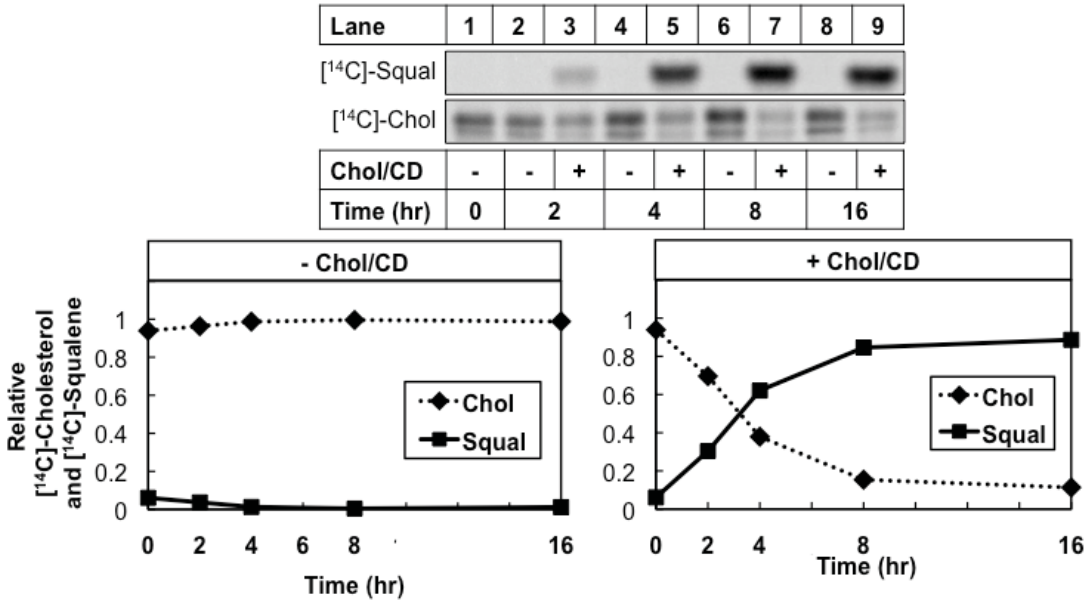

Figure 3.4 Cholesterol-dependent squalene accumulation over 16 hr

CHO-7 cells were statin pretreated overnight, and the following day were treated in medium B with or without Chol/CD (20 μg/ml) as indicated, labeled with [^{14}C]-acetate in medium A during treatment 2 hr prior to harvesting, and then assayed for [^{14}C]-cholesterol and [^{14}C]-squalene accumulation. Relative accumulation was calculated so that [^{14}C]-squalene + [^{14}C]-cholesterol = 1 at each time point. Error bars (±SEM) are contained within the symbols (representative of n=6 separate experiments).

3.3.3 Cholesterol-dependent post-transcriptional regulation of SM

To uncover this mechanism, we first examined transcriptional regulation using quantitative (real-time) PCR, and compared the mRNA levels of *SQLE* (SM) to that of *HMGCR* (HMGR). In the absence of added cholesterol, the mRNA levels of both genes were constant and remained unaffected over 16 hr (Figure 3.5). The addition of cholesterol caused a decrease in expression levels of both genes with similar kinetics and magnitude. Therefore, there is a dissociation of mRNA levels from flux through the pathway, suggesting post-transcriptional regulation of SM.

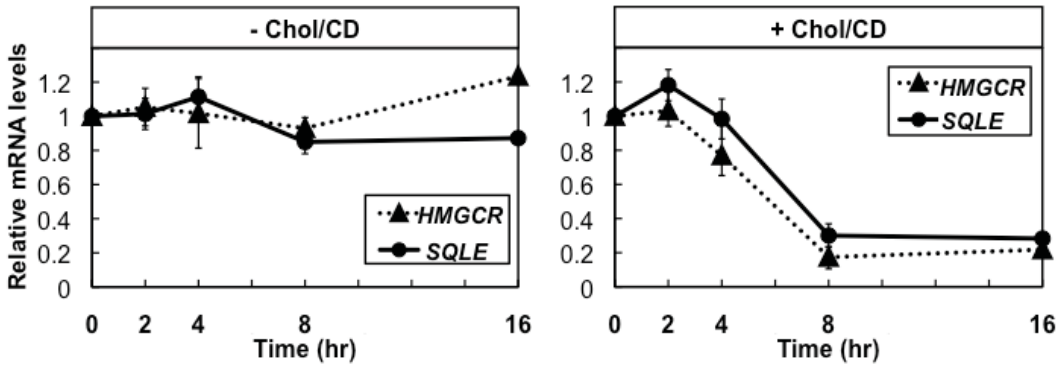

Figure 3.5 Cholesterol decreases mRNA levels of HMGCR and SQLE at a similar rate

CHO-7 cells were statin pretreated overnight in medium B, and the following day were treated in medium B with or without Chol/CD (20 μg/ml) as indicated and mRNA levels for hamster *SQLE* (SM) and *HMGCR* (HMGR) determined by quantitative Real-Time PCR. The values are normalized to the control condition which was set to 1, and are ± SEM (n=3, each performed in triplicate).

To exclude transcriptional regulation, we utilized SRD-1 cells, a mutant line of CHO cells which exhibit sterol-independent expression of SREBP-2 target genes (Yang et al., 1994). These cells overexpress a truncated form of SREBP-2, bypassing the sterol-regulated proteolytic step, leading to constant transcriptional activation independent of sterol levels. Therefore in the SRD-1 cells, mRNA levels of *HMGCR* and *SQLE* were similarly unaffected by cholesterol addition (Figure 3.6).

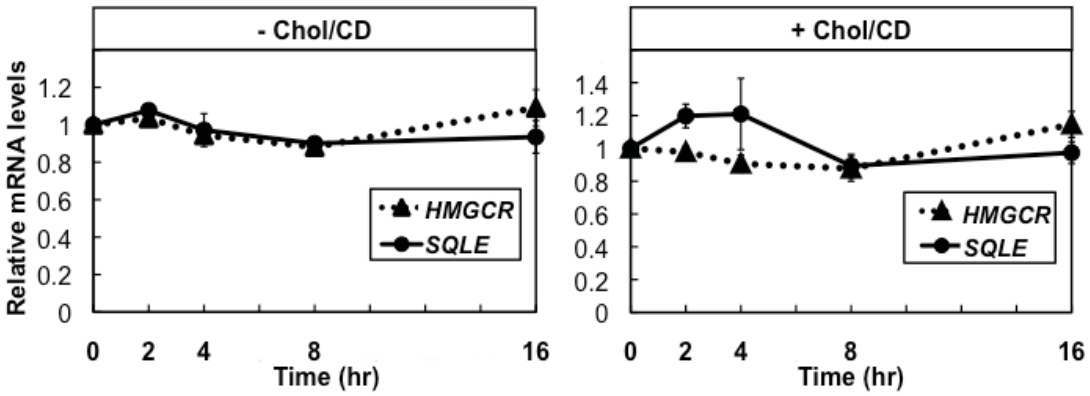

Figure 3.6 mRNA levels of HMGCR and SQLE remain unaffected by the addition of cholesterol in the mutant SRD-1 cells

SRD-1 cells were statin pretreated overnight in medium B, and the following day were treated in medium B with or without Chol/CD (20 μg/ml) as indicated and mRNA levels for hamster *SQLE* (SM) and *HMGCR* (HMGR) determined by quantitative Real-Time PCR. The values are normalized to the control condition which was set to 1, and are ± SEM (n=3, each performed in triplicate).

Despite lack of transcriptional regulation, cholesterol-dependent squalene accumulation was still evident in SRD-1 cells (Figure 3.7). A considerable amount of squalene was observed even without cholesterol treatment because the SRD-1 cells have a higher basal level of sterol synthesis. However, cholesterol-dependent squalene accumulation was still observed after 2 hr. Together, this is consistent with SM being post-transcriptionally regulated by cholesterol, which may impact on the control of cholesterol synthesis.

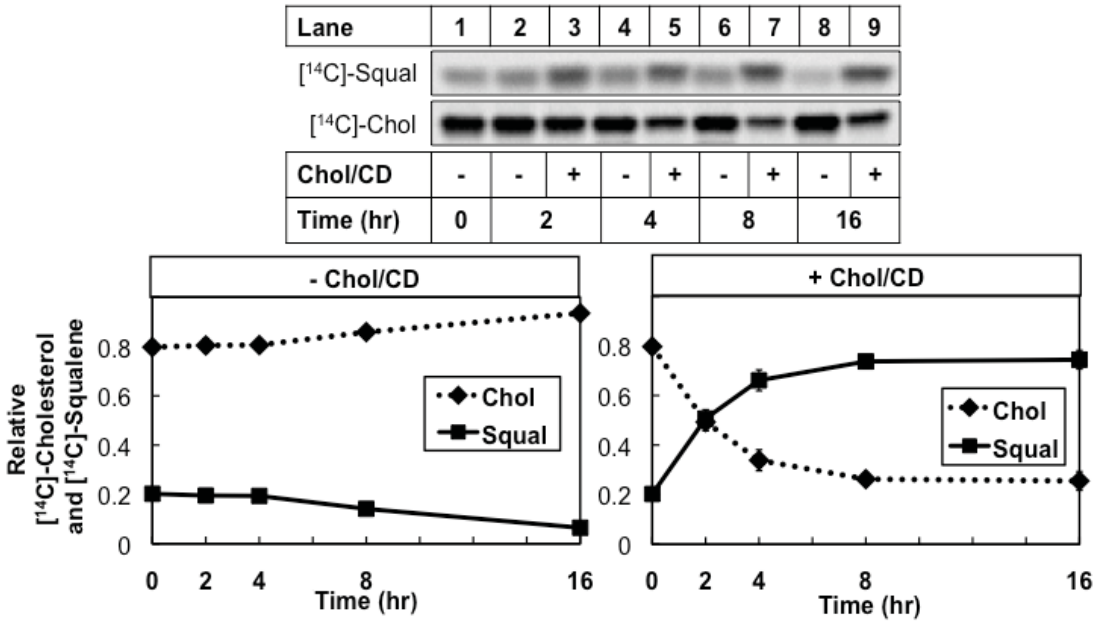

Figure 3.7 Cholesterol treatment causes squalene to accumulate in SRD-1 cells

Cells were statin pretreated overnight in medium B, and the following day were treated in medium B with or without Chol/CD (20 μg/ml) as indicated, labeled with [^{14}C]-acetate in medium A during treatment 2 hr prior to harvesting, and then assayed for [^{14}C]-cholesterol and [^{14}C]-squalene. Relative accumulation was calculated so that [^{14}C]-squalene + [^{14}C]-cholesterol = 1 at each time point. Error bars (±SEM) are contained within the symbols (representative of n=4 separate experiments).

3.4 DISCUSSION

In this chapter, we document the cholesterol-induced accumulation of squalene in CHO-7 cells, and observe this phenomenon in a variety of human hepatic as well as non-hepatic cell-types (Figures 3.1 and 3.3). Using a more physiological setting, this occurs even under full serum conditions and no statin pretreatment, either by Chol/CD or LDL treatment (Figure 3.2). The time taken by cholesterol to reduce mRNA levels of *SQLE* and *HMGCR* was similar, and did not correspond to the accumulation of squalene, which started to occur within 2 hr of cholesterol treatment (Figures 3.4 and 3.5). This hinted at the involvement of another mechanism beyond the transcriptional level. We confirmed this by using mutant cells lacking transcriptional control by SREBP-2 to show that squalene accumulates in the presence of cholesterol (Figure 3.7).

In 1979, Gonzalez and colleagues provided evidence for two major regulatory steps in the cholesterol biosynthesis pathway, the first being HMGR and the other SM (Gonzalez et al., 1979). They showed that in human renal cancer cells exogenous cholesterol not only decreased the activity of HMGR, which was already considered to be a rate-limiting enzyme, but also inhibited the downstream conversion of mevalonate to cholesterol, resulting in the accumulation of squalene. Although the cholesterol-mediated accumulation of squalene has been documented in a number of different studies (Brown and Goldstein, 1980; Eilenberg and Shechter, 1984; Raskin and Siperstein, 1974), the mechanism behind this effect was never explored. Most of these studies utilized radiolabeled mevalonate as a source for cholesterol synthesis, bypassing the first flux-controlling step catalyzed by HMGR. However, we have shown that even when radiolabeled acetate, the first precursor feeding into the cholesterol synthesis pathway is used, squalene accumulates in a cholesterol-enriched environment. This indicates that in the presence of a sufficient amount of cholesterol, SM becomes ‘rate-limiting’ independently of HMGR, causing squalene build-up in cells. Furthermore, the concept that SM may be a largely overlooked control point in cholesterol synthesis is suggested by its much lower specific activity in liver cells compared to that of HMGR (Hidaka et al., 1990). It is also interesting to note that the isoprenoid

squalene is believed to be stable and non-toxic to cells (Chugh et al., 2003), which could potentially imply that higher circulating levels of squalene could be less toxic compared to cholesterol.

In conclusion, we have provided evidence for cholesterol having an acute post-transcriptional effect on SM. In order to further explore the mechanism involved, we postulated that cholesterol could be lowering SM protein levels, in turn causing squalene to accumulate. We investigate the cholesterol-dependent effect on endogenous SM protein as well as in an ectopic system in the following chapter.

CHAPTER 4

POST-TRANSLATIONAL REGULATION OF SQUALENE MONOOXYGENASE

4. POST-TRANSLATIONAL REGULATION OF SQUALENE MONOOXYGENASE

4.1 INTRODUCTION

Sterol regulatory element binding protein-2 (SREBP-2) mediates the transcriptional expression of more than 20 different enzymes involved in cholesterol synthesis (Horton et al., 2003). Of these, extensive research has mostly been done on the regulation of HMGR, the 'rate-limiting' enzyme in cholesterol synthesis (Rodwell et al., 1976). In contrast, even though a number of earlier studies had identified squalene monooxygenase (SM) as a potential second 'rate-limiting' enzyme in the cholesterol synthesis pathway [e.g. (Gonzalez et al., 1979; Hidaka et al., 1990)], the initial key observation of squalene accumulating in a lipid-enriched environment in cells was not pursued further.

Transcriptionally, SM and HMGR are regulated by cholesterol [reviewed in (Horton et al., 2002)]. However, in the previous chapter we provided evidence that the accumulation of squalene observed in cells treated with cholesterol occurs via a mechanism beyond the transcriptional level. Also, from the well-elucidated post-translational regulatory mechanism of HMGR (Jo and DeBose-Boyd, 2010), it can be inferred that the metabolic flux of a pathway depends on changes in activity levels of its regulatory enzymes. Hence, we hypothesized that the presence of sufficient cholesterol in cells destabilizes SM protein levels, causing squalene to accumulate.

Furthermore, other sterols may also play a role in the regulation of cholesterol synthesis. For example, side-chain oxidized sterols such as 25-hydroxycholesterol (25HC), 27-hydroxycholesterol (27HC), and 24(*S*),25-epoxycholesterol (24,25EC) are potent regulators of the SREBP pathway [reviewed in (Gill et al., 2008)], and also induce degradation of HMGR (Song and DeBose-Boyd, 2004). Thus, we also explored the possibility of whether other sterol intermediates in the cholesterol synthesis pathway, and/or oxysterols could be involved in regulating SM.

The specific aims of this chapter are as follows:

a. **Test the effect of cholesterol on endogenous as well as ectopic human SM protein levels**
b. **Identify if other sterols and/or oxysterols affect SM protein levels**

Together, this data should bring us one step closer to uncovering the mechanism behind the cholesterol-dependent accumulation of squalene observed in Chapter 3.

4.2 MATERIALS AND METHODS

Detailed lists of materials and methods are given in Chapter 2. The specific reagents and materials used for this chapter are given below.

4.2.1 Materials

Lipofectamine LTX, Opti-MEM I medium, Amplex Red Cholesterol Assay kit, and anti-V5 antibody were purchased from Invitrogen (Carlsbad, CA). Anti-SQLE (SM) antibody was purchased from Protein Tech Group (Chicago, IL). Peroxidase-conjugated AffiniPure Donkey Anti-Mouse IgG and Peroxidase-conjugated AffiniPure Donkey Anti-Rabbit IgG were obtained from Jackson ImmunoResearch Laboratories (West Grove, PA). Anti-α-tubulin antibody, compactin, cycloheximide, methyl-β-cyclodextrin, mevalonate, and protease inhibitor were obtained from Sigma (St. Louis, MO). 24(*S*),24-Epoxycholesterol (24,25EC) was obtained from Enzo Life Sciences (Farmingdale, NY). Cholesterol, lanosterol, lathosterol, 7-dehydrocholesterol (7DHC), 24,25-dihydrolanosterol (24,25DHL), 7α-hydroxycholesterol (7αHC), 7β-hydroxycholesterol (7βHC), 7-ketocholesterol (7KC), 19-hydroxycholesterol (19HC), 25-hydroxycholesterol (25HC), and 27-hydroxycholesterol (27HC) were obtained from Steraloids (Newport, RI).

4.2.2 Methods

4.2.2.1 Cell Culture

All cells were maintained in monolayer at 37°C in 5% CO_2. Cells were seeded at a density of 2×10^5 cells/well in 6-well plates for all other experiments. CHO-7and SRD-1 cells were maintained in medium A. Unless otherwise stated, cells were statin pretreated in media containing 5 μM statin (compactin) and 50 μM mevalonate overnight (CHO-7 and SRD-1 cells in medium B). Cells were then treated with test agents (added in ethanol or dimethylsulfoxide to refreshed media) as indicated in the figure legends. Within an experiment, the final concentrations of solvent were kept constant between conditions and did not exceed 0.28 % (v/v).

4.2.2.2 Transfection

CHO cells in 6-well plates were grown in medium A (without antibiotics) and transfected the following day using Lipofectamine LTX reagent (Invitrogen) according to the manufacturer's instructions, using a ratio of 1 μg of DNA: 4 μl of transfection reagent. DNA was equalized with empty vector between different conditions. Following 24 hr transfection, cells were statin pretreated overnight, and then treated as indicated in the respective figure legends.

4.2.2.3 Western Blotting

During harvest, after rinsing once with 1X PBS, cells were lyzed in 100 μl 10% (w/v) SDS with 5 μl protease inhibitor cocktail. Lysates were passed through 18G needles, and were vortexed vigorously for 20 min at room temperature. After equalizing protein concentrations using the BCA assay Chapter 2 (Section 2.2.2), samples (usually 40 μg of protein) were analyzed by 10% SDS-PAGE, and transferred onto nitrocellulose membrane. The membrane was then incubated in blocking solution [5% (w/v) skim milk, 0.1% (v/v) Tween-20 in PBS] for 1 hr, and immunoblotted with the following antibodies: anti-V5 (1:10 000), anti-SM (1:5 000), and anti-α-tubulin (1:200 000). The observed protein bands migrated according to their calculated molecular weight: 64 kDa for SM and 50 kDa for α-tubulin. The relative intensities of bands were quantified by densitometry using ImageJ Software (1.36b).

4.2.2.4 Cholesterol Mass Determination

Cells were washed with cold 1X PBS, harvested in RIPA buffer (50 mM NaCl, 1.0% IGEPAL CA-630, 0.5% sodium deoxycholate, 0.1% SDS, 200 mM Tris, pH 8.0) and passed through an 18G needle 20 times. Total cellular cholesterol content was determined using the Amplex Red Cholesterol assay kit (Invitrogen), according to the manufacturer's instructions (with an Fmax microplate spectrofluorometer (Molecular Devices, CA), excitation λ = 544 nm, emission λ = 590 nm), and expressed relative to protein (measured by the BCA assay, Chapter 2, Section 2.2.2).

4.3 RESULTS

4.3.1 Cholesterol-dependent degradation of SM

One explanation for the accumulation of squalene (Chapter 3) is that cholesterol also acts post-translationally, accelerating the degradation of SM. We investigated this possibility independently of SREBP-2 activity using SRD-1 cells. Chol/CD caused a reduction in endogenous SM protein by 4 hr, with negligible levels by 8 hr (Figure 4.1A, lane 7). This effect was not observed when cells were treated with methyl-β-cyclodextrin (CD) without cholesterol (Figure 4.1B, lane 3). A second band (~50 kDa) sometimes evident in the immunoblots of the endogenous protein, likely reflects partial degradation (Sakakibara et al., 1995), but not an intermediate in sterol regulated degradation, since it appears unaffected by cholesterol treatment. Protein synthesis was inhibited with cycloheximide (CHX) during cholesterol treatment, showing that the regulation was post-translational, through degradation of SM. This cholesterol-mediated degradation of SM was on a comparably acute timescale to squalene accumulation (Chapter 3, Figure 3.7). Overall, addition of cholesterol increased SM turnover several-fold, with the estimated half-life decreasing from ~14 hr to ~4 hr.

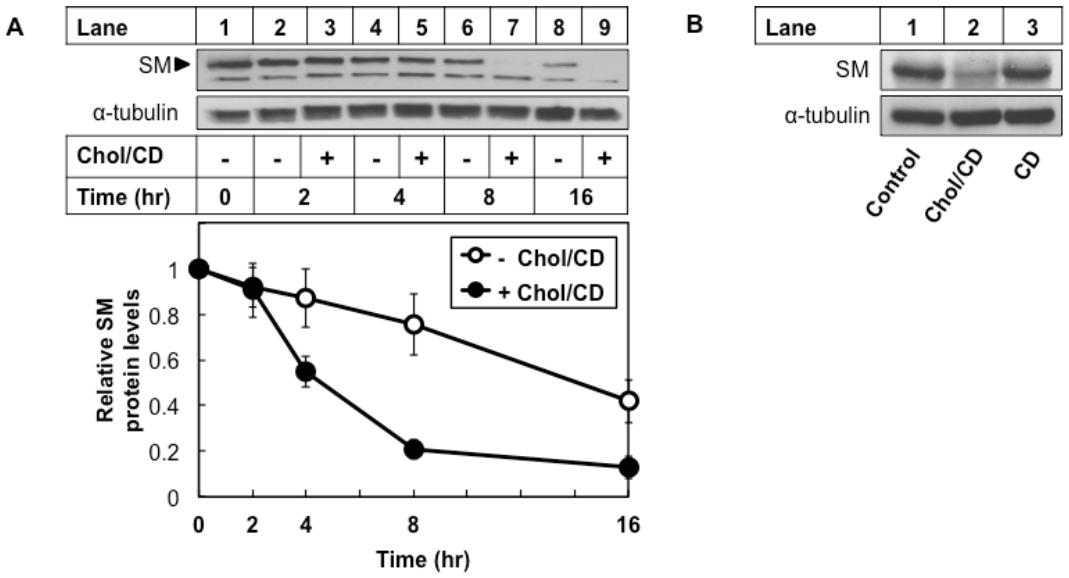

Figure 4.1 Cholesterol reduces SM protein levels post-translationally in SRD-1 cells

(A and B) SRD-1 cells were statin pretreated overnight in medium B, and treated as indicated in medium A containing cycloheximide (10 μg/ml) and Chol/CD (20 μg/ml), or (B) additionally with methyl-β-cyclodextrin (CD) for 8 hr. Cell lysates were assayed for endogenous SM and α-tubulin by immunoblotting (representative of n=3 separate experiments for each). Densitometry values for (A) are standardized to the vehicle treated control condition, and are ± SEM.

4.3.2 Sterol Specificity - Cholesterol as the principal degradation signal

Next, we examined whether endogenously synthesized sterols could regulate SM. We pretreated cells for 16 hr with a statin to inhibit sterol synthesis, lowering cholesterol levels and upregulating SREBP-2 target genes. The removal of the statin from the media then allows increased sterol synthesis due to the higher level of biosynthetic enzymes (Wong et al., 2008). Total cellular cholesterol at 8 hr increased by ~20% when statin was withdrawn from SRD-1 cells (an increase of 7 μg/mg from 34 μg cholesterol/mg cell protein). This newly synthesized sterol was sufficient to accelerate the degradation of SM (Figure 4.2A). Inhibiting later steps in the mevalonate pathway, at SM and lanosterol synthase (the first sterol generating enzyme), preserved SM protein levels to the same extent as statin (Figure 4.2B lanes 1, 3 and 5), indicating that the degradation signal is a sterol.

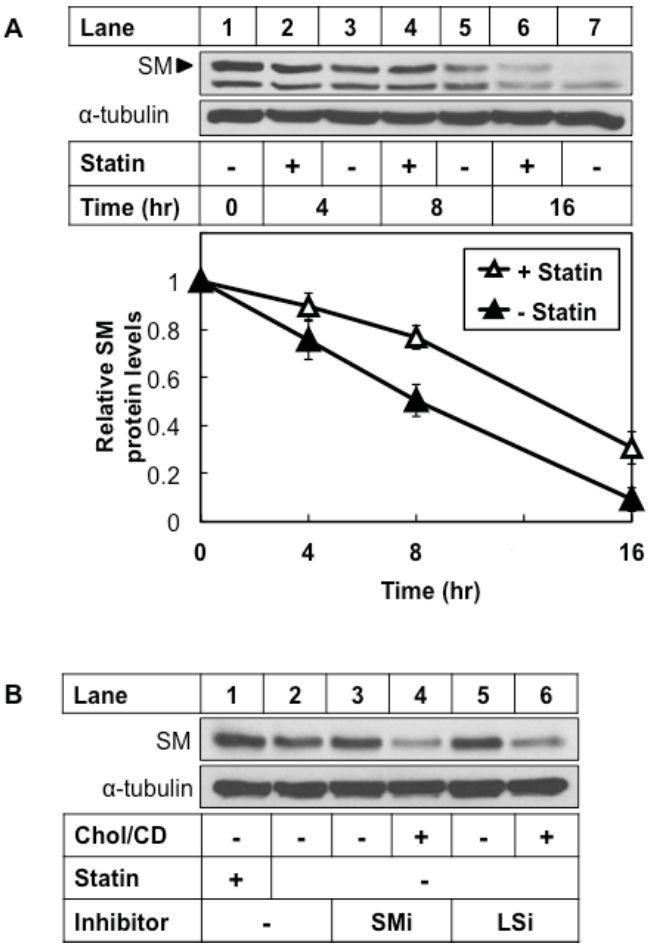

Figure 4.2 Endogenous cholesterol reduces SM protein levels

(A and B) SRD-1 cells were statin pretreated overnight in medium B, and treated as indicated in medium A containing cycloheximide (10 μg/ml) and either statin (compactin, 5 μM), SM inhibitor (SMi, 10 μM), lanosterol synthase inhibitor (LSi, 10 μM), and/or Chol/CD (20 μg/ml) for 8 hr. Cell lysates were assayed for endogenous SM and α-tubulin by immunoblotting (representative of n=4 separate experiments for each). Densitometry values for (A) are standardized to the vehicle treated control condition, and are ± SEM.

After establishing the effect of cholesterol on endogenous SM protein, we setup a system to test ectopic human SM regulation. Consistent with our results for endogenous hamster protein, there was a cholesterol-dependent reduction in human SM [expressed in CHO-7 cells driven with a viral thymidine kinase (TK) promoter] (Figure 4.3, lanes 3-4). In contrast, a construct with a higher expression cytomegalovirus (CMV) promoter did not show clear sterol regulation (Figure 4.3, lanes 7-8).

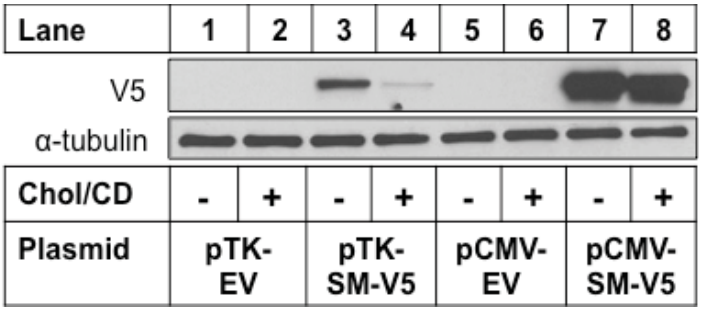

Figure 4.3 Cholesterol reduces ectopic human SM protein levels

CHO-7 cells were transfected with 1 μg of either empty vector (EV), or plasmids encoding human SM constructs as indicated. Following overnight statin pretreatment, CHO-7 cells were treated for 8 hr in medium B containing cycloheximide (10 μg/ml) with or without Chol/CD (20 μg/ml or as indicated). SM-V5 and α-tubulin were analyzed by immunoblotting (representative of n=4 separate experiments).

Thus, to examine the sterol specificity of this potential regulatory mechanism, the TK-driven SM expression vector was used. We tested the ability of a selection of sterol pathway intermediates and oxysterols, which have one or more additional oxygen-containing groups on the carbon backbone of cholesterol to cause degradation of ectopic human SM (Figure 4.4). 25HC at a concentration that inhibits SREBP processing (1 μg/ml) (Adams et al., 2004) did not destabilize SM, nor did 24,25EC (1 μg/ml), a physiological regulator of cholesterol synthesis (Wong et al., 2008) (Figure 4.4A, lane 3). A range of sterols and oxysterols were also delivered complexed to methyl-β-cyclodextrin at the same concentration as cholesterol (20 μg/ml) (Figures 4.4B and C). Treatment with the side-chain oxysterols 24,25EC, 25HC and 27-hydroxycholesterol (27HC) again had no effect on SM protein levels (Figure 4.4B, lanes 6-8), in contrast to what has been observed for HMGR (Song and DeBose-Boyd, 2004b). However, the steroid-ring oxysterols 7α-hydroxycholesterol (7αHC), 7β-hydroxycholesterol (7βHC), 7-ketocholesterol (7KC) and synthetic 19-hydroxycholesterol (19HC) induced degradation (Figure 4.4C, lanes 2-5). For the pathway sterols, the major methyl-sterol intermediates lanosterol and 24,25-dihydrolanosterol (24,25DHL) – the latter of which also accelerates degradation of HMGR (Lange et al., 2008; Song et al., 2005b) – had no effect on SM (Figure 4.4C, lanes 7-8). 7-Dehydrocholesterol (7DHC) and

lathosterol, both with double bonds on the steroid ring, also did not reduce SM protein levels (lane 5-6), whereas desmosterol which differs only by a double bond on the side chain was as effective as cholesterol (Figure 4.4C, lane 4 vs 3).

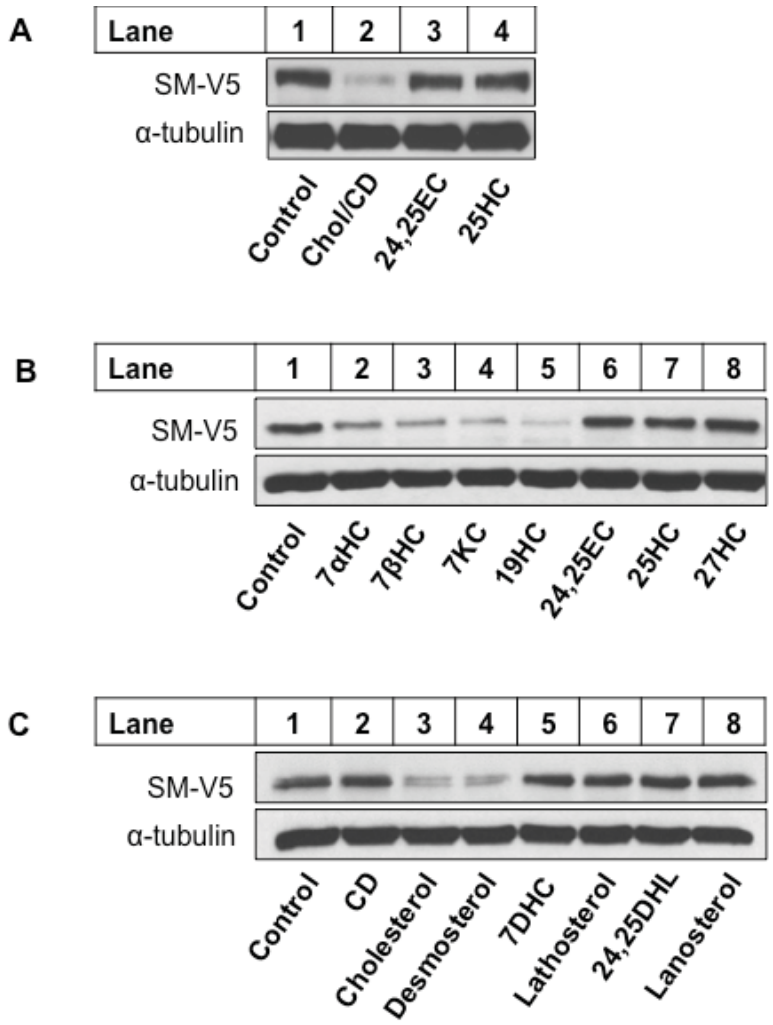

Figure 4.4 Degradation of SM is accelerated by cholesterol rather than oxygenated side-chain oxysterols

(A, B, C) CHO-7 cells were transfected with 1 μg of pTK-SM-V5. Following overnight statin pretreatment, CHO-7 cells were treated for 8 hr in medium B containing cycloheximide (10 μg/ml) with or without: **(A)** Chol/CD (20 μg/ml or as indicated), 24(*S*),25-epoxycholesterol (24,25EC, 1 μg/ml) or 25-hydroxycholesterol (25HC, 1 μg/ml); **(B, C)** An equivalent concentration of CD alone or CD complexed with the following sterols (20 μg/ml): 7α-hydroxycholesterol (7αHC), 7β-hydroxycholesterol (7βHC), 7-ketocholesterol (7KC), 19-hydroxycholesterol (19HC), 24,25EC, 25HC, 27-hydroxycholesterol (27HC), cholesterol, desmosterol, 7-dehydrocholesterol (7DHC), lathosterol, 24,25-dihydrolanosterol (24,25DHL), or lanosterol. SM-V5 and α-tubulin were analyzed by immunoblotting (each representative of n=4 separate experiments).

4.3.3 Cholesterol threshold for degradation of SM

The inverse curvilinear relationship (Figure 4.5A) between cholesterol and SM protein levels suggests the presence of a threshold required to trigger rapid degradation, approximately 15-20 μg total cholesterol/mg total protein in CHO-7 cells (Figure 4.5A, right panel). This threshold is close to the basal cholesterol value of ~15 μg/mg protein observed in full serum (NCS) without statin pretreatment (Figure 4.5B), consistent with a physiological feedback role for SM degradation in control of cholesterol synthesis. It is also worth noting that compared to lipoprotein-deficient serum (LPDS), full serum (NCS) has only marginally higher cholesterol content (Figure 4.5B). This explains the modest decrease observed in ectopic SM protein levels in full serum (NCS) compared with lipoprotein-depleted serum (LPDS) after 8 hr (Figure 4.5B, right panel). The different serum conditions together with statin were included as controls for the cholesterol assay.

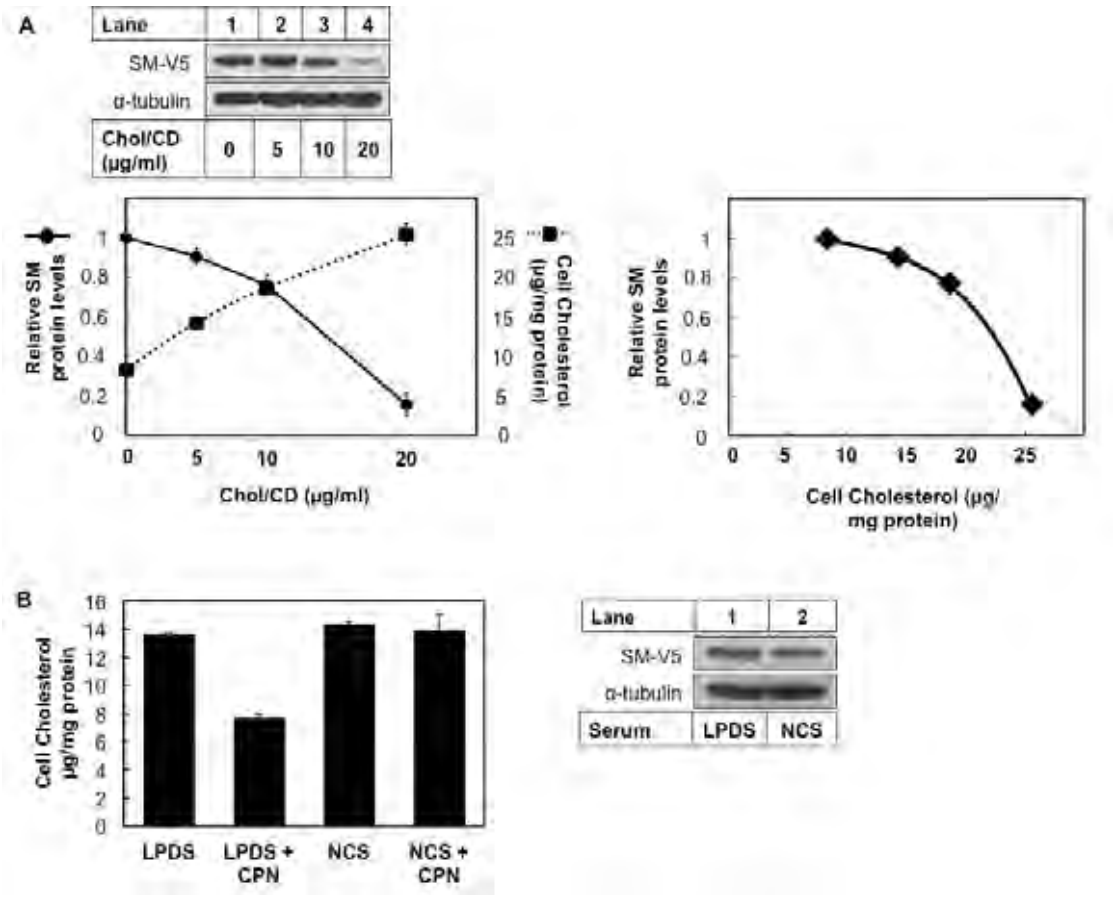

Figure 4.5 The relationship between the amount of cholesterol and SM protein levels, and the effect of serum derived cholesterol on degradation of SM

(A and B) CHO-7 cells were transfected with 1 μg pTK-SM-V5 and statin pretreated in medium B overnight. **(A)** Cells were treated for 8 hr in medium B containing cycloheximide (10 μg/ml) with varying concentrations of Chol/CD (0-20 μg/ml) for 8 hr. SM-V5 protein and α-tubulin were analyzed by immunoblotting (n=8). Total cellular cholesterol levels were measured in parallel experiments (n=3). The error bars (±SEM) presented are sometimes contained within the symbols. **(B)** Cells were treated in medium B or C (supplemented with 5 μM compactin and 50 μM mevalonate) as indicated for 8 hr, both containing 10 μg/ml cycloheximide. The immunoblot shown is representative of at least 2 separate experiments. For the graph- Cells were pretreated overnight in either medium A, medium B, medium C, or medium C with 5 μM compactin (statin) and 50 μM mevalonate. The media was then refreshed with the same formulations between conditions as for the pretreatments, but with the addition of 10 μg/ml cycloheximide, and harvested after 8 hr for cholesterol mass determination similarly to (A). The data are presented as mean + SEM from 3 separate experiments.

4.4 DISCUSSION

In the present study, we showed that cholesterol treatment led to a reduction in endogenous and ectopic SM protein levels, evident at 4 hr (Figure 4.1A and 4.3). SM protein levels remained unaffected when endogenous sterol synthesis was inhibited, indicating that it is indeed a sterol that accelerates the degradation of SM (Figure 4.2). After establishing that cholesterol itself feeds back and accelerates turnover of SM, we explored the sterol specificity of this phenomenon beyond cholesterol. Even though certain steroid-ring oxysterols appeared to destabilize SM (Figure 4.4), the likely cellular concentrations of these oxysterols are dramatically supraphysiological, and the most potent oxysterol tested, 19HC, is not found in nature (Brown and Jessup, 1999; Brown et al., 1997). Also, due to its much greater relative abundance compared to 7-oxygenated sterols (Brown and Jessup, 1999) or desmosterol (Yang et al., 2006), cholesterol itself appears to be the primary signal that mediates accelerated turnover of SM. Therefore, unlike HMGR, which has multiple degradation signals that include 24,25-dihydrolanosterol and certain side-chain oxysterols (Song and DeBose-Boyd, 2004; Lange et al., 2008), our results indicate that cholesterol is the major physiologically relevant regulator of SM.

Studies on cholesterol homeostasis routinely pretreat cells with a statin or under serum-depleted conditions to greatly reduce cellular cholesterol levels. It could be argued that such a lipid-deficient environment is not physiological for testing the cholesterol-dependent regulation of SM. To address this issue, we grew cells using full serum (NCS), and found that even the amount of cholesterol in NCS was sufficient to lower SM protein levels, albeit to a lesser extent (Figure 4.5B). Interestingly, our cholesterol assay revealed that the 20 μg/ml Chol/CD routinely used as treatment is comparable to the basal cell cholesterol level in NCS (Figures 4.2 and 4.5B). Therefore, the cholesterol mediated turnover of SM does not require an overload of cholesterol in cells, further strengthening the possibility of this being a physiological occurrence.

This mechanism is important from a cholesterol homeostasis viewpoint because cholesterol acutely regulates SM protein levels, thereby decreasing *de novo* cholesterol synthesis acutely (as seen in Chapter 3) before transcriptional regulation

via the SREBP-2 pathway (Chapter 3, Figure 3.5). This introduces a new form of post-translational regulation in the cholesterol synthesis pathway.

In conclusion, in this chapter, we used a number of different approaches to show that through feedback inhibition, cholesterol degrades SM protein. This could partially explain the accumulation of squalene in cells treated with cholesterol, and contribute to the 'rate-limiting' activity of this enzyme. In the next chapter, we further elucidate the cholesterol-dependent degradation mechanism for SM.

CHAPTER 5

CHOLESTEROL-REGULATED PROTEASOMAL DEGRADATION OF SQUALENE MONOOXYGENASE: CLUES INTO THE MECHANISM

5. CHOLESTEROL-REGULATED PROTEASOMAL DEGRADATION OF SQUALENE MONOOXYGENASE: CLUES INTO THE MECHANISM

5.1 INTRODUCTION

In Chapters 3 and 4, we established that cholesterol accelerates the degradation of SM through an unknown post-translational mechanism. This is associated with an accumulation of squalene, consistent with the possibility of SM being an important flux-controlling enzyme in cholesterol synthesis.

SM and HMGR are associated with the endoplasmic reticulum (ER), and the fate of many ER-bound proteins is destruction by the proteasome (Hampton, 2002). Based on the well-elucidated proteasomal degradation of HMGR (DeBose-Boyd, 2008a; Jo and DeBose-Boyd, 2010a), we hypothesized that the cholesterol-dependent degradation of SM is also proteasomal. Briefly, ER-associated degradation (ERAD) is a protein 'quality control' process that degrades misfolded proteins or proteins that do not form oligomeric complexes due to cellular stress, genetic mutations, or transcriptional and translational errors, and certain membrane-bound proteins when no longer required by the cell. These proteins are ubiquitinated by a suite of ubiquitin conjugating and ligating enzymes, and transported into the cytosol, before being recognized by the 26S proteasome for breakdown (Meusser et al., 2005; Vembar and Brodsky, 2008).

In this chapter, we set out to delineate the precise post-translational mechanism leading to the proteasomal degradation of SM. The specific aims of this chapter are as follows:

a. Determine whether the cholesterol-dependent degradation of SM is via the ubiquitin-proteasome pathway

b. Investigate the effect of proteasomal inhibition on the accumulation of squalene

c. Identify the regulatory domain of SM involved in the cholesterol-dependent degradation of this enzyme

The mechanistic detail obtained from this chapter should shed light on how SM becomes ‘rate-limiting’: correlating the decrease in enzyme protein levels and an increase in squalene accumulation upon cholesterol treatment in cells.

5.2 MATERIALS AND METHODS

Detailed lists of materials and methods are given in Chapter 2. The specific reagents and materials used in this chapter are given below.

5.2.1 Materials

Lipofectamine LTX, Opti-MEM I medium, Dynabeads, Amplex Red Cholesterol Assay kit, and anti-V5 antibody were purchased from Invitrogen (Carlsbad, CA). [1-^{14}C]-acetic acid sodium salt (specific radioactivity: 56 mCi/mmol) and Glutathione Sepharose 4B beads were purchased from GE Healthcare (Chalfont St. Giles, UK). [2-^{14}C]-mevalonolactone (mevalonate) (specific radioactivity: 40-60 mCi/mmol) and [^{35}S]-Protein Labeling Mix (EXPRE^{35}S^{35}S Protein Labeling Mix, specific radioactivity: >1000 Ci/mmol) were purchased from Perkin Elmer (Waltham, MA). Anti-SQLE (SM) antibody was purchased from Protein Tech Group (Chicago, IL). HA.11 monoclonal antibody was purchased from Covance (Princeton, NJ). Peroxidase-conjugated AffiniPure Donkey Anti-Mouse IgG and Peroxidase-conjugated AffiniPure Donkey Anti-Rabbit IgG were obtained from Jackson ImmunoResearch Laboratories (West Grove, PA). N-Acetyl-Leu-Leu-Norleu-al (ALLN), anti-α-tubulin antibody, butylated hydroxytoluene, chloroquine, compactin (also called mevastatin), cycloheximide, Dulbecco's phosphate buffered saline (PBS), lactacystin, methyl-β-cyclodextrin, mevalonate, Z-Leu-Leu-Leu-al (MG132), primers, protease inhibitor cocktail, N-ethylmaleimide, sodium oleate, sodium dodecyl sulphate (SDS), IGEPAL CA-630, sodium deoxycholate, methionine, and cysteine were obtained from Sigma (St. Louis, MO). The HA-tagged ubiquitin plasmid, pMT123, encoding 8 tandem HA-ubiquitins (Treier et al., 1994), was a gift from Dr Dirk Bohmann (University of Rochester Medical Centre, Rochester, NY).

5.2.2 Methods

5.2.2.1 Cell Culture

All cells were maintained in monolayer at 37°C in 5% CO_2. Cells were seeded at the following densities: 2×10^6 cells/6 cm dish for immunoprecipitation; 4×10^6 cells/10 cm dish for glutathione sepharose pulldown; 2×10^5 cells/well in 6-well plates for all other experiments. CHO-7, SRD-1, and SRD-15 cells were maintained in medium A, and SRD-13A cells were maintained in medium C supplemented with 5 μg/ml cholesterol, 1 mM mevalonate, and 20 μM sodium oleate. Unless otherwise stated, cells were statin pretreated in media containing 5 μM statin (compactin) and 50 μM mevalonate overnight (CHO-7, SRD-1, SRD-13A, and SRD-15 cells in medium B). Cells were then treated with test agents (added in ethanol or dimethylsulfoxide to refreshed media) as indicated in the figure legends. Within an experiment, the final concentrations of solvent were kept constant between conditions and did not exceed 0.28 % (v/v).

5.2.2.2 Transfection

CHO cells in 6-well plates were grown in medium A (without antibiotics) and transfected the following day using Lipofectamine LTX reagent (Invitrogen) according to the manufacturer's instructions, using a ratio of 1 μg of DNA: 4 μl of transfection reagent. DNA was equalized with empty vector between different conditions. Following 24 hr transfection, cells were statin pretreated overnight, and then treated as indicated in the respective figure legends.

5.2.2.3 Western Blotting

During harvest, after rinsing once with 1X PBS, cells were lyzed in 100 μl 10% (w/v) SDS with 5 μl protease inhibitor cocktail. Lysates were passed through 18G needles, and were vortexed vigorously for 20 min at room temperature. After equalizing protein concentrations using the BCA assay Chapter 2 (Section 2.2.2), samples (usually 40 μg of protein) were analyzed by 10% SDS-PAGE, and transferred onto nitrocellulose membrane. The membrane was then incubated in

blocking solution [5% (w/v) skim milk, 0.1% (v/v) Tween-20 in PBS] for 1 hr, and immunoblotted with the following antibodies: anti-V5 (1:10 000), anti-SM (1:5 000), anti-HA (1:10 000) and anti-α-tubulin (1:200 000). The observed protein bands migrated according to their calculated molecular weight: 64 kDa for SM and 50 kDa for α-tubulin. The relative intensities of bands were quantified by densitometry using ImageJ Software (1.36b).

5.2.2.4 Lipid Extraction and Thin Layer Chromatography

Following statin pretreatment, cells were metabolically labeled with 1 μCi/well [^{14}C]-acetate or [^{14}C]-mevalonate added to the existing media for the last 2 or 4 hr of treatment, as indicated in the respective figure legends. Cells were washed once with PBS, lyzed in 500 μl 0.1 M NaOH, and rinsed with 1.25 ml H_2O. Protein concentrations were measured using the BCA assay method (Section 2.2.2). Lysates were saponified with 500 μl 20% KOH (w/v) in methanol, butylated hydroxytoluene (1 μl, 20 mM), and EDTA (20 μl, 20 mM) at 70ºC for 1 hr. After cooling, the lipids were extracted with 2 ml hexane and evaporated to dryness. Extracts were re-dissolved in 60 μl hexane, and aliquots corresponding to equivalent amounts of protein separated on Silica Gel 60 F_{254} plates (Merck, Whitehouse Station, NJ) with a mobile phase of hexane: diethyl ether: glacial acetic acid (60:40:1, v/v/v). Bands corresponding to cholesterol, MOS, and squalene were visualized using the FLA-5100 phosphorimager (Fujifilm, Tokyo, Japan). The relative intensities of bands were quantified using Sciencelab ImageGauge 4.0 Software (Fujifilm).

5.2.2.5 Metabolic Labeling of N100-GST with [^{35}S]-Methionine/Cysteine

CHO-7 cells were transiently transfected as indicated in the figure legend. After statin pretreatment, cells were labeled in methionine-free medium (Invitrogen) supplemented with 5 μM compactin and 50 μM mevalonate containing 250 μCi/ml [^{35}S]-Protein Labeling Mix (Perkin Elmer) for 3 hr, then washed and chased in medium B containing 2 mM methionine and cysteine with or without Chol/CD, for 0-8 h. [^{35}S]-labeled N100-GST was pulled down from lysates with equal cell protein using glutathione sepharose beads (GST Pulldown- Section 5.2.2.6), and

pellets were subjected to 4-20% or 10% SDS-PAGE. Bands were visualized by phosphorimaging, and their relative intensities were quantified using Sciencelab ImageGauge 4.0 Software (Fujifilm).

5.2.2.6 Ubiquitination assays for Human SM

Following transfection and treatment (as indicated in the figure legends), CHO-7 cells were harvested by washing twice with cold 1X PBS. Cells were then scraped in 1X PBS, transferred to a 50 ml tube, and centrifuged at 1000 g for 5 min. After discarding the supernatant, the pellet (lysate) was resuspended in 500 µl RIPA buffer (50 mM NaCl, 1.0% IGEPAL CA-630, 0.5% sodium deoxycholate, 0.1% SDS, 200 mM Tris, pH 8.0) supplemented with N-ethylmaleimide (10 mM), protease inhibitor cocktail and ALLN (25 µg/ml), and lyzed by passing through an 18G needle 50-60 times.

Immunoprecipitation

Lysates were immunoprecipitated with monoclonal anti-V5-conjugated Dynabeads (Invitrogen), according to the manufacturer's instructions, with some modifications. Dynabeads (80 µl/500 µg protein) were prepared by washing three times (5 min each) with RIPA buffer. Fresh RIPA buffer (250 µl) was then added to the tube containing the beads, followed by 2 µg anti-V5 antibody (2 µg), and the antibody-beads mixture was allowed to rotate overnight at 4^{o}C. The next day, the microfuge tubes were placed on the magnetic stand and the supernatant (RIPA buffer) was removed. Lysates with equal cell protein (standardized using the BCA assay) were added to the antibody-beads mixture. These were then rotated for 4 h at 4^{o}C. The supernatant was then collected and stored for analyze the efficiency of the IP, and the pellets (antibody-beads-protein of interest) mixture were washed three times for 30 min each. After the final wash, the supernatant was discarded, the pellets were resuspended in 50 µl modified loading buffer (2 volumes RIPA buffer + 2 volumes 10% SDS + 1 volume fresh 5X Laemmli Buffer/β-mercaptoethanol), and boiled for 5-10 min at 95^{o}C. Pellets were subjected to 7.5% SDS-PAGE, followed by immunoblot analysis with anti-V5 (for SM) and anti-HA (for ubiquitin) antibodies

GST Pulldown Assay

Pull-down of the N100-GST fusion protein was achieved using glutathione sepharose beads. The beads (80 µl/500 µg protein) were prepared by adding 500 µl RIPA buffer, rotating for 2 min, and then centrifuging at 16 000 g for 1 min. This was repeated 3 times. After the final wash, the supernatant was replaced with the lysates with equal cell protein (standardized using the BCA assay). These were then rotated overnight at 4^{o}C. The next day, samples were centrifuged at 16 000 g for 5 min, and the supernatant was collected for analysis of the pulldown. The pellets (GST beads-protein of interest) were then resuspended in 1 ml RIPA buffer and allowed to rotate at 4^{o}C for 1 hr after which they were centrifuged at 16 000 g for 5 min. This step was repeated twice, however, pellets were allowed to rotate for 30 min instead. After the final wash, the supernatant was discarded, the pellets were resuspended in 50 µl modified loading buffer (2 volumes RIPA buffer + 2 volumes 10% SDS + 1 volume fresh 5X Laemmli Buffer/β-mercaptoethanol), and boiled for 10 min at 95^{o}C with occasional vortexing. Pellets were subjected to 7.5% SDS-PAGE, followed by Immunoblot analysis with anti-V5 (for SM) and anti-HA (for ubiquitin) antibodies.

5.3 RESULTS

5.3.1 Cholesterol-dependent degradation of SM is proteasomal

Based on the idea that SM could be degraded via the ERAD pathway, we tested whether the cholesterol-accelerated degradation of SM is proteasomal. In support of this, a range of proteasomal inhibitors (ALLN, MG132, and lactacystin) preserved endogenous SM protein levels (Figure 5.1A). On the contrary, a lysosomal inhibitor (chloroquine) had no effect (Figure 5.1B).

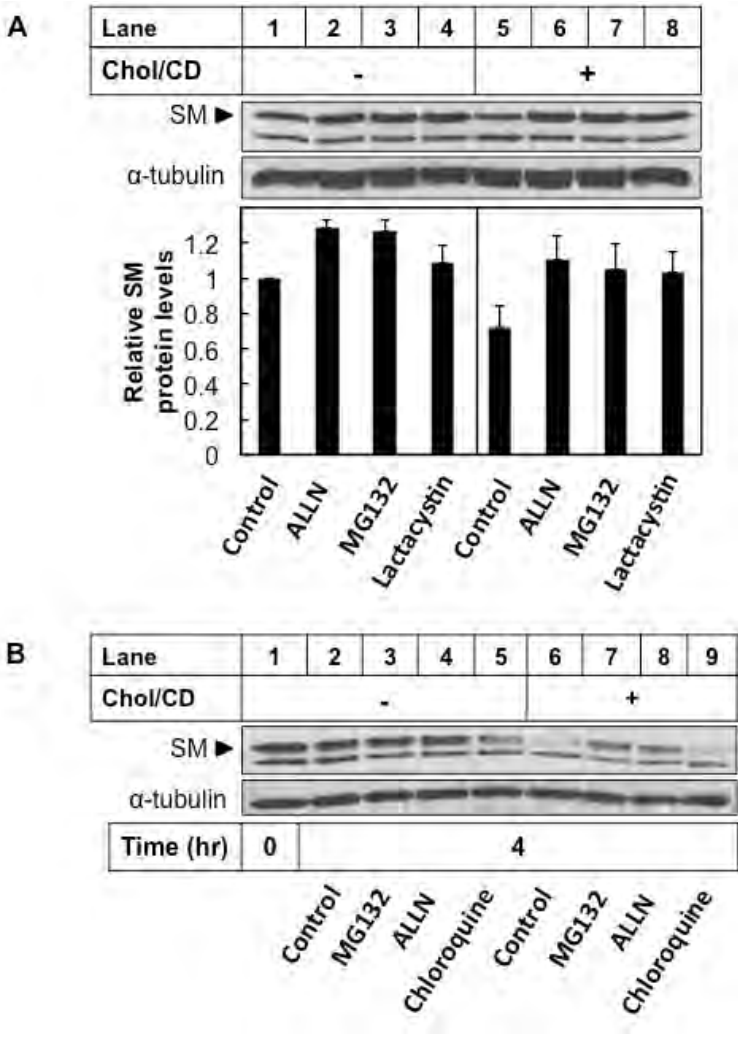

Figure 5.1 Effect of proteasomal and lysosomal inhibitors on cholesterol-regulated turnover of SM

SRD-1 cells were statin pretreated overnight in medium B, and treated in medium B containing cycloheximide (10 μg/ml) with or without Chol/CD (20 μg/ml) and with MG132 (10 μM), ALLN (25 μg/ml), lactacystin (10 μM) and chloroquine (200 μM) as indicated for 4 hr. **(A)** Densitometric values for SM protein were normalized to the vehicle-treated control condition, which was set to 1. The data is presented as mean + SEM from 4 separate experiments. In cholesterol-treated cells, all three proteasomal inhibitors significantly increased SM levels above control values ($p < 0.05$ by paired t-test). **(B)** This immunoblot is representative of 3 separate experiments.

Over a period of 8 hr, cholesterol-mediated degradation of the enzyme could be prevented with the proteasomal inhibitor MG132 (Figure 5.2A). As observed with endogenous hamster SM, the cholesterol-dependent reduction in ectopic human enzyme was also rescued by the addition of MG132 (Figure 5.2B, lanes 2 vs 4).

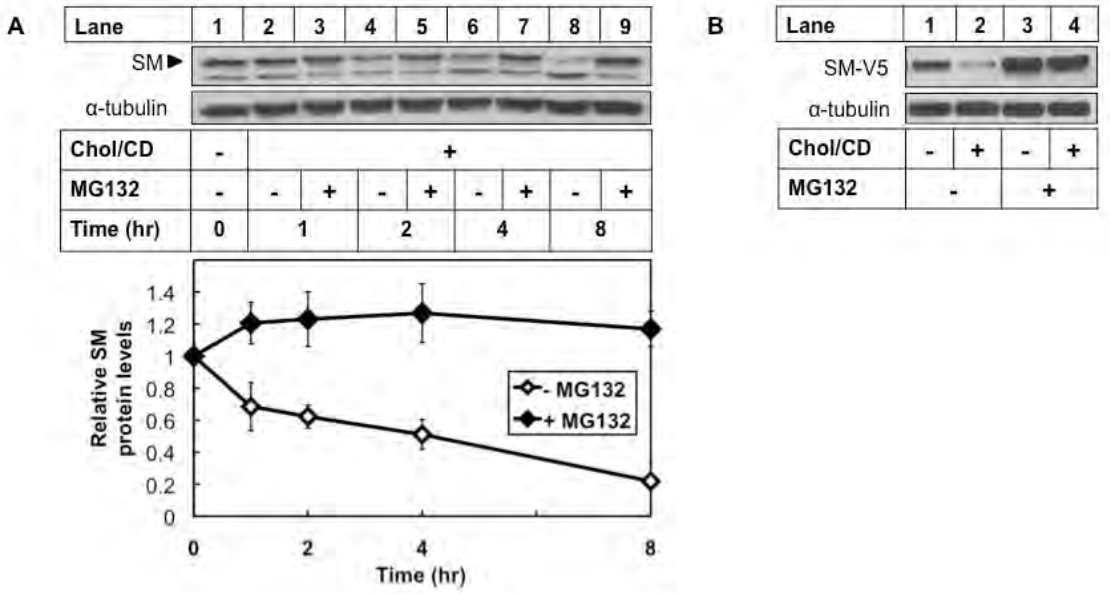

Figure 5.2 Proteasomal inhibition reverses cholesterol-dependent reduction in SM protein levels

(A) SRD-1 cells were statin pretreated overnight in medium B, and treated in medium B containing cycloheximide (10 μg/ml), Chol/CD (20 μg/ml) and MG132 (10 μM), as indicated. Cell lysates were assayed for SM and α-tubulin by immunoblotting. Densitometric values for SM protein were normalized to the vehicle-treated control condition, which was set to 1 (representative of n=3 separate experiments) **(B)** CHO-7 cells were transfected with 1 μg pTK-SM-V5 plasmid as indicated, statin pretreated and treated as in (A) for 8 hr (representative of n=4 separate experiments).

Alternatively, glycine-alanine repeats (GAr) from Epstein-Barr virus nuclear antigen-1 were added to the ends of the human SM protein to provide resistance to proteasomal degradation (Sharipo et al., 1998). The effect of the GAr repeats is similar to that of a proteasomal inhibitor, and there are a few postulated mechanisms via which the GAr repeats achieve this. One example is whereby GAr repeats interfere with the ATP-driven insertion of a substrate into the 19S proteasome regulatory complex, thus halting the proteolytic degradation process (Zhang and

Coffino, 2004). A single 30 amino-acid repeat at the C-terminus slightly increased protein levels (Figure 5.3, lanes 3 vs 1), whereas repeats on both the N- and C-termini blunted cholesterol-dependent degradation (Figure 5.3, lanes 5-6).

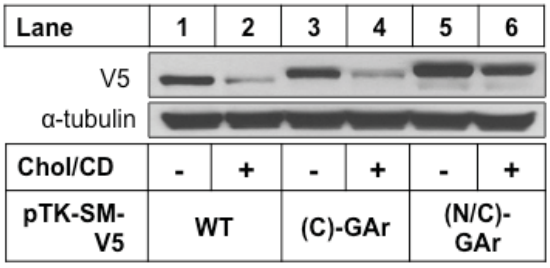

Figure 5.3 Glycine-alanine repeats (GAr) provide marginal resistance to SM when subjected to cholesterol-dependent proteasomal degradation

CHO-7 cells were transfected with 1 μg of plasmid as indicated. The SM constructs contain glycine-alanine repeats at the C- and/or N-termini of wild-type (WT) SM-V5 as indicated. Cells were statin pretreated overnight in medium B containing cycloheximide (10 μg/ml) and treated with Chol/CD (20 μg/ml) as indicated for 8 hr. Cell lysates were assayed for SM-V5 and α-tubulin by immunoblotting (representative of n=2 separate experiments).

In co-expression experiments with HA-tagged ubiquitin, human SM was polyubiquitinated in the presence of MG132, which was greater in the presence of cholesterol (Figure 5.4, lanes 4 vs 3). Thus, SM is degraded by the ubiquitin-proteasomal system, enhanced by increased cholesterol levels.

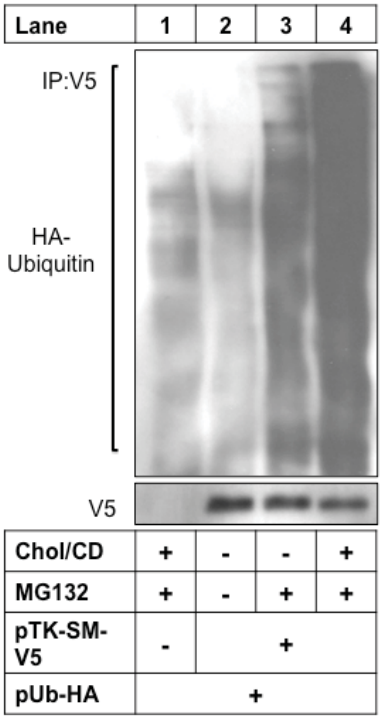

Figure 5.4 Cholesterol enhances the polyubiquitination of SM

CHO-7 cells were transfected with 1.5 μg of pTK-SM-V5 and 0.5 μg of pUb-HA (HA-tagged ubiquitin), statin pretreated overnight in medium B, treated in medium B with or without Chol/CD (20 μg/ml) and MG132 (10 μM) for 4 hr as indicated. SM-V5 was immunoprecipitated from cell lysates. Immunoprecipitated pellets were assayed for SM-V5 and HA-ubiquitin by immunoblotting (representative of n=2 separate experiments).

Importantly, in SRD-1 cells, proteasomal inhibition dramatically reduced the accumulation of squalene after 4 hr of cholesterol treatment and increased cholesterol synthesis from acetate (Figure 5.5A, lane 4 vs 3). The same effect was also observed using radiolabeled mevalonate in both SRD-1 and CHO-7 cells (Figures 5.5B and C, respectively), thus bypassing HMGR. This is consistent with the cholesterol-dependent proteasomal degradation of SM having functional consequences, by contributing to the squalene accumulation observed.

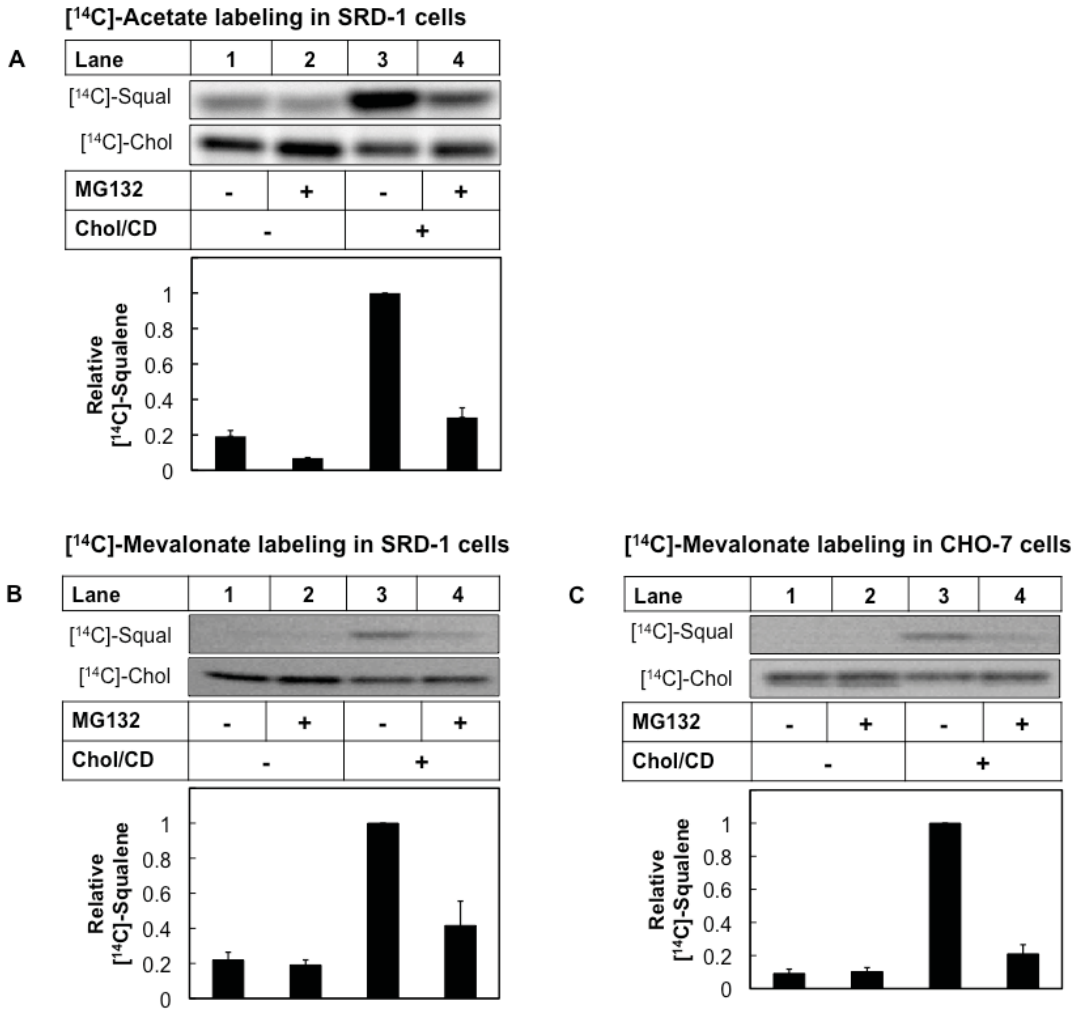

Figure 5.5 Proteasomal inhibition with MG132 reduces squalene accumulation after cholesterol treatment

Statin pretreated in medium B, SRD-1 **(A, B)** or CHO-7 **(C)** cells were treated in medium A with or without Chol/CD (20 μg/ml) and/or MG132 (10 μM), and labeled with [^{14}C]-acetate (A) or [^{14}C]-mevalonate (B, C) for 4 hr. [^{14}C]-Squalene accumulation was expressed relative to the maximal condition (Chol/CD), which was set to 1 [representative of n=4 separate experiments (A); 5 (B); and 3 (C)].

5.3.2 Insig and Scap are not required for the cholesterol-dependent degradation of SM

Sterol-dependent degradation of HMGR requires its sterol-sensing domain, which binds the Insig retention protein that in turn recruits a ubiquitin ligase into contact with HMGR (DeBose-Boyd, 2008b). To determine whether Insig is required for degradation of SM, we observed lipid synthesis and SM turnover in SRD-15 cells. These mutant CHO cells are deficient in Insig, with no functional Insig-1 isoform, and an extremely low level of Insig-2 (Lee et al., 2005). When SRD-15 cells were treated with cholesterol, squalene still accumulated (Figure 5.6), with similar kinetics to CHO-7 and SRD-1 cells (Chapter 3, Figures 3.4 and 3.7).

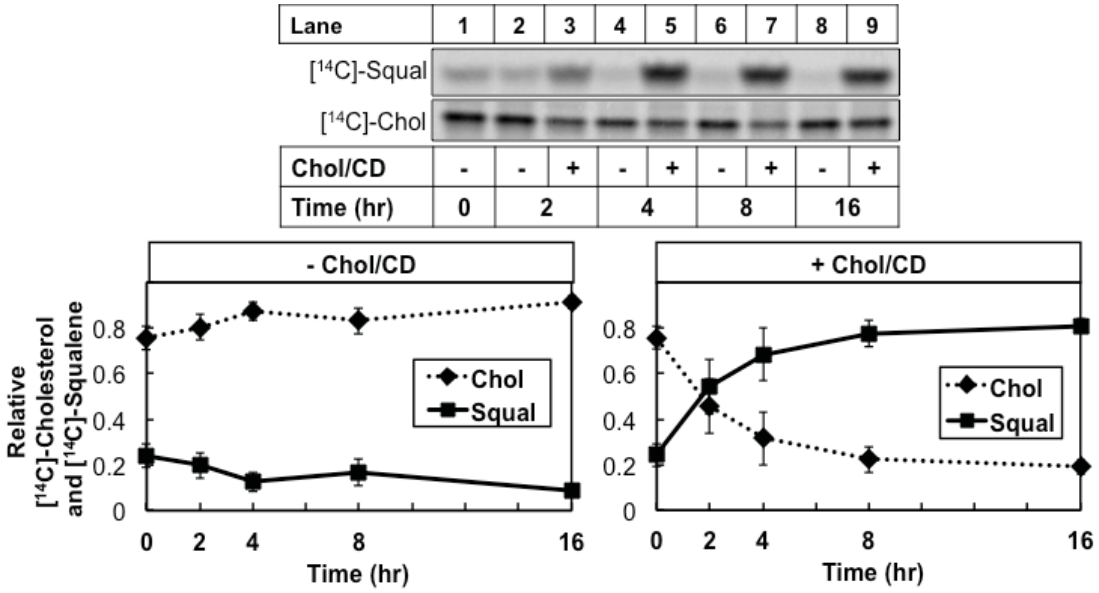

Figure 5.6 Cholesterol-dependent squalene accumulation in Insig-deficient SRD-15 cells

SRD-15 cells were statin pretreated overnight in medium B, and treated in medium B with or without Chol/CD (20 μg/ml) as indicated and labeled with [^{14}C]-acetate in medium A during treatment 2 hr prior to harvesting. Relative accumulation was calculated so that [^{14}C]-squalene + [^{14}C]-cholesterol = 1 at each time point. Error bars (±SEM) are contained within the symbols (representative of n=5 separate experiments).

In addition, protein degradation was still observed in SRD-15 cells for both endogenous SM (Figure 5.7A, lane 2) and ectopic human SM (Figure 5.7B, left panel, lane 4). Cholesterol-dependent degradation of SM also occurred in SRD-13A cells (Rawson et al., 1999), mutant CHO cells which lack the cholesterol-sensing protein Scap and consequently do not have a functional SREBP pathway (Figure 5.7B, right panel, lane 2). Thus, Insig and Scap are not required for degradation of SM. Furthermore, if additional regulatory machinery is necessary, then the genes are unlikely to be strict SREBP-2 targets.

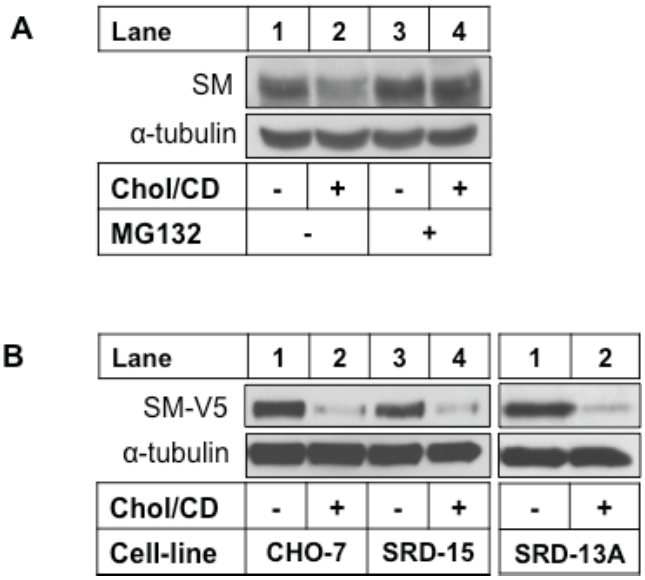

Figure 5.7 Cholesterol reduces SM protein levels independently in the absence of Insig and Scap

(A) SRD-15 cells were statin pretreated overnight in medium B, and treated in medium B containing cycloheximide (10 μg/ml), Chol/CD (20 μg/ml) and MG132 (10 μM) for 8 hr, as indicated. Cell lysates were assayed for SM and α-tubulin by immunoblotting (representative of n=4 separate experiments). **(B)** The indicated cell-lines were transfected with 1 μg pTK-SM-V5, statin pretreated overnight in medium B, and treated in medium B containing cycloheximide (10 μg/ml) with or without Chol/CD (20 μg/ml) for 8 hr. SM-V5 protein was analyzed by immunoblotting (each representative of n=2 separate experiments).

5.3.3 Cholesterol-dependent proteasomal degradation of SM requires its N-terminal domain

The N-terminus of SM, encoded by the first exon, is partially conserved in vertebrates but lacking in lower organisms [Figure 5.8A (full version in the Appendix)]. In addition, a recombinant truncated rat enzyme missing the first 99 residues retains full activity (Sakakibara et al., 1995). This led us to suspect that the vertebrate N-terminal region is a structurally and functionally distinct domain that may play a role in post-transcriptional regulation.

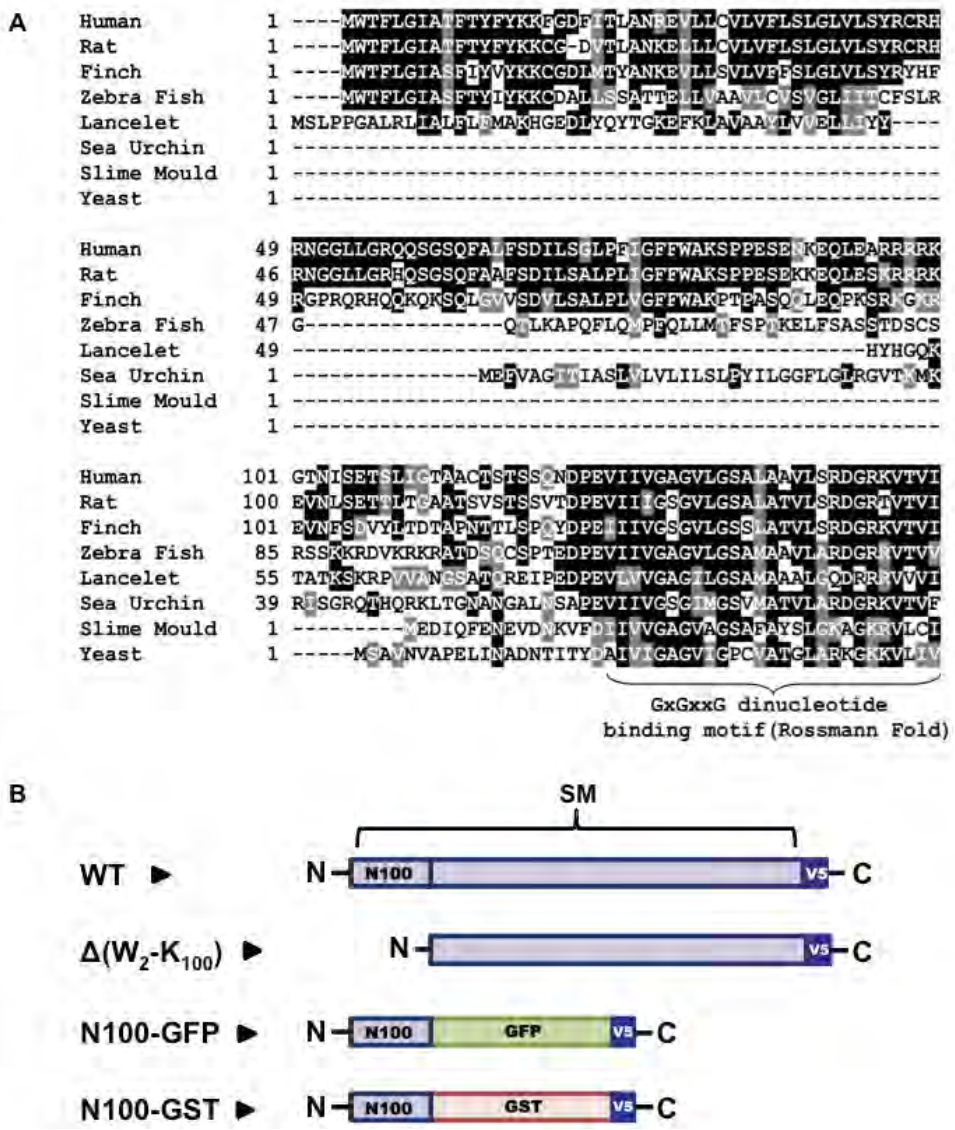

Figure 5.8 The N-terminal domain of SM is conserved in vertebrates, but lacking in invertebrates

(A) Multiple sequence alignment of the first ~150 amino acids of SM for selected species (full version in Appendix). **(B)** Schematic of SM fusion and deletion constructs.

We constructed a corresponding human version that is missing the N-terminal region ($\Delta(W_2\text{-}K_{100})$; Figure 5.8B), and examined its response to cholesterol treatment (Figure 5.9A). Unlike full-length SM (WT, Figure 5.9A, lane 2 vs 1), turnover of this deletion construct was unaffected by cholesterol (Figure 5.9A, lane

5 vs 4), and levels were further increased by addition of MG132 (Figure 5.9A, lane 6 vs 4).

We then determined if ablating the cholesterol-regulation of the deletion construct has functional consequences, by acutely labeling transfected cells with [^{14}C]-acetate. Importantly, we observed that MOS, the product of SM, accumulates preferentially in cholesterol-treated cells transfected with the N-terminal deletion construct compared to full-length SM (Figure 5.9B, lanes 4 vs 2). Accordingly, densitometric analysis showed that the precursor squalene to product MOS ratio was 30-40% lower in the cholesterol-treated cells transfected with the truncated construct, in keeping with the failure of cholesterol to accelerate degradation of this variant. It should be noted that the squalene accumulation observed in cells transfected with the [$\Delta(W_2\text{-}K_{100})$] (Figure 5.9B) can be due to the endogenous SM.

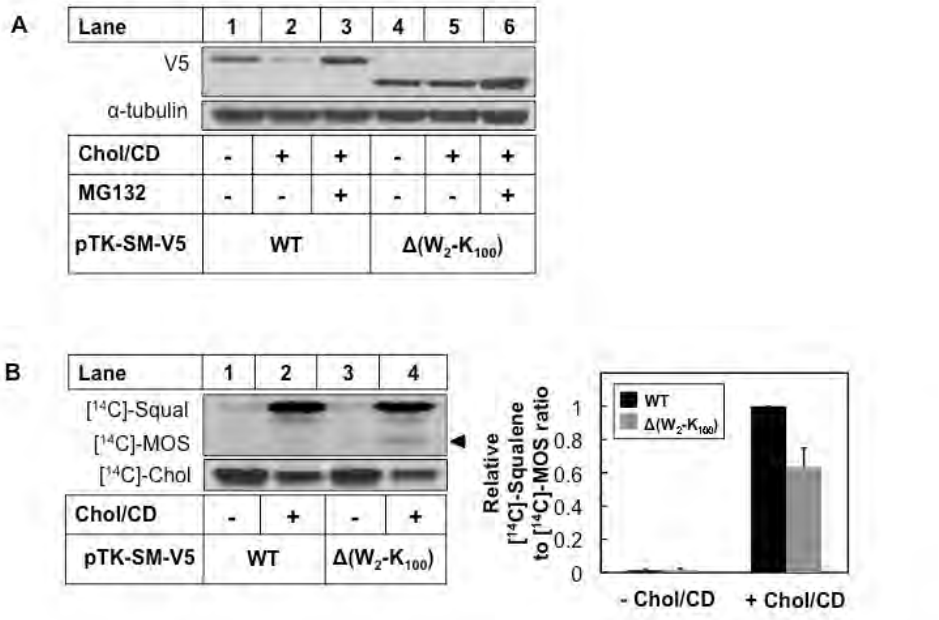

Figure 5.9 SM deletion construct [Δ(W_2-K_{100})] lacks cholesterol regulation

CHO-7 cells were transfected with 1 μg pTK-SM-V5 (WT) or pTK-SM-Δ(W_2-K_{100})-V5 [Δ(W_2-K_{100})] as indicated and statin pretreated overnight in medium B. **(A)** Following statin pretreatment, cells were treated in medium B containing cycloheximide (10 μg/ml), with or without Chol/CD (20 μg/ml), and/or MG132 (10 μM) for 8 hr. V5-tagged SM constructs were analyzed by immunoblotting. (n=2). **(B)** Transfected and statin pretreated CHO-7 cells were labeled with [^{14}C]-acetate in medium A, and treated with or without Chol/CD (20 μg/ml) for 4 hr. Cells were assayed for accumulation of [^{14}C]-cholesterol, [^{14}C]-squalene and [^{14}C]-2,3-monooxidosqualene (MOS). The [^{14}C]-MOS band is indicated with an arrow. The [^{14}C]-squalene to [^{14}C]-MOS ratio was expressed relative to the maximal condition (cells transfected with pTK-SM-V5 and treated with Chol/CD), which was set to 1. For the Chol/CD conditions, the Δ(W_2-K_{100}) construct produced a lower [^{14}C]-squalene to [^{14}C]-MOS ratio than the wild-type (WT) construct (p<0.05 by t-test; n=5).

We next prepared a complementary construct of the first 100 amino acids of epitope-tagged human SM, but it failed to express (data not shown). This may be due to the extremely hydrophobic character of this region, previously proposed to contain transmembrane domains (Ono, 2002; Sakakibara et al., 1995). To assist folding or solubilization and enable expression, we fused the first 100 amino acids (N100) to green fluorescent protein (N100-GFP) or glutathione *S*-transferase (N100-GST) under the control of the TK promoter (Figure 5.8B). Importantly, turnover of both heterologous fusion constructs was robustly regulated by cholesterol (Figure

5.10A, lane 4 vs 3; Figure 5.10B, lane 2 vs 1), whereas expression of either GFP or GST alone was unaffected by cholesterol treatment (data not shown).

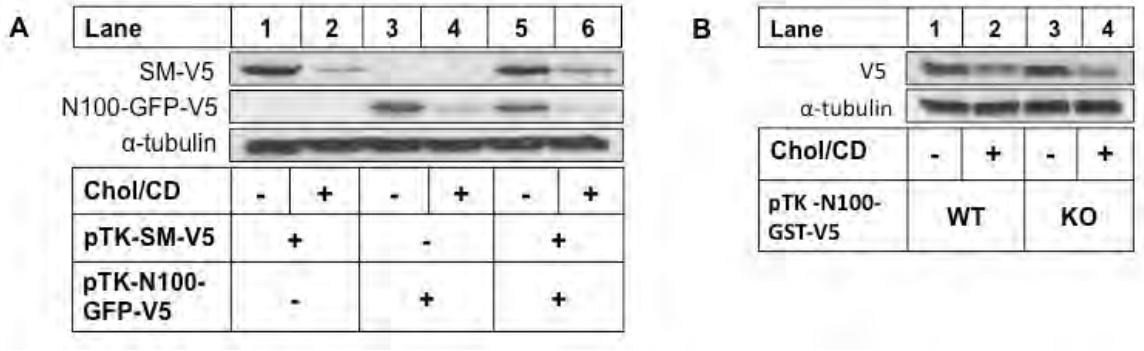

Figure 5.10 Cholesterol regulated turnover of N100 fused to GFP or GST

(A and B) CHO-7 cells were transfected as indicated and statin pretreated overnight in medium B. Following statin pretreatment, cells were treated in medium B containing cycloheximide (10 μg/ml), with or without Chol/CD (20 μg/ml) for 8 hr. V5-tagged SM constructs were analyzed by immunoblotting. **(A)** 0.5 μg pTK-SM-V5 (WT) and/or 0.5 μg pTK-SM-N100-GFP-V5 (N100-GFP) as indicated, (n=3). **(B)** 0.25 μg of pTK-SM-N100-GST-V5 (WT) or pTK-SM-N100-KO-GST-V5 (KO) containing no lysines in the first 100 amino acids, but others remain within GST and the V5 tag, (n=2).

When the full-length protein and truncated chimera were co-transfected, cholesterol-dependent turnover of each was also unaffected (Figure 5.10A, lane 6 vs 5). This was surprising in light of the marked blunting of regulation seen for the CMV system earlier (Chapter 4), because expression of the TK-driven truncated fusion protein (N100-GFP) was much higher than the full-length non-fusion protein (data not shown).

A pulse-chase approach, which permits the study of protein degradation without the use of cycloheximide, confirmed that Chol/CD treatment accelerates degradation of the N100-GST (Figure 5.11), and suggests a comparable half-life (~3 hr) to that seen in the cycloheximide-containing studies on full-length endogenous SM [~4 hr, Figures 4.1A (Chapter 4) and 5.2A]. Without added cholesterol, the N100-GST appeared remarkably stable over the 8 hr. Cholesterol began to degrade this truncated version of SM by 2 hr (Figure 5.11), in line with the timing observed for squalene accumulation (Chapter 3: Figures 3.4 and 3.7).

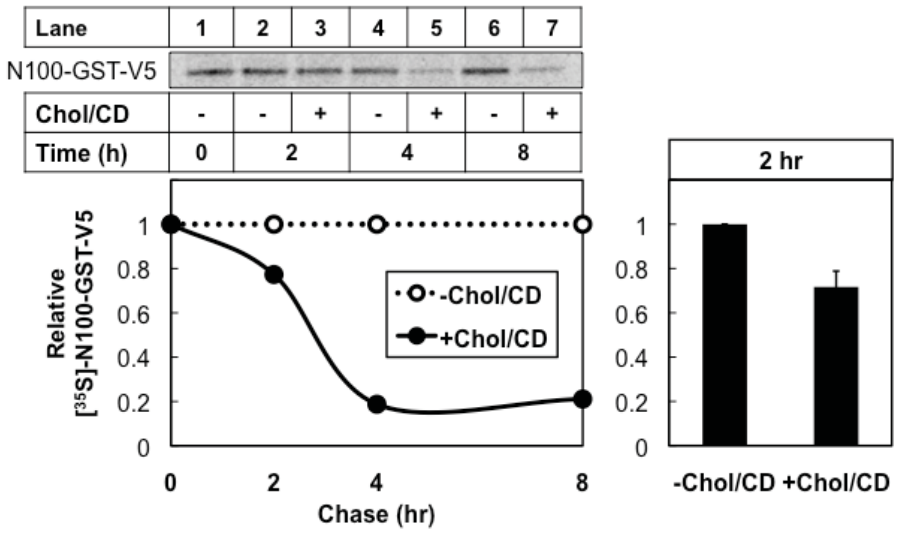

Figure 5.11 Cholesterol accelerates the degradation of N100-GST even in the absence of cycloheximide

CHO-7 cells were transfected with 0.25 μg of pTK-SM-N100-GST-V5 (N100-GST). Following statin pretreatment, cells were pulsed for 3 hr with [^{35}S]-methionine/cysteine and then chased in medium B with or without Chol/CD (20 μg/ml) for 0-8 hr. [^{35}S]-N100-GST protein was pulled down with glutathione sepharose, analyzed by SDS-PAGE and the gel visualized by phosphorimaging (n=2). For the image shown, densitometric values were plotted for the +Chol/CD conditions. The –Chol/CD values, which did not change over the 8 hr, were each set to 1. Right hand panel: Cholesterol significantly degraded N100-GST at 2 hr (p<0.05 by t-test; n=4).

Moreover, GST pull-down of the N100-GST chimera co-expressed with HA-tagged ubiquitin revealed clear cholesterol-dependent polyubiquitination (Figure 5.12A, lane 1 vs 2) at 4 hr. This effect was also observed as early as 1 hr after cholesterol treatment (Figure 5.12B), which probably explains why squalene accumulation is observed within 2 hr of cholesterol treatment (Chapter 3: Figures 3.4 and 3.7).

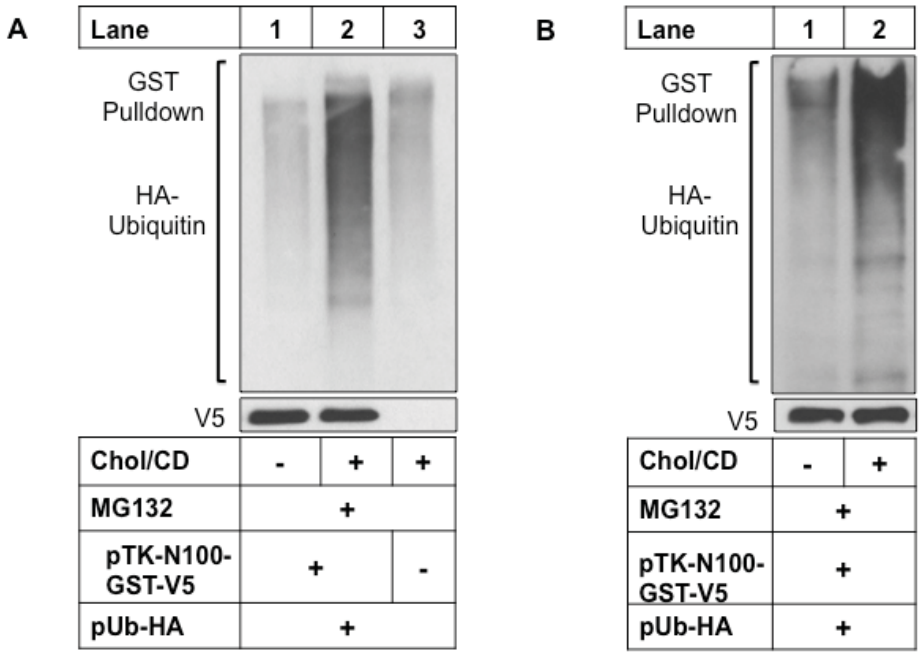

Figure 5.12 Cholesterol-dependent polyubiquitination of N100-GST at 1 and 4 hr

(A and B) CHO-7 cells were transfected with 1.5 μg of pTK-SM-N100-GST-V5 (N100-GST) and 0.5 μg of pMT123 (pUb-HA, HA-tagged ubiquitin). Following statin pretreatment, cells were treated in medium B with or without Chol/CD (20 μg/ml) and MG132 (10 μM) for (A) 4 hr or (B) 1 hr. N100-GST protein was pulled down with glutathione sepharose and immunoblotted for V5 (N100-GST) and HA-ubiquitin. Representative of **(A)** n=2 **(B)** n=3 separate experiments.

Together, these data suggest that the N-terminal region forms a regulatory domain, which is both necessary and sufficient for post-translational regulation of SM by the proteasome, which in turn helps regulate flux through the cholesterol biosynthetic pathway.

5.4 DISCUSSION

In this chapter, we showed that the cholesterol-dependent degradation of SM occurs via the ubiquitin-proteasome system: protein levels were rescued through proteasomal inhibition with MG132 (Figure 5.2), and polyubiquitination increased with cholesterol treatment (Figure 5.4). Importantly, MG132 reversed the accumulation of squalene, suggesting that accelerated proteasomal degradation of SM may help to acutely control flux through the cholesterol biosynthetic pathway. This effect was observed in cells radiolabelled with [^{14}C]-acetate as well as [^{14}C]-mevalonate (bypassing HMGR) (Figure 5.5), showing that HMGR activity has no influence over the rate-limiting step catalyzed by SM. Also, cholesterol-mediated turnover of SM did not require Insig or Scap (Figure 5.7).

In order to elucidate the degradation mechanism for SM, it was necessary to identify its regulatory domain. We hypothesized that a well-conserved N-terminal region distinct from the enzyme's catalytic site could be the region of interest (Sakakibara et al., 1995). Appropriate constructs showed that cholesterol-regulated turnover of SM was mediated by the N-terminal domain of human SM (N100). The turnover of the N100-GFP and -GST tagged constructs were sterol-regulated, indicating that this region is responsible for conferring sterol responsiveness on the enzyme. Moreover, the enzyme lacking the N100 region [$\Delta(W_2\text{-}K_{100})$] did not show cholesterol-dependent regulation (Figure 5.9A). Also, a relatively higher amount of MOS, product of the SM-catalyzed reaction, was observed in $\Delta(W_2\text{-}K_{100})$-transfected cells treated with cholesterol implying that cholesterol had a reduced effect on the functionality of the truncated enzyme compared to the full length version, due to the absence of the N100 region.

An ^{35}S labeling pulse-chase approach (Figure 5.11) further strengthened our finding (as reported in Chapter 4) that by 2 hr, cholesterol begins to cause degradation of SM, leading to a build-up of squalene. Due to technical and time constraints, only the N100 region and not full length SM was used for the pulse-chase experiment. Even then, a comparable half-life of ~ 3 hr to that determined using endogenous SM (Chapter 4) was obtained (Figure 5.11). Similar to full-length SM, the N100 region also undergoes polyubiquitination upon proteasomal inhibition

in a cholesterol-enriched environment as early as 1 hr (Figure 5.12). Together, this supports the argument that the N100 region of SM is responsible for cholesterol-induced degradation of the enzyme.

Even though SM is proposed to be the second flux-controlling enzyme in the cholesterol synthesis pathway, and like HMGR, is degraded via the ubiquitin-proteasome pathway, current evidence suggests that SM has a distinct degradation mechanism. Firstly, a key difference is that SM lacks the five transmembrane sterol-sensing domain present in sterol-responsive proteins such as HMGR, the SREBP-escort protein Scap (Hua et al., 1996), and the intracellular cholesterol trafficking protein Niemann Pick C1 (NPC1) (Loftus et al., 1997). Secondly, Insig, which is required to initiate ubiquitination of HMGR, and is also responsible for retaining the SREBP-Scap complex in the ER to prevent proteolytic activation of SREBP, is not required for cholesterol-dependent degradation of SM. Thirdly, as investigated in Chapter 4, the degradation signals for HMGR such as 24,25-dihydrolanosterol, and oxysterols like 25-hydroxycholesterol, 27-hydroxycholesterol, and 24(*S*),25-epoxycholesterol, are unable to destabilize SM. Even though, we have outlined the key components of the feedback mechanism via which cholesterol promotes the degradation of SM, certain details about the ubiquitination process, for example, identifying specific ubiquitinating enzymes, for example, ubiquitin E3 ligases, are yet to be found.

Our numerous attempts at identifying an ubiquitination site for SM using site-directed mutagenesis have been unsuccessful to date. This involved mutating groups of lysines to arginine, including selected conserved residues, or all lysines from the heterologous fusions (Figure 5.10B), which all retained cholesterol-regulated turnover. These data suggest that a specific regulated ubiquitination site may be unnecessary, and/or that ubiquitination may occur on the N-terminal amino group (Breitschopf et al., 1998).

With this chapter, we conclude our work that highlights SM as a significant regulatory enzyme in the cholesterol synthesis pathway. In the next chapter, we focus on SM and 2,3-oxidosqualene cyclase with respect to their involvement in manipulating 24(*S*),25-epoxycholesterol levels and its significance.

CHAPTER 6

24(*S*),25-EPOXYCHOLESTEROL AND ITS INVOLVEMENT IN CHOLESTEROL HOMEOSTASIS

6. 24(*S*),25-EPOXYCHOLESTEROL AND ITS INVOLVEMENT IN CHOLESTEROL HOMEOSTASIS

6.1 INTRODUCTION

Cholesterol is known to be the principal regulator of its own synthesis. It achieves this by a complex feedback system that is mediated by a number of ER-associated proteins that are involved in its synthesis as well as its sensing (Goldstein et al., 2006a). Over the past few decades, oxysterols have developed the reputation of being potent molecules that have a diverse contribution to cholesterol homeostasis [reviewed in (Gill et al., 2008)]. A fitting example is 24(*S*),25-epoxycholesterol (24,25EC; systematic name: 24(*S*),25-epoxy-cholest-5-en-3β-ol).

24,25EC has a unique origin: instead of being an oxygenated derivative of cholesterol like all the other known oxysterols, it is synthesized *de novo* from acetate during the normal course of cholesterol synthesis (Figure 6.1) (Nelson et al., 1981b). Nelson and colleagues detected significant levels of this oxysterol in human cells of hepatic as well as non-hepatic origin (Nelson et al., 1981b). Additionally, when added to cultured cells, 24,25EC inhibited the activity of HMGR (Spencer et al., 1985). Furthermore, 24,25EC suppresses SREBP processing (Janowski et al., 2001), and is the most potent oxysterol activator of LXR target genes (Janowski et al., 1999; Lehmann et al., 1997a; Spencer et al., 2001), thus influencing the amount of cholesterol at the transcriptional level as well. Therefore, in the recent years, 24,25EC has become a widely recognized significant modulator of cholesterol homeostasis (Björkhem and Diczfalusy, 2004; Brown, 2009; Huff and Telford, 2005).

Since 24,25EC is synthesized in a shunt of the mevalonate pathway alongside cholesterol (Figure 6.1), two enzymes are essential to ensure that both 24,25EC and cholesterol are being produced. The first enzyme, SM, which in addition to catalyzing the conversion of squalene into MOS, initiates the shunt pathway by acting a second time to convert MOS into 2,3*(S)*:22*(S)*,23-dioxidosqualene (DOS), the substrate for the next important enzyme 2,3-oxidosqualene cyclase (OSC) to act upon.

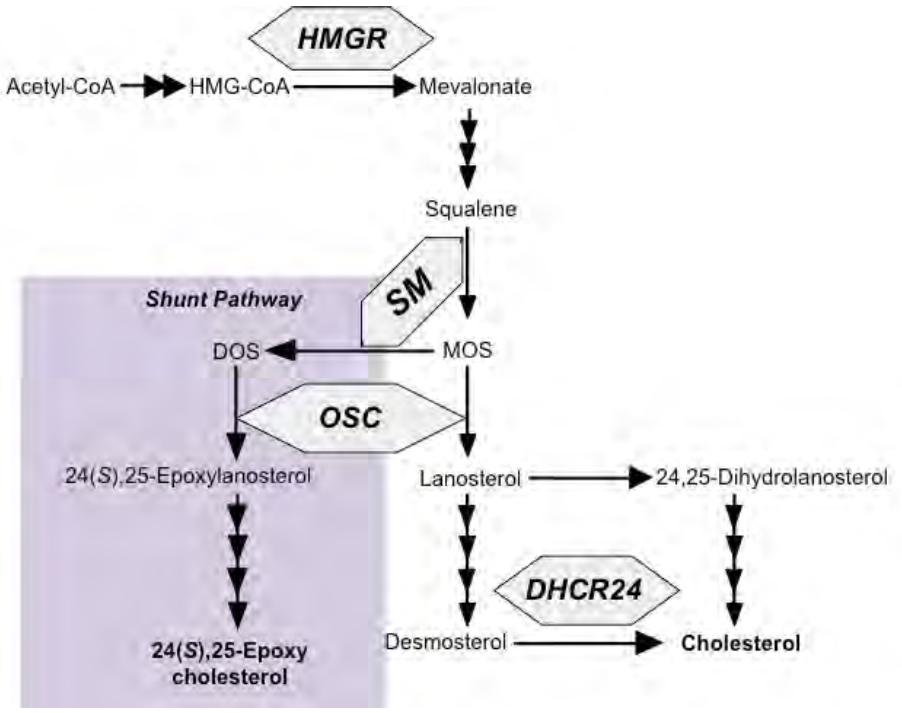

Figure 6.1 The mevalonate pathway featuring key enzymes of cholesterol homeostasis

(HMGR: 3-hydroxy-3-methylglutaryl coenzyme A reductase; SM: squalene monooxygenase; MOS: 2,3(S)-monooxidosqualene; DOS: 2,3(S):22(S),23-dioxidosqualene; OSC: 2,3-oxidosqualene cyclase; DHCR24: 3β-hydroxysterol-Δ24-reductase)

Like SM, OSC is also equally involved in the production of cholesterol (Figure 6.1). An interesting characteristic of OSC is that when partially inhibited, it favors the production of 24,25EC over cholesterol because OSC has a higher affinity for DOS (precursor for 24,25EC) than MOS (Boutaud et al., 1992). Having increased levels of 24,25EC could potentially be beneficial for cells to keep their cholesterol status in check, since 24,25EC has been shown to acutely control the level of newly synthesized cholesterol in cultured cells (Wong et al., 2008).

The unique location of OSC in the cholesterol synthesis pathway, and the fact that minor manipulations to the enzyme levels can lead to a shift in the balance of cholesterol and 24,25EC synthesis, in recent years has made this enzyme an attractive pharmacological target for treatment of hypercholesterolemia (Björkhem and Diczfalusy, 2004). However, trials done on hamsters and dogs have shown that

high doses of OSC inhibitors increased the risk of cataracts (Funk and Landes, 2005). There has not been much recent progress made in evaluating inhibitors of cholesterol synthesis for lowering blood cholesterol levels.This is probably because all the attention has always been concentrated on statins, which monopolize the market for the treatment of hypercholesterolemia. However, with the use of high doses of statins on the rise, there is a concern of increasing adverse effects, the most common being myalgia (Brown, 2010). Also, the inhibitory effect of statin on cholesterol synthesis leads to a compensatory increase in expression of several key cholesterol biosynthetic enzymes, including HMGR. Hence, removal of the statin results in a concentration-dependent surge in cholesterol synthesis (Wong et al., 2007a). Accordingly in normal subjects, stopping statin therapy caused a rebound of serum cholesterol levels, monocyte HMGR activity and sterol synthesis (Stone et al., 1989). This has been termed the 'Statin Rebound Phenomenon', and has been especially observed after an acute vascular event, when statin discontinuation results in an erratic increase in cholesterol levels in patients (Daskalopoulou, 2009).

In this chapter, we propose a novel lipid lowering treatment that combines the advantages of both statins and OSC inhibitors. In cultured cells, we show that the partial inhibition of OSC, which raises endogenous 24,25EC levels, can synergize with statins to modulate newly synthesized elevated cholesterol levels, a consequence of the 'Statin Rebound Phenomenon'. Additionally, as part of investigating the involvement of 24,25EC at different levels in cholesterol homeostasis, the specific aims are the following:

a. **To investigate the effect of cholesterol treatment on 24,25EC levels with the cell**
b. **To characterize stable cells that have higher levels of 24,25EC**
c. **To determine the effect of 24,25EC on modulating the 'Statin Rebound Phenomenon' in cultured cells**

6.2 MATERIALS AND METHODS

A detailed list of materials and methods is given in Chapter 2. The specific reagents and materials used for this chapter are given below.

6.2.1 Materials

TRIzol Reagent, SuperScript III First Strand cDNA Synthesis Kit, and anti-Myc were purchased from Invitrogen (Carlsbad, CA). SYBR Green SensiMix dT was from Quantace (Norwood, MA). 24(*S*),24-Epoxycholesterol (24,25EC) was obtained from Enzo Life Sciences (Farmingdale, NY). The OSC stable cell line was prepared by Dr Jenny Wong.

6.2.2 Methods

6.2.2.1 Cell Culture

All cells were maintained in monolayer at 37°C in 5% CO_2. Cells were seeded at the following densities: 2×10^6 cells/6 cm dish for immunoprecipitation; 4×10^6 cells/10 cm dish for glutathione sepharose pulldown; 2×10^5 cells/well in 6-well plates for all other experiments. CHO-7 cells were maintained in medium A, and SM and OSC overexpressing cell lines were maintained in medium A supplemented with 100 μg/ml zeocin. Unless otherwise stated, cells were statin pretreated in media containing 5 μM statin (compactin) and 50 μM mevalonate overnight (CHO-7 cells in medium B). Cells were then treated with test agents (added in ethanol or dimethylsulfoxide to refreshed media) as indicated in the figure legends. Within an experiment, the final concentrations of solvent were kept constant between conditions and did not exceed 0.28 % (v/v).

6.2.2.2 Western Blotting

During harvest, after rinsing once with 1X PBS, cells were lyzed in 100 µl 10% (w/v) SDS with 5 µl protease inhibitor cocktail. Lysates were passed through 18G needles, and were vortexed vigorously for 20 min at room temperature. After equalizing protein concentrations using the BCA assay Chapter 2 (Section 2.2.2), samples (usually 40 µg of protein) were analyzed by 10% SDS-PAGE, and transferred onto nitrocellulose membrane. The membrane was then incubated in blocking solution [5% (w/v) skim milk, 0.1% (v/v) Tween-20 in PBS] for 1 hr, and immunoblotted with the following antibodies: anti-myc (1:10 000) and anti-α-tubulin (1:200 000). The observed protein bands migrated according to their calculated molecular weight: 64 kDa for SM, 78 kDa for OSC, and 50 kDa for α-tubulin. The relative intensities of bands were quantified by densitometry using ImageJ Software (1.36b).

6.2.2.3 Lipid Extraction and Thin Layer Chromatography

Following statin pretreatment, cells were metabolically labeled with 1 µCi/well [^{14}C]-acetate or [^{14}C]-mevalonate added to the existing media for the last 2 or 4 hr of treatment, as indicated in the respective figure legends. Cells were washed once with PBS, lyzed in 500 µl 0.1 M NaOH, and rinsed with 1.25 ml H_2O. Protein concentrations were measured using the BCA assay method (Section 2.2.2). Lysates were saponified with 500 µl 20% KOH (w/v) in methanol, butylated hydroxytoluene (1 µl, 20 mM), and EDTA (20 µl, 20 mM) at 70ºC for 1 hr. After cooling, the lipids were extracted with 2 ml hexane and evaporated to dryness. Extracts were re-dissolved in 60 µl hexane, and aliquots corresponding to equivalent amounts of protein separated on Silica Gel 60 F_{254} plates (Merck, Whitehouse Station, NJ) with a mobile phase of hexane: diethyl ether: glacial acetic acid (60:40:1, v/v/v). Bands corresponding to cholesterol, MOS, and squalene were visualized using the FLA-5100 phosphorimager (Fujifilm, Tokyo, Japan). The relative intensities of bands were quantified using Sciencelab ImageGauge 4.0 Software (Fujifilm).

Argentation TLC

Cells were then lysed in 500 µl 0.1 M NaOH and protein concentrations measured using the BCA assay. Lysates were saponified with 1 ml ethanol, 500 µl 75% (w/v) KOH in H_2O, 1 µl 20 mM butylated hydroxyltoluene, and 20 µl 20 mM EDTA at 70ºC for 1 h. After cooling, non-saponifiable lipids were extracted into 2.5 ml hexane and evaporated to dryness. Lipid extracts were re-dissolved in 60 µl hexane, and aliquots corresponding to equivalent amounts of protein were separated by Arg-TLC using 4% (w/v) silver-coated Silica Gel 60 F_{254} plates with a mobile phase of heptane:ethyl acetate (2:1, v/v), run four times. Bands corresponding to cholesterol and desmosterol were visualized using the FLA-5100 phosphorimager (Fujifilm, Tokyo, Japan). The relative intensities of bands were quantified using Sciencelab ImageGauge 4.0 Software (Fujifilm).

6.2.2.4 Quantitative Real-Time PCR

As described in Chapter 2 (Section 2.2.6), RNA was harvested in triplicate using TRIzol reagent, reverse transcribed to yield cDNA using the SuperScript III First Strand cDNA Synthesis kit (Invitrogen), and mRNA levels determined relative to the housekeeping gene by quantitative real-time PCR using SYBR Green and a Corbett Rotorgene 3000. Primers were directed against SM (*SQLE*) and HMGR (*HMGCR*), with porphobilinogen deaminase (*Pbgd*) as the housekeeping gene (refer to Chapter 2, Table 2.4). Values were expressed relative to the vehicle-treated control, which was set to 1.

6.2.2.5 Generation of SM overexpressing stable cell line

CHO-7 cells were transfected with pCMV-SM-myc (1 µg) for 24 hr using Lipofectamine LTX transfection reagent (4 µl/well in a 6 well plate) and stable transfectants were selected for zeocin (500 µg/ml) resistance. Pure clones were obtained by limiting dilution, and were screened for SM-myc expression by Western blotting. The SM overexpressing stable cells were characterized by qRT-PCR (SM expression levels) and TLC (cholesterol, squalene, and 24,25EC synthesis).

6.3 RESULTS

6.3.1 24*(S)*,25-Epoxycholesterol is effluxed from cells under various conditions

In Chapters 3 and 5, we have established that squalene accumulates when cells are treated with cholesterol. Generally, this was accompanied by a corresponding decrease in *de novo* cholesterol synthesis (Chapter 3). We attributed this to cholesterol feeding back and inhibiting SM, creating a bottleneck at this step. As a result, the precursor squalene builds up in the cell. SM normally also catalyzes the formation of DOS, which eventually goes on to form 24,25EC. Therefore, we predicted that inhibiting SM should not only reduce cholesterol synthesis, but would decrease 24,25EC synthesis. We hypothesized that any reduction seen in 24,25EC levels in response to cholesterol treatment would reflect SM degradation, and the shutting down of its own synthesis.

We found that when CHO-7 cells were treated with Chol/CD, LDL, or 25HC, 24,25EC levels appeared to decrease compared to the control (Figure 6.2). This was most apparent in the Chol/CD-treated condition (Figure 6.2 lane 3 and 7). This effect was observed regardless of the cells being pretreated overnight with statin.

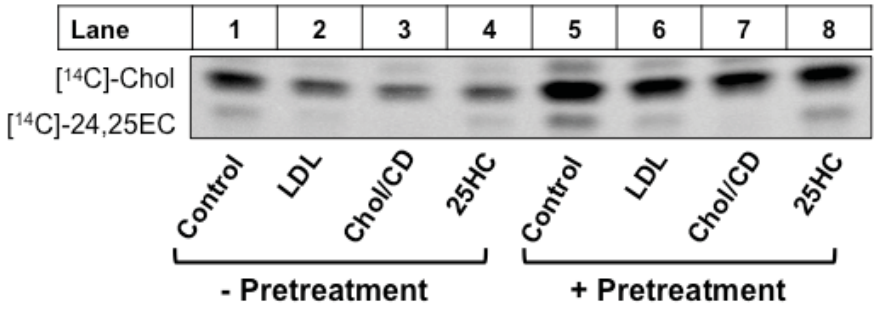

Figure 6.2 24,25EC disappears from cells treated with cholesterol

CHO-7 cells were statin pretreated overnight as indicated and then treated with 50 μg/ml LDL, 20 μg/ml Chol/CD, or 1 μg/ml 25HC and labeled with [^{14}C]-acetate for 4 hr. Neutral lipid extracts were separated using radio-TLC and bands corresponding to cholesterol and 24,25EC were visualized by phosphorimaging and the image shown is representative of at least 2 separate experiments.

Based on our knowledge about SM catalyzing the first step of 24,25EC production, we assumed that adding cholesterol (which degrades SM) was leading to a decrease in 24,25EC synthesis. However, we could not rule out increased degradation or efflux into the media. To differentiate between these possibilities, an experiment was set up in which CHO-7 cells were pretreated overnight with 10 nM OSC inhibitor (OSCi, Ro-488071), and radiolabelled with [^{14}C]-acetate to facilitate the build-up of [^{14}C]-24,25EC. The following day, after washing off the pretreatment media, cells were treated with or without cholesterol. To block any further flux of [^{14}C]-acetate or early derivatives through the pathway which could confound the results, a statin, and squalene synthase inhibitor (SSi) were included in the treatment media. During the harvest, neutral lipids were extracted from cells as well as from the media and were analyzed using radio-Thin Layer Chromatography (radio-TLC).

This experiment showed that the 24,25EC, but not cholesterol, was being effluxed from the cells upon cholesterol treatment, appearing in the media (Figure 6.3A). It was therefore clear that cholesterol was not having an effect on the synthesis or degradation of 24,24EC, but rather could be involved in inducing the export of this oxysterol out of the cell. Before pursuing this observation further, it

was important to determine if the methyl-β-cyclodextrin (MβCD) alone was having an effect on 24,25EC (Figure 6.3B and 6.3C). We tested this under normal lipoprotein-deficient serum (LPDS) as well as starvation conditions using 0.1% Bovine Serum Albumin (0.1% BSA). The starvation media was compared alongside with the LPDS to shed light on whether the effluxed 24,25EC in the media was being taken up by any residual apolipoproteins present in the LPDS. We found that in the presence of MβCD alone, 24,25EC was being effluxed into the media, to a similar extent in the 0.1% BSA and LPDS conditions, ruling out the possibility of apolipoprotein cholesterol acceptors being involved (Figure 6.3B versus C). Interestingly, even though MβCD alone had an effect on 24,25EC efflux, cholesterol had a slightly greater effect, suggesting that cholesterol may have an additive effect on the removal of 24,25EC from the cell.

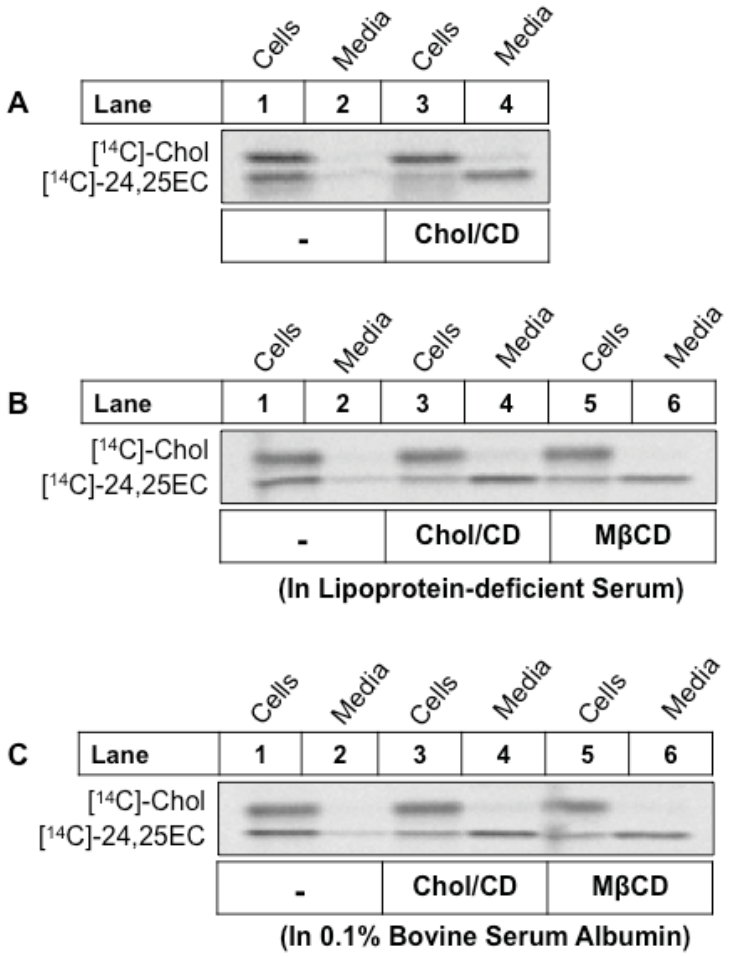

Figure 6.3 Methyl-β-cyclodextrin alone causes the efflux of 24,25EC into the media

(A-C) CHO-7 cells were pretreated overnight with 10 nM OSCi (Ro-488071) and radiolabelled with 1 μCi/well [^{14}C]-acetate. The next day, cells were treated with 20 μg/ml Chol/CD or the equivalent amount MβCD alone for 4 hr as indicated in media containing 5 μM compactin and 150 μM SSi (Zaragozic acid). Neutral lipid extracts from the cells and media were separated using radio-TLC and bands corresponding to cholesterol, and 24,25EC were visualized by phosphorimaging.

Since cholesterol did not have a marked specific effect on the transport of 24,25EC, we decided not to pursue this any further. Even though the fate of 24,25EC once effluxed from the cell remains an area of uncertainty, through the next series of experiments, we aimed to focus on the implications of 24,25EC on cholesterol synthesis within cells.

6.3.2 Generation of a stable cell line that has increased production of 24,25EC

A stable cell line can be a valuable tool for studying the role of a certain enzyme, or how manipulating enzyme levels influences the flux of a pathway. Our laboratory has previously generated a cell line that overexpresses OSC (Wong et al., 2008). OSC, the next enzyme in cholesterol synthesis pathway after SM, converts MOS into lanosterol *en route* to cholesterol, and DOS into 24(*S*),25-epoxylanosterol (Figure 6.1). An interesting characteristic of OSC is that when partially inhibited, it produces more 24,25EC than under normal conditions [refer to Chapter 1, Section 1.8.3 (Boutaud et al., 1992; Huff and Telford, 2005). However, overexpression of OSC inhibits 24,25EC synthesis, and leads to an increase in acute cholesterol production as illustrated in Figure 6.4 (Wong et al., 2008).

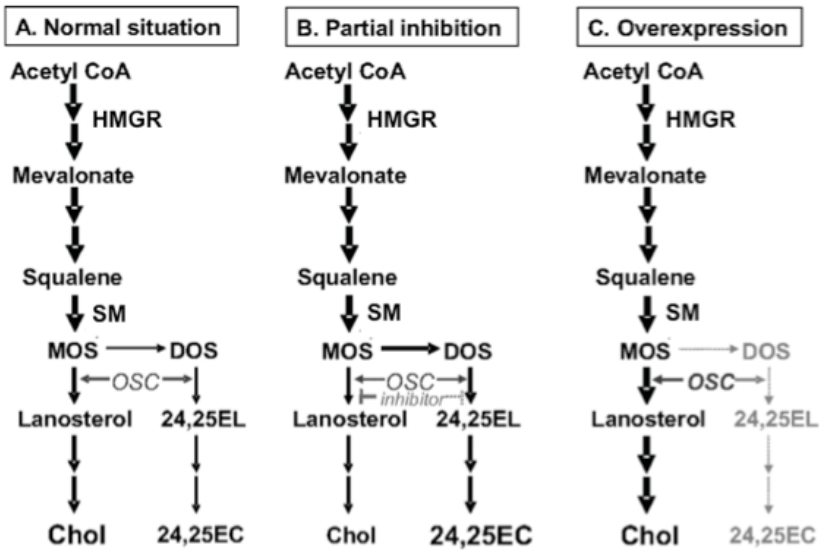

Figure 6.4 Manipulations of OSC enzyme levels determine the amount of 24,25EC being synthesized in cells

(A) Under normal conditions, OSC favors the synthesis of cholesterol (Chol), but some 24,25EC is still produced. **(B)** When partially inhibited, OSC preferentially cyclizes DOS over MOS, leading to an increase in 24,25EC synthesis. **(C)** When overexpressed, OSC acts upon MOS alone, which leads to an increase in cholesterol synthesis, and the shunt pathway used to produce 24,25EC is no longer active. (24,25EL: 24(S),25-epoxylanosterol). Figure modified from (Wong et al., 2008).

Our starting point was to determine how overexpression of SM, an important flux controlling point in cholesterol synthesis (Chapters 3, 4, and 5), affects cellular cholesterol homeostasis in cells. To this end, we cloned human SM into a pcDNA4-myc-tagged vector that has a zeocin resistance gene, and colonies were selected using the antibiotic zeocin. Seven colonies were screened, out of which one of them had a relatively higher SM expression level. Thus, cells from this colony were picked for limiting dilution, a process by which a clonal cell line can be obtained from a single cell. The colony obtained from one of the clones was then expanded, grown on a larger scale, and used for the initial characterization experiments aimed at testing SM mRNA and protein levels. These SM overexpressing stable cells (SM6.12), exhibited only a modest increase in SM mRNA and protein levels compared to parental CHO cells (Figure 6.5A and B). Also, when tested alongside the OSC stable cell line, SM6.12 expression levels were extremely low, and only showed up after a longer exposure (Figure 6.5 C).

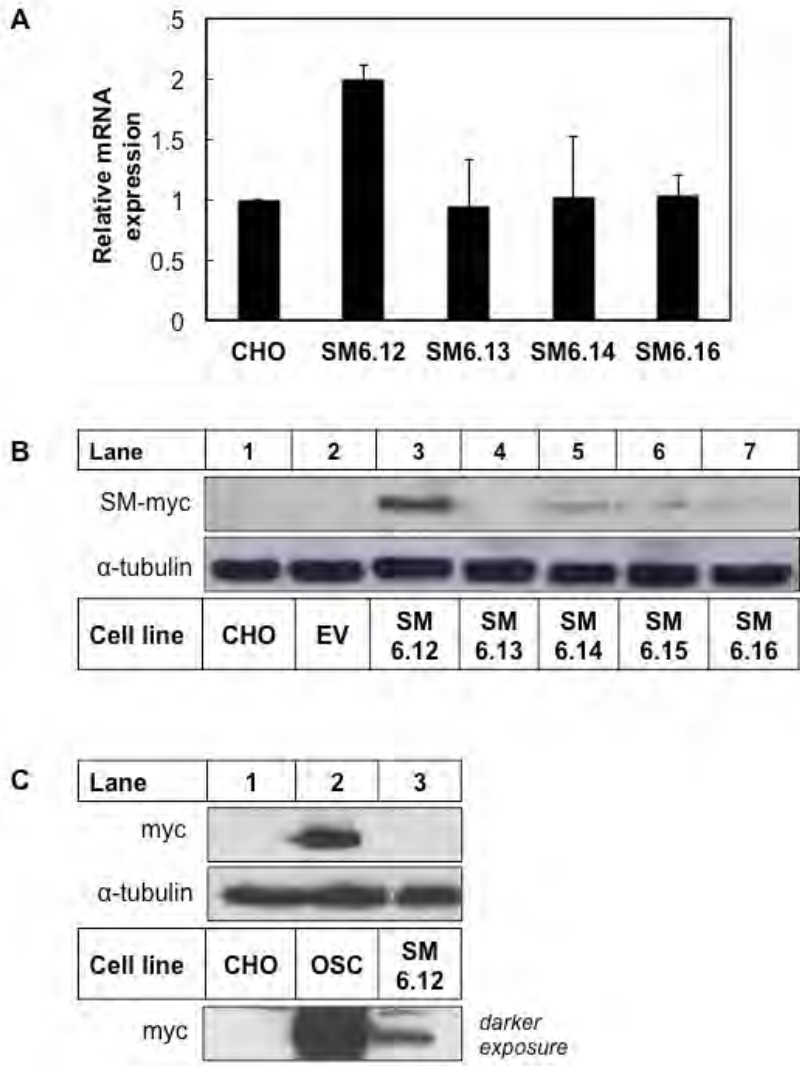

Figure 6.5 Screening of SM overexpressing stable cells

(A) SM mRNA levels of CHO cells and 4 SM stable cell lines, designated SM6.12, SM6.13, SM6.14, and SM6.16 were determined by qRT-PCR relative to the housekeeping gene PBGD. Values are mean +half range normalized to the control cell line (CHO) which is set to 1, and are from n=2 separate experiments (each performed in triplicate). **(B)** 50 μg protein from whole cell lysates were separated by 10% SDS-PAGE and immunoblotted with anti-myc (1:10 000) and anti-α-tubulin (1:200 000) antibodies, n=1. **(C)** 90 μg of protein from whole cell lysates were separated by 10% SDS-PAGE and immunoblotted with anti-myc (1:10 000) for OSC (78 kDa) and SM (64 kDa) and anti-α-tubulin (1:200 000) antibodies.

Further characterization of the SM6.12 stable cells led to an interesting observation that these cells made more 24,25EC than wild-type CHO cells. The 24,25EC to cholesterol ratio in the SM6.12 cells was approximately twice that of the wild-type cells (Figure 6.6 lane 3 versus lane 1).

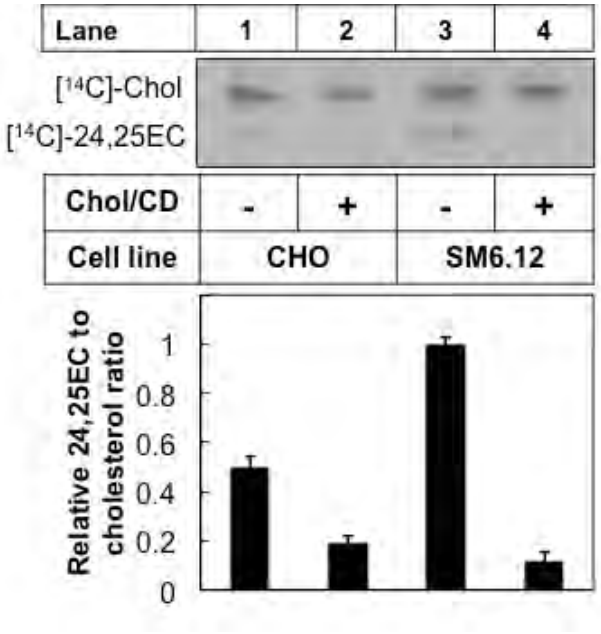

Figure 6.6 SM overexpressing cell line SM6.12 produces more 24,25EC than wild-type CHO cells

CHO-7 and SM6.12 cells were treated in medium A with 20 μg/ml Chol/CD as indicated and radiolabelled with 1 μCi/ml [^{14}C]-acetate for 6 hr, and then harvested. Neutral lipid extracts (with equal protein levels) were separated by radio-TLC and bands corresponding to cholesterol and 24,25EC were visualized, and their relative intensities quantified by densitometry. Values are relative to the vehicle-treated condition of SM6.12 which has been set to 1, and are mean + half range, representative of n=2 separate experiments.

Our laboratory has also shown that 24,25EC also regulates the synthesis of cholesterol by inhibiting the enzyme 3β-hydroxysterol-Δ24-reductase (DHCR24) (Zerenturk, E. and Kristiana, I., unpublished data). This enzyme catalyzes the conversion of desmosterol into cholesterol (Figure 6.1). The SM6.12 cells were utilized to show that endogenous 24,25EC inhibited the activity of DHCR24, decreasing cholesterol synthesis with a corresponding increase in desmosterol accumulation (Figure 6.7 lanes 7-9). As seen previously in Figure 6.6, SM6.12 cells

synthesize proportionally more 24,25EC compared to the wild-type CHO cells, whereas the OSC overexpressing stable cells in agreement with Wong et al., essentially lack 24,25EC production (Wong et al., 2008). Thus, relative 24,25EC synthesis by these three cell-lines is inversely proportional to the cholesterol to desmosterol ratio, an indicator of DHCR24 activity (Figure 6.7).

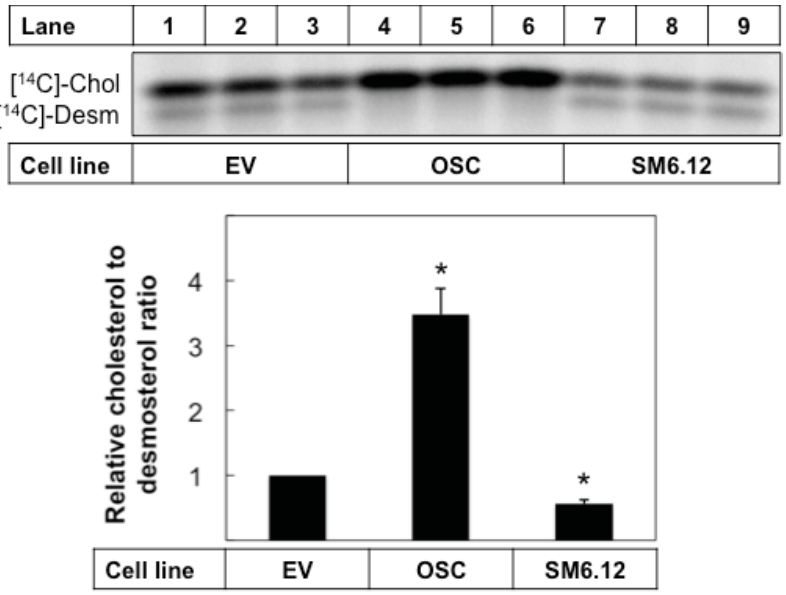

Figure 6.7 SM6.12 cells have lower cholesterol synthesis and increased desmosterol levels

Stable cell lines overexpressing 2,3-oxidosqualene cyclase (OSC), squalene monooxygenase (SM6.12), and empty vector (EV) were radiolabelled with 1 μCi/ml [^{14}C]-acetate for 4 hr. Lipid extracts were separated by argentation TLC and bands corresponding to cholesterol and desmosterol were visualized by phosphorimager and quantified by densitometry. Data was obtained from at least n=3 separate experiments and is set relative to the control cell line (EV). Densitometry was performed and is presented as mean + SEM, and $p<0.05$, using a paired t-test versus the vehicle condition.

6.3.3 24,25EC moderates the 'statin rebound effect' in cultured cells

Our laboratory previously demonstrated that endogenous 24,25EC acts as a physiological regulator by acutely controlling the *de novo* synthesis of cholesterol (Wong et al., 2008). Without 24,25EC, cholesterol synthesis was erratic and exaggerated. This effect was seen by pretreating with a statin, which induces

cholesterol biosynthetic enzymes (under the influence of SREBP-2). Consequently, after removal of the statin, there is a burst of cholesterol synthesis. This is termed the 'Statin Rebound Phenomenon'. We set out to test if endogenous 24,25EC may ameliorate the 'Statin Rebound Phenomenon' in CHO cells, by incubating them with different concentrations of a statin with or without a very low dose of an OSC inhibitor (OSCi, GW534511X) for a period of 24 hr. The OSCi dose was just enough to partially inhibit the enzyme, which then led to an increase in the production of 24,25EC (Boutaud et al., 1992; Wong et al., 2008). After washing away the drugs, the cells were radiolabelled with [^{14}C]-acetate for 2 hr in order to capture the 'Statin Rebound Phenomenon'.

Thus, with increasing statin concentrations, the amount of cholesterol synthesized during the 2 hr post-treatment period also increased. However, having the OSCi and statin together, blunted the surge seen in the levels of newly synthesized cholesterol compared to the conditions with statin alone (Figure 6.8A). This 'smoothening' effect on cholesterol levels was attributed to the increase in 24,25EC synthesis caused by the partial inhibition of OSC. We tested this directly by incubating cells with different concentrations of 24,25EC, the highest being 1 μM. When a statin was included in the treatment, there was a clear spike in cholesterol synthesis (Figure 6.8B, lane 1 versus 5), however, once the oxysterol was present along with the statin, it seemed to control and gradually decrease the level of cholesterol synthesis during the post-treatment labeling period. Our results therefore support previous work done in our laboratory that 24,25EC is indeed a physiological modulator of cholesterol levels, and have further extended this observation by showing that it is effective in blunting the burst in cholesterol synthesis, which is a consequence of the 'Statin Rebound Phenomenon'.

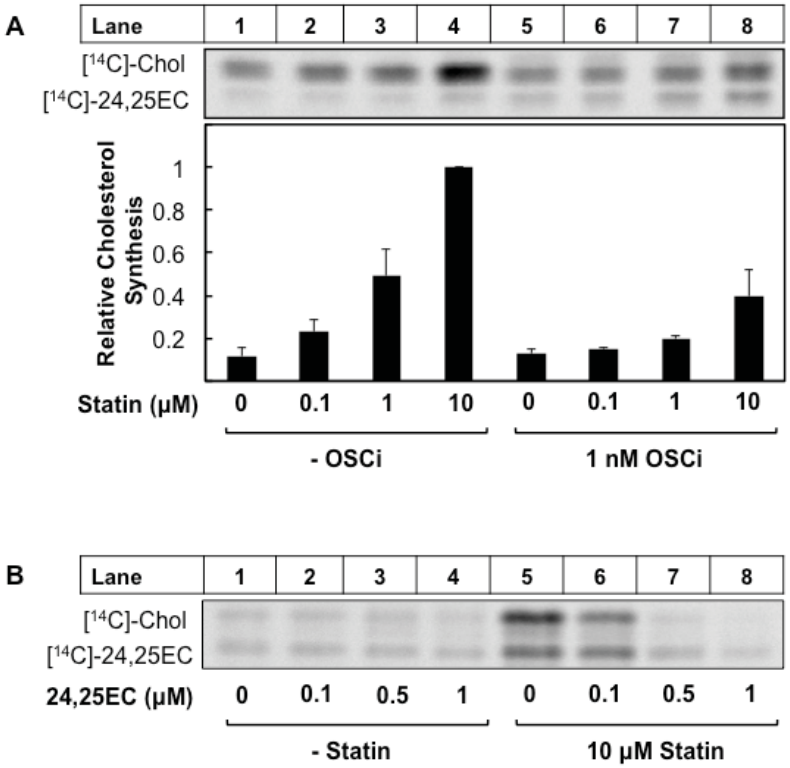

Figure 6.8 Partial inhibition of OSC leads to an increase in 24,25EC, smoothening the statin rebound effect.

CHO-7 cells were pretreated with test agents as indicated for 24 hr. After removal of the test agents, cells were radiolabeled with 1 μCi/ml [^{14}C]-acetate for 2 hr. Cell lysates were subjected to neutral lipid extraction and were analyzed by radio-TLC, and the cholesterol and 24,25EC bands were visualized using a phosphorimager, and their relative intensities were quantified (for A). **(A)** Cells were pretreated with the indicated concentrations of statin (compactin) with or without 1 nM OSCi (GW534511X) for 24 hr. The values are relative to the condition treated with 10 μM statin, which is set to 1, and are mean +SEM from 3 separate experiments. **(B)** CHO-7 cells were pretreated with the indicated concentrations of 24,25EC with or without 10 μM statin (compactin) for 24 hr, representative of n=2 separate experiments.

6.4 DISCUSSION

In this chapter, we have focused on examining various levels of cholesterol homeostasis in which the oxysterol 24,25EC could be involved. An interesting observation was made during one set of experiments where we found that the addition of cholesterol led to the disappearance of 24,25EC from the cells, giving rise to the question- does cholesterol play a role in determining the fate of this oxysterol? Initially, we assumed that this was due to cholesterol accelerating the degradation of SM, thus decreasing 24,25EC synthesis, but instead Chol/CD treatment induced efflux of 24,25EC into the media. Little is known about what happens to 24,2EC after it performs its regulatory role, including how the cell eliminates it. 24,25EC synthesized in astrocytes is secreted into culture media, and can be taken up by neurons where it can regulate neuronal cholesterol synthesis (Wong et al., 2007b). Like cholesterol, some oxysterols are known to be exported out of the cell by ABCA1 or ABCG1 transporter proteins [reviewed in (Gill et al., 2008)]. Although involvement of these ABC transporters in the efflux of 24,25EC is not known, it is noteworthy that protein expression of ABCA1 increased with cholesterol treatment under these culturing conditions (W. Luu, unpublished observations). However, the efflux of 24,25EC into the media was mostly cholesterol independent (Figure 6.3), and it is possible that the more polar nature of 24,25EC compared to cholesterol means that it does not require an active transport mechanism.

Another level of 24,25EC-dependent cholesterol regulation was observed in experiments that involved the use of the SM overexpressing stable cells (SM6.12). Since these cells overexpress SM, which we have shown is a flux-controlling enzyme in cholesterol synthesis (Chapters 3,4, and 5), we expected them to have increased cholesterol synthesis. On the contrary, instead of having more cholesterol, these cells had higher levels of 24,25EC compared to the wild-type CHO cells (Figure 6.6). This interesting feature reinforces the importance of SM in 24,25EC synthesis, and could represent a compensatory mechanism. Having increased levels of cholesterol could be toxic to cells, and therefore, the SM6.12 stable cells probably maintain their homeostasis by synthesizing more 24,25EC, which feeds back on cholesterol synthesis. Furthermore, it can be speculated that due to the role of SM

as a rate-limiting enzyme in cholesterol synthesis, it is probably not possible to obtain SM stable cells with relatively higher overexpression levels, as that would go against the natural flux of the cholesterol synthesis pathway.

Since SM6.12 synthesize more 24,25EC, they proved to be a valuable tool for studying the effect of endogenous 24,25EC on the enzyme activity of DHCR24. By inhibiting this enzyme, 24,25EC regulates cholesterol synthesis post-translationally, by blocking the penultimate step of the pathway, and also at a transcriptional level by restricting the activation of SREBP-2.

Our laboratory has previously shown that this oxysterol acutely regulates the levels of newly synthesized cholesterol (Wong et al., 2008). Considering that partial inhibition of OSC increases 24,25EC levels in cells, we aimed to test if statins could be augmented by OSC inhibitors (OSCi). Indeed, a low concentration of OSC inhibitor significantly reduced the rebound effect that occurs post-statin removal (Figure 6.8A, lanes 5-8), and this could be reproduced with added 24,25EC. This pilot data supports the idea that partial inhibition of OSC can synergize with statins and reduce the 'Statin Rebound Phenomenon'. Using this approach of combination therapy can improve drug efficacy, leading to a possibility of using a lower dose of statin, thus alleviating side effects associated with high doses of statins (Gill and Brown, 2011).

Taken together, the results presented in this chapter further strengthen the role of 24,25EC as a quintessential modulator of cholesterol synthesis.

CHAPTER 7

GENERAL DISCUSSION

7. GENERAL DISCUSSION

The importance of a regulatory enzyme in contributing to the essential and intricate process of cholesterol homeostasis has been exemplified by HMGR, the first rate-limiting enzyme in cholesterol synthesis. However, over the past four decades, a modest amount of evidence has accumulated suggesting that SM is the second rate-limiting enzyme in cholesterol synthesis (Gonzalez et al., 1979; Hidaka et al., 1990), a concept that has remained largely overlooked. In this thesis, we have provided mechanistic detail for a cholesterol-mediated, post-translational degradation of SM, which participates in controlling the overall flux of the cholesterol synthesis pathway.

7.1 Overall findings

We established that the cholesterol-dependent accumulation of squalene precedes the transcriptional downregulation of SM (Chapter 3), and is a functional consequence of the degradation of SM protein under cholesterol replete conditions (Chapter 5). The cholesterol-dependent degradation of SM requires the ubiquitin-proteasome system: protein levels were rescued through proteasomal inhibition with MG132, and polyubiquitination increased upon cholesterol treatment (Chapter 5, Figure 5.12). This regulatory mechanism for SM did not require Insig or Scap (Chapter 5, Figure 5.7), but was mediated by the N-terminal region of human SM, which also conferred sterol-regulated turnover on heterologous fusion proteins (Chapter 5, Figure 5.10). Importantly, the proteasome inhibitor MG132 reversed the accumulation of squalene, indicating that the cholesterol-accelerated proteasomal degradation of SM may help to acutely control flux through the cholesterol synthesis pathway. This concept is further strengthened by the observation that cholesterol was unable to induce the degradation of the SM construct lacking the N-terminal domain [$\Delta(W_2\text{-}K_{100})$], as demonstrated by increased formation of the product MOS in cells transfected with this construct [$\Delta(W_2\text{-}K_{100})$] compared to wild-type SM upon cholesterol enrichment (Chapter 5, Figure 5.9). Importantly, the cholesterol-dependent degradation could be recapitulated with just the N-terminal domain

(comprising the first 100 amino acids of SM) fused either to GFP or GST (Chapter 5, Figure 5.10).

Whilst generally comparable, the time course of squalene accumulation did not exactly mirror falling SM protein levels in the presence of cycloheximide: a clear cholesterol effect on protein levels was observed starting at 4 hr (Chapter 4, Figure 4.1), whereas, squalene began to accumulate as early as 2 hr of cholesterol treatment (Chapter 3, Figure 3.4 and 3.7). However, it is noteworthy that in experiments without cycloheximide, cholesterol-mediated effects on the N-terminal domain were observed as early as at 1 hr (polyubiquitination, as demonstrated in Chapter 5, Figure 5.12), and at 2 hr, using a pulse-chase approach (Chapter 5, Figure 5.11). This more rapid timing is compatible with that observed for squalene accumulation (obtained without cycloheximide). It is possible that cycloheximide may alter the kinetics of SM degradation, as has been noted previously for HMGR (Grayson et al., 1985). Nevertheless, there is a chance that other post-transcriptional mechanisms or other intricacies about this proposed model may be involved in the control of mammalian SM activity, which remain to be revealed.

The importance of SM as a regulatory enzyme is also highlighted from the unique characteristics of cells overexpressing the enzyme (SM6.12, Chapter 6, Figures 6.5 and 6.6). Owing to its strategic location at the start of the shunt pathway, 24,25EC synthesis and its modulation depends on SM protein levels. Thus, the SM6.12 cells synthesize relatively more 24,25EC and less cholesterol than wild type CHO cells, suggesting that the increased 24,25EC acutely regulates the amount of cholesterol being synthesized, thus preventing overaccumulation of cholesterol.

7.2 A distinct degradation mechanism for SM

The ubiquitination and proteasomal degradation process for HMGR has been well characterized, and the enzyme represents an ideal model for the ERAD of polytopic membrane proteins [reviewed in (Youngah and DeBose-Boyd, 2010)]. Even though SM is a second example of regulated proteasomal degradation for the control of cholesterol synthesis, it is important to note that its degradation mechanism is

distinct from that of HMGR. To begin with, the degradation signals for SM and HMGR differ: cholesterol is the only physiologically relevant sterol that degrades SM (details in Chapter 4), whereas HMGR is degraded by 24,25-dihydrolanosterol, and the oxysterols 25HC, 27HC, and 24,25EC (Song et al., 2005), all of which have no effect on SM protein levels (Chapter 4, Figure 4.4A, B, and C). SM lacks the five transmembrane sterol-sensing domain and its degradation is not mediated by Insig. Notably, the sterol specificity of SM degradation is also strikingly different than that previously shown to inhibit SREBP processing, and/or binding to Scap or Insig (summarized in Table 7.1).

7.2.1 Role of the N-terminal domain of SM

The first 100 amino acids of SM (comprising 17% of the protein) are well-conserved between mammals and birds, and are not required for the catalytic activity of the enzyme (Sakakibara et al., 1995). This region was sufficient to mediate cholesterol-regulated turnover of GST or GFP, when GFP alone for example is otherwise remarkably stable (Corish and Tyler-Smith, 1999). However, it is not known if regulated degradation of the enzyme requires direct binding of cholesterol to the N-terminus. Mutation of a single tyrosine, a residue known to be essential for cholesterol interaction, from a motif fulfilling the CRAC cholesterol binding consensus sequence (Epand, 2006; Jamin et al., 2005), had no effect on regulation (data not shown). Furthermore, it is not known if regulated degradation requires a conformational change mediated by altered membrane structure, or requires a second sensing protein. Further insight into this would require the delineation of SM membrane topology.

The blunted regulation seen for the CMV-driven expression vector (Chapter 4, Figure 4.3) hints at the presence of additional regulatory proteins. By contrast, competition for a limiting factor(s) did not appear to occur when we co-transfected full-length SM and the very highly expressed N100-GFP fusion protein (Chapter 5, Figure 5.9A). Thus, this question remains an area of uncertainty.

Table 7.1 Comparison of the ability of the listed sterols to inhibit SREBP processing, bind to SCAP or Insig, and stimulate ubiquitination (or degradation) of HMGR or SM (high, ++ ; moderate, + ; negligible, - ; not determined, nd)

Sterol	SREBP Inhibition	*In vitro* Binding		Ub/Deg.	
		Scap	Insig	HMGR	SM
7α-Hydroxycholesterol	+	-	+	-	++
7β-Hydroxycholesterol	+	-	+	-	++
7-Ketocholesterol	+	-	+	-	++
19-Hydroxycholesterol	-	-	-	++	++
24(*S*),25-Epoxycholesterol	++	-	++	++	-
25-Hydroxycholesterol	++	-	++	++	-
27-Hydroxycholesterol	++	-	++	++	-
Cholesterol	++	++	-	-	++
Desmosterol	++	++	-	-	++
7-Dehydrocholesterol	-	**nd**	**nd**	+	-
Lathosterol	-	**nd**	**nd**	**nd**	-
24,25-Dihydrolanosterol	-	**nd**	**nd**	++	-
Lanosterol	-	-	-	-	-

Partly derived from data from (Adams et al., 2004; Song and DeBose-Boyd, 2004b; Song et al., 2005b). The last column summarizes the results from Chapter 4, Figure 4.4A, B, and C of the current work.

7.3 Advantage of an additional control point in cholesterol synthesis

What might be the evolutionary advantage of having an additional post-translational control point for regulating cholesterol synthesis beyond HMGR? Transcriptional downregulation of the SREBP pathway is relatively slow, with mRNA levels of target genes only appreciably decreasing hours after treatment (Chapter 3, Figures 3.5 and 3.6), potentially leaving active enzyme with a relatively long half-life. More rapid shutdown of cholesterol synthesis requires post-transcriptional control, such as the well-documented proteasome-mediated degradation of HMGR (DeBose-Boyd, 2008b). However, HMGR activity can vary widely (DeBose-Boyd, 2008b), such that sterol synthesis could be difficult to dampen in a timely manner. Moreover, some HMGR activity is needed for isoprenoid production (Brown and Goldstein, 1980). In contrast, SM appears to have much lower activity than HMGR (Hidaka et al., 1990) and is committed to sterol production, making it suitable for rapid modulation of cholesterol synthesis independently from isoprenoid synthesis.

We propose a model whereby the mevalonate pathway is controlled rapidly and segmentally at HMGR and SM (Figure 7.1). One situation where this could be useful would be to respond to a sudden influx of exogenous cholesterol while the demand for isoprenoids such as farnesol or geranylgeraniol remains high. This argument is consistent with the observation that the physiologically relevant cholesterol molecule itself appears to be the major signal for SM degradation (Chapter 4, Figure 4.4). This raises the possibility that SM may constitute a second important control point in cholesterol synthesis, serving as a reminder that flux control of metabolic pathways tends to be shared by multiple enzymes (Thomas and Fell, 1998), which could facilitate flexible control of different intermediates. However, to what extent degradation of SM normally regulates cholesterol synthesis *in vivo* remains to be determined.

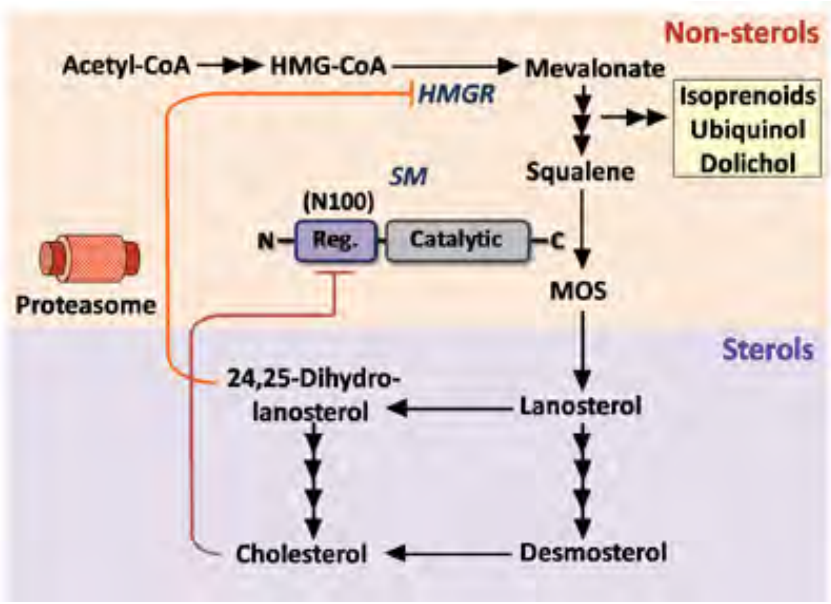

Figure 7.1 Segmental control of the cholesterol synthesis pathway

Sterol-dependent, post-translational control of the mevalonate pathway is mediated in large part by the ubiquitin-proteasome system. 3-Hydroxy-3-methylglutaryl-coenzyme A reductase (HMGR) is degraded in response to 24,25-dihydrolanosterol and side-chain oxysterols (not shown), which will consequently also reduce flux into the non-sterol branch of the pathway. In contrast, turnover of squalene monooxygenase (SM) is accelerated by the end-product, cholesterol itself, specifically inhibiting sterol production. This cholesterol-dependent degradation of SM requires its N-terminal 100 amino acids, here designated as the regulatory domain (Reg.), which is separate from the catalytic portion of the enzyme.

7.4 Implications and Significance

This work may have important implications for human health and disease, notably in relation to cardiovascular disease, but also other conditions such as, neurodegenerative diseases and certain cancers, in which cholesterol has also been implicated. The SM inhibitors NB-598 and FR194738 have been successful in inhibiting cholesterol synthesis in animal models such as dogs, hamsters, and rats (Horie et al., 1991; Sawada et al., 2001), however, have not been tested in humans. SM inhibitors could arguably be a better treatment for hypercholesterolemia than statins. This is because a number of statin-related side-effects occur due to the inhibition of isoprenoid synthesis, which is a consequence of inhibiting cholesterol synthesis at HMGR, a very early step in the pathway. Therefore, there is a need to

develop alternatives to statin therapy. Moreover, our work may rekindle interest in SM as a potential therapeutic target for hypercholesterolemia and other cholesterol-related diseases.

7.5 Future Directions

There remain some unanswered questions that could shed light on important aspects of the mechanism underlying the cholesterol-mediated degradation of SM via the ubiquitin-proteasome system.

7.5.1 Binding of cholesterol to SM

It is important to know whether cholesterol binds SM directly or indirectly, involving an interacting partner. There is also a possibility that cholesterol could induce membrane effects, such as a conformational change in SM. However, the membrane topology of SM would have to be known before investigating such effects. Nonetheless, a first useful step would be to perform cholesterol-binding assays using the N-terminal construct of SM, as this is the regulatory region of the enzyme that causes the whole enzyme to degrade in a cholesterol-dependent manner. One approach that we have begun to utilize in our laboratory is the use of [^{3}H]-photocholesterol - a photoactivatable analogue of cholesterol, in which the Δ5 double bond and the hydrogen at C-6 are replaced by the photoactivatable diazirine ring (Thiele et al., 2000). The suitability of [^{3}H]-photocholesterol labeling has been demonstrated for known cholesterol-interacting proteins such as NPC1 (Liu et al., 2009), caveolin-1 (Haberkant et al., 2008), and apolipoprotein A1 and apolipoprotein B (Thiele et al., 2000). We have begun optimizing this approach, and in the future, it would be very informative to know whether [^{3}H]-photocholesterol directly and specifically binds to the N-terminal region of SM.

7.5.2 E3 Ubiquitin Ligases

In order to completely elucidate the polyubiquitination process that SM is subjected to, the E3 ubiquitin ligase interacting with SM needs to be identified. Gp78, the

membrane-bound ubiquitin ligase that initiates sterol-dependent degradation of HMGR, associates with Insig-1 during the ubiquitination of HMGR (Song et al., 2005a). Since we have ruled out the involvement of Insig in the proteasomal degradation of SM, gp78 would most likely not be the interacting E3 ubiquitin ligase for SM. Other precedents include IDOL (Inducible Degrader of the LDLR) and TRC8, both containing the RING domain, which confers them with E3 ligase activity, and are associated with initiating the ubiquitination process of proteins involved in cholesterol homeostasis. For example, LXR regulates the uptake of cholesterol through IDOL-mediated ubiquitination of the LDL receptor (Zelcer et al., 2009). However, we have shown that 24,25EC, the most potent oxysterol ligand for LXR, has no effect on SM protein levels, possibly ruling out the involvement of IDOL in the degradation of SM. TRC8 binds to, and stimulates the ubiquitination of Insig-1 (Lee et al., 2010). Interestingly, TRC8 contains a sterol-sensing domain, and its protein levels are regulated in a sterol-dependent manner (Lee et al., 2010), such that when the cholesterol status of cells is low, TRC8 is upregulated and vice versa. Therefore, TRC8 is most likely not involved in the cholesterol-mediated degradation of SM. There is yet another ER-associated E3 ligase known as HRD1, the human orthologue of the yeast E3 ligase Hrd1p/Der3p involved in the ERAD of HMGR (Kikkert et al., 2004). Relatively little is known about HRD1, other than it being involved in the basal proteasomal degradation of mammalian HMGR, and two other ER substrates TCR-α and CD3-δ (Kikkert et al., 2004).

Coimmunoprecipitation coupled with *in vitro* ubiquitination assays could be useful to identify other likely E3 ubiquitin ligases for SM. Once the appropriate E3 ubiquitin ligase for SM is identified, other cofactors and/or proteins that interact with the E3 ligase-SM complex can be identified using affinity purification with tandem mass spectrometry.

7.5.3 SM localization to lipid droplets

Cytoplasmic lipid droplets consist of a neutral lipid core with a surrounding phospholipid monolayer. In recent years, studies have shown that a variety of

proteins are localized in lipid droplets, suggesting that they may play a more active functional role than previously thought. In addition to a wide array of signaling proteins, caveolins, and Rab proteins, SM is also localized to lipid droplets in an active state in yeast (Leber et al., 1998). Furthermore, studies have shown that other ERAD substrates such as HMGR and apolipoprotein B-100 localize to lipid droplets when proteasomal activity is blocked (Hartman et al., 2010; Ohsaki et al., 2006). In the case of HMGR, it has been speculated that after the enzyme is ubiquitinated in a sterol-dependent manner, it is translocated into a lipid droplet-associated sub-domain of the ER, where it is deglycosylated and subsequently degraded by the proteasome (Hartman et al., 2010). Furthermore, the VCP/p97 complex, which participates in the extraction of HMGR from the ER membrane, also associates with lipid droplets (Hartman et al., 2010). In light of these studies, it would be interesting to explore if mammalian SM has dual localization in the ER and lipid droplets, or whether it only localizes to lipid droplets en route to the proteasome.

7.6 Conclusion

In conclusion, our results present an example of end-product inhibition, cholesterol feeds back to promote the proteasomal degradation of SM through a mechanism distinct from that previously established for HMGR. This demonstrates yet another layer of complexity in the control of cholesterol synthesis.

APPENDICES

Table A1 Selected discoveries impacting on the Oxysterol Hypothesis

Year	Milestone
1769	Characterization of cholesterol by Poulletier de la Salle (Fieser, 1959)
1816	Named as ‘cholesterine’ by Chevreul (Chevreul, 1816)
1906	Identification of ‘oxycholesterol’ (oxysterols) by Lifschütz (Smith, 1981)
1927–8	Nobel Prizes awarded to Windaus and Wieland for elucidation of the structure of cholesterol and bile acids respectively
1933	Feedback control by cholesterol first observed (Schoenheimer and Breusch, 1933)
1953	Feedback regulation of cholesterol synthesis by other cholesterol-like compounds noted (Tomkins et al., 1953) 24(*S*)-hydroxycholesterol (cerebrosterol) discovered in human brain (Di Frisco et al., 1953)
1956	27-Hydroxycholesterol discovered to be produced from cholesterol by liver mitochondria (Fredrickson and Ono, 1956)
1964	Nobel Prize awarded to Bloch and Lynen for elucidating the cholesterol and fatty acid biosynthetic pathways
1973	Possible role of oxysterols as cholesterol synthesis mediators (Kandutsch and Chen, 1973)
1978	The Oxysterol Hypothesis formulated (Kandutsch et al., 1978)
1981	24(*S*),25-Epoxycholesterol discovered in human liver (Nelson et al., 1981a)
1985	Nobel Prize awarded to Brown and Goldstein for their discoveries concerning the regulation of cholesterol metabolism, including discovery of the LDL receptor
1993	Certain oxysterols suppress activation of SREBP (master regulators of cholesterol homeostasis) (Briggs et al., 1993)
1994	Evidence that 27-hydroxycholesterol provides a mechanism for cholesterol elimination from macrophages (Björkhem et al., 1994)

1996	Evidence that 24(*S*)-hydroxycholesterol provides a mechanism for cholesterol elimination from the brain (Lütjohann et al., 1996)
1997	Certain oxysterols proposed as natural ligands for the liver X receptors (Lehmann et al., 1997a)
2005	Certain oxysterols, and some sterol intermediates of cholesterol, accelerate degradation of HMGR (Song et al., 2005b)
2007	Evidence that certain oxysterols are important ligands for LXR *in vivo* (Chen et al., 2007); Identification of Insig as the oxysterol sensing protein in the ER (Radhakrishnan et al., 2007)
2008	Evidence that an endogenous oxysterol [24(*S*),25-epoxycholesterol] plays an acute role in smoothing cholesterol homeostatic responses (Wong et al., 2008)

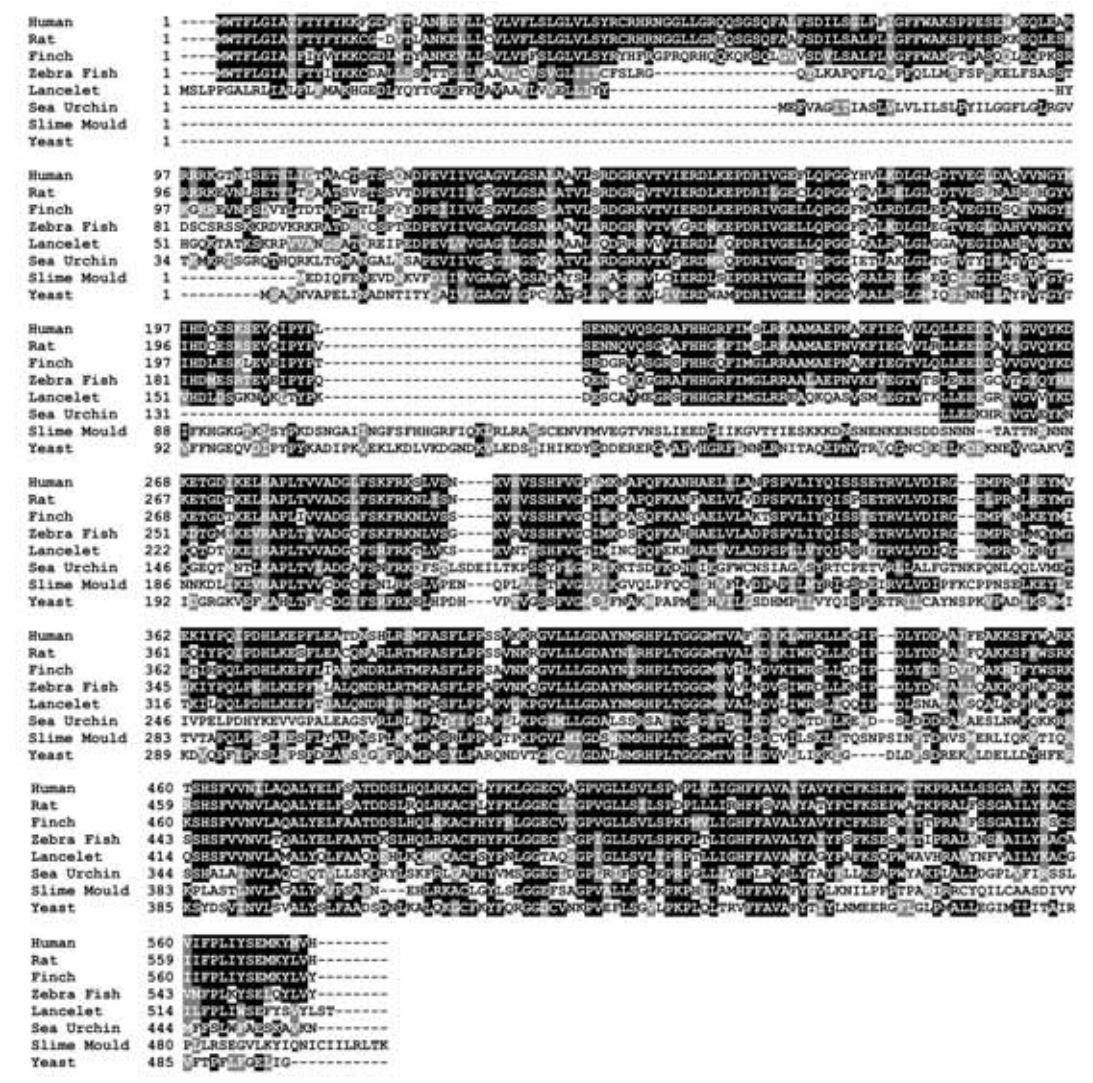

Figure A1 Multiple sequence alignment of SM protein for selected species, constructed using ClustalW2.

Alignment of human (*Homo sapiens*, NP_003120), rat (*Rattus norvegicus*, P52020), finch (*Taeniopygia guttata*, XP_002187271), zebra fish (*Danio rerio*, NP_001103509), lancelet (*Branchiostoma floridae*, XP_002594656), slime mould (*Dictyostelium discoideum*, XP_629022) and yeast (*Saccharomyces cerevisiae*, P32476).

REFERENCES

Abe, I., Seki, T., Umehara, K., Miyase, T., Noguchi, H., Sakakibara, J., and Ono, T. (2000). Green tea polyphenols: novel and potent inhibitors of squalene epoxidase. Biochem Biophys Res Commun *268*, 767-771.

Adams, C.M., Reitz, J., De Brabander, J.K., Feramisco, J.D., Li, L., Brown, M.S., and Goldstein, J.L. (2004). Cholesterol and 25-hydroxycholesterol inhibit activation of SREBPs by different mechanisms, both involving SCAP and Insigs. J Biol Chem *279*, 52772-52780.

Ahner, A., and Brodsky, J.L. (2004). Checkpoints in ER-associated degradation: excuse me, which way to the proteasome? Trends in Cell Biology *14*, 474-478.

Aikawa, M., and Libby, P. (2004). The vulnerable atherosclerotic plaque: Pathogenesis and therapeutic approach. Cardiovascular Pathology *13*, 125-138.

Beyea, M.M., Heslop, C.L., Sawyez, C.G., Edwards, J.Y., Markle, J.G., Hegele, R.A., and Huff, M.W. (2007). Selective up-regulation of LXR-regulated genes ABCA1, ABCG1, and APOE in macrophages through increased endogenous synthesis of 24(S),25-epoxycholesterol. J Biol Chem *282*, 5207-5216.

Björkhem, I. (2007). Rediscovery of cerebrosterol. Lipids *42*, 5-15.

Björkhem, I., Andersson, O., Diczfalusy, U., Sevastik, B., Xiu, R.J., Duan, C., and Lund, E. (1994). Atherosclerosis and sterol 27-hydroxylase: evidence for a role of this enzyme in elimination of cholesterol from human macrophages. Proc Natl Acad Sci U S A *91*, 8592-8596.

Björkhem, I., and Diczfalusy, U. (2004). 24(S),25-epoxycholesterol-a potential friend. Arterioscler Thromb Vasc Biol *24*, 2209-2210.

Boutaud, O., Dolis, D., and Schuber, F. (1992). Preferential cyclization of 2,3(S):22(S),23-dioxidosqualene by mammalian 2,3-oxidosqualene-lanosterol cyclase. Biochem Biophys Res Commun *188*, 898-904.

Breitschopf, K., Bengal, E., Ziv, T., Admon, A., and Ciechanover, A. (1998). A novel site for ubiquitination: the N-terminal residue, and not internal lysines of MyoD, is essential for conjugation and degradation of the protein. Embo J *17*, 5964-5973.

Briggs, M.R., Yokoyama, C., Wang, X., Brown, M.S., and Goldstein, J.L. (1993). Nuclear protein that binds sterol regulatory element of low density lipoprotein receptor promoter. I. Identification of the protein and delineation of its target nucleotide sequence. J Biol Chem *268*, 14490-14496.

Brown, A.J. (2007). Cholesterol, Statins and Cancer. Clin Exper Pharm Physiol *34*, 135-141.

Brown, A.J. (2009). 24(S),25-epoxycholesterol: a messenger for cholesterol homeostasis. Int J Biochem Cell Biol *41*, 744-747.

Brown, A.J. (2010). Does Upsizing Statins have a Downside? Drug Safety *33*, 435-436 410.2165/11532370-000000000-000000000.

Brown, A.J., Dean, R.T., and Jessup, W. (1996). Free and esterified oxysterol: formation during copper-oxidation of low density lipoprotein and uptake by macrophages. J Lipid Res *37*, 320-335.

Brown, A.J., and Jessup, W. (1999). Oxysterols and atherosclerosis. Atherosclerosis *142*, 1-28.

Brown, A.J., Leong, S.L., Dean, R.T., and Jessup, W. (1997). 7-Hydroperoxycholesterol and its products in oxidized low density lipoprotein and human atherosclerotic plaque. J Lipid Res *38*, 1730-1745.

Brown, A.J., Sun, L., Feramisco, J.D., Brown, M.S., and Goldstein, J.L. (2002). Cholesterol addition to ER membranes alters conformation of SCAP, the SREBP escort protein that regulates cholesterol metabolism. Mol Cell *10*, 237-245.

Brown, A.J., Watts, G.F., Burnett, J.R., Dean, R.T., and Jessup, W. (2000). Sterol 27-hydroxylase acts on 7-ketocholesterol in human atherosclerotic lesions and macrophages in culture. J Biol Chem *275*, 27627-27633.

Brown, M.S., and Goldstein, J.L. (1976). The low density lipoprotein pathway in human fibroblasts: Relation between cell surface receptor binding and endocytosis of low density lipoprotein Annals of the New York Academy of Sciences *275*, 19.

Brown, M.S., and Goldstein, J.L. (1980). Multivalent feedback regulation of HMG CoA reductase, a control mechanism coordinating isoprenoid synthesis and cell growth. J Lipid Res *21*, 505-517.

Brown, M.S., and Goldstein, J.L. (1986). A receptor-mediated pathway for cholesterol homeostasis. Science *232*, 34-47.

Chen, W., Chen, G., Head, D.L., Mangelsdorf, D.J., and Russell, D.W. (2007). Enzymatic reduction of oxysterols impairs LXR signaling in cultured cells and the livers of mice. Cell Metab *5*, 73-79.

Chevreul, M.E. (1816). Examen des graisses d'homme, de mouton, de boeuf, de jaguar et d'oie. Ann Chim Phys *2*, 339-372.

Chugh, A., Ray, A., and Gupta, J.B. (2003). Squalene epoxidase as hypocholesterolemic drug target revisited. Prog Lipid Res *42*, 37-50.

Click, E.M., and Balian, G. (1985). Domain structure of human plasma and cellular fibronectin. Use of a monoclonal antibody and heparin affinity to identify three different subunit chains. Biochemistry *24*, 6685-6696.

Corey, E.J., Russey, W.E., and de Montellano, P.R.O. (1966). 2,3-Oxidosqualene, an Intermediate in the Biological Synthesis of Sterols from Squalene1. Journal of the American Chemical Society *88*, 4750-4751.

Corish, P., and Tyler-Smith, C. (1999). Attenuation of green fluorescent protein half-life in mammalian cells. Protein Eng *12*, 1035-1040.

Cummins, C.L., and Mangelsdorf, D.J. (2006). Liver X receptors and cholesterol homoeostasis: spotlight on the adrenal gland. Biochem Soc Trans *34*, 1110-1113.

Daskalopoulou, S.S. (2009). When statin therapy stops: implications for the patient. Current Opinion in Cardiology *24*, 454-460 410.1097/HCO.1090b1013e32832ebf32892.

DeBose-Boyd, R.A. (2008a). Feedback regulation of cholesterol synthesis: sterol-accelerated ubiquitination and degradation of HMG CoA reductase. Cell research *18*, 609-621.

DeBose-Boyd, R.A. (2008b). Feedback regulation of cholesterol synthesis: sterol-accelerated ubiquitination and degradation of HMG CoA reductase. Cell Res *18*, 609-621.

Deshaies, R.J., and Joazeiro, C.A.P. (2009). RING Domain E3 Ubiquitin Ligases. Annu Rev Biochem *78*, 35.

Di Frisco, S., De Ruggieri, P., and Ercoli, A. (1953). Isolation of cerebrosterol from human brain. Boll Soc Ital Biol Sper *29*, 1351-1352.

Dollis, D., and Schuber, F. (1994). Effects of a 2,3-oxidosqualene-lanosterol cyclase inhibitor, 2,3:22,23-dioxidosqualene and 24,25-epoxycholesterol on the regulation of cholesterol biosynthesis in human hepatoma cell line HepG2. Biochem Pharmacol *48*, 49-57.

Du, X., Kristiana, I., Wong, J., and Brown, A.J. (2006). Involvement of Akt in ER-to-Golgi transport of SCAP/SREBP: a link between a key cell proliferative pathway and membrane synthesis. Mol Biol Cell *17*, 2735-2745.

Dzeletovic, S., Breuer, O., Lund, E., and Diczfalusy, U. (1995). Determination of cholesterol oxidation products in human plasma by isotope Dilution-Mass Spectrometry. Anal Biochem *225*, 73-80.

Eilenberg, H., and Shechter, I. (1984). A possible regulatory role of squalene epoxidase in Chinese hamster ovary cells. Lipids *19*, 539-543.

Endo, A., Kuroda, M., and Tsujita, Y. (1976). ML-236A, ML-236B, and ML-236C, new inhibitors of cholesterogenesis produced by Penicillium citrinium J Antiobiot (Tokyo) *29*, 3.

Engel, T., Kannenberg, F., Fobker, M., Nofer, J.-R., Bode, G., Lueken, A., Assmann, G., and Seedorf, U. (2007). Expression of ATP binding cassette-transporter ABCG1 prevents cell death by transporting cytotoxic 7β-hydroxycholesterol. FEBS Letters *581*, 1673-1680.

Epand, R.M. (2006). Cholesterol and the interaction of proteins with membrane domains. Prog Lipid Res *45*, 279-294.

Espenshade, P.J. (2006). SREBPs: sterol-regulated transcription factors. Journal of cell science *119*, 973-976.

Espenshade, P.J., Li, W.P., and Yabe, D. (2002). Sterols block binding of COPII proteins to SCAP, thereby controlling SCAP sorting in ER. Proc Natl Acad Sci U S A *99*, 11694-11699.

Favre, B., and Ryder, N.S. (1997). Cloning and expression of squalene epoxidase from the pathogenic yeast Candida albicans. Gene *189*, 119-126.

Ferguson, J.B., and Bloch, K. (1977). Purification and properties of a soluble protein activator of rat liver squalene epoxidase. The Journal of biological chemistry *252*, 5381-5385.

Fieser, L.F., Fieser, M (1959). Steroids (New York, Reinhold Publishing Corporation).

Folkers, K., Langsjoen, P., Willis, R., Richardson, P., Xia, L.J., Ye, C.Q., and Tamagawa, H. (1990). Lovastatin decreases coenzyme Q levels in humans. Proceedings of the National Academy of Sciences *87*, 8931-8934.

Fredrickson, D.S., and Ono, K. (1956). The in vitro production of 25- and 26-hydroxycholesterol and their in vivo metabolism. Biochim Biophys Acta *22*, 183-184.

Fuks-Holmberg, D., and Bloch, K. (1983). Intermembrane transfer of squalene promoted by supernatant protein factor. Journal of Lipid Research *24*, 402-408.

Funk, J., and Landes, C. (2005). Histopathologic findings after treatment with different oxidosqualene cyclase (OSC) inhibitors in hamsters and dogs. Experimental and toxicologic pathology : official journal of the Gesellschaft fur Toxikologische Pathologie *57*, 29-38.

Furberg, C., and Pitt, B. (2001). Withdrawal of cerivastatin from the world market. Current Controlled Trials in Cardiovascular Medicine *2*, 205 - 207.

Garza, R., Tran, P., and Hampton, R.Y. (2009). Geranylgeranyl pyrophosphate (GGPP) is a potent regulator of HRD-dependent HMG-CoA reductase degradation in yeast. J Biol Chem *284*, 12.

Gelissen, I.C., Brown, A.J., Mander, E.L., Kritharides, L., Dean, R.T., and Jessup, W. (1996). Sterol efflux is impaired from macrophage foam cells selectively enriched with 7-ketocholesterol. J Biol Chem *271*, 17852-17860.

Gil, G., Faust, J.R., Chin, D.J., Goldstein, J.L., and Brown, M.S. (1985). Membrane-bound domain of HMG CoA reductase is required for sterol-enhanced degradation of the enzyme. Cell *41*, 249-258.

Gill, S., and Brown, A. (2011). Exploiting a Physiological Regulator to Improve the Efficacy and Safety of Statins. Cardiovascular Drugs and Therapy *25*, 183-185.

Gill, S., Chow, R., and Brown, A.J. (2008). Sterol regulators of cholesterol homeostasis and beyond: the oxysterol hypothesis revisited and revised. Prog Lipid Res *47*, 391-404.

Goldstein, J.L., Basu, S.K., and Brown, M.S. (1983). Receptor-mediated endocytosis of low-density lipoprotein in cultured cells. Methods Enzymol *98*, 241-260.

Goldstein, J.L., and Brown, M.S. (1990). Regulation of the mevalonate pathway. Nature *343*, 425-430.

Goldstein, J.L., and Brown, M.S. (2009). The LDL Receptor. Arteriosclerosis, Thrombosis, and Vascular Biology *29*, 431-438.

Goldstein, J.L., DeBose-Boyd, R.A., and Brown, M.S. (2006a). Protein sensors for membrane sterols. Cell *124*, 35-46.

Goldstein, J.L., DeBose-Boyd, R.A., and Brown, M.S. (2006b). Protein sensors for membrane sterols. Cell *124*, 35-46.

Gong, Y., Lee, J.N., Lee, P.C.W., Goldstein, J.L., Brown, M.S., and Ye, J. (2006). Sterol-regulated ubiquitination and degradation of Insig-1 creates a convergent mechanism for feedback control of cholesterol synthesis and uptake. Cell Metabolism *3*, 15-24.

Gonzalez, R., Carlson, J.P., and Dempsey, M.E. (1979). Two major regulatory steps in cholesterol synthesis by human renal cancer cells. Arch Biochem Biophys *196*, 574-580.

Gould, R.G., Taylor, C.B., Hangerman, J.S., Warner, I., and Campbell, D.J. (1952). Cholesterol metabolism I. Effect of dietary cholesterol on the synthesis of cholesterol in dog tissue in vitro. J Biol Chem *201*, 519-528.

Graham, D.J., Staffa, J.A., Shatin, D., Andrade, S.E., Schech, S.D., La Grenade, L., Gurwitz, J.H., Chan, K.A., Goodman, M.J., and Platt, R. (2004). Incidence of Hospitalized Rhabdomyolysis in Patients Treated With Lipid-Lowering Drugs. JAMA: The Journal of the American Medical Association *292*, 2585-2590.

Grayson, D.R., Lee, L., and Evans, D.R. (1985). Immunochemical analysis of the domain structure of CAD, the multifunctional protein that initiates pyrimidine biosynthesis in mammalian cells. The Journal of biological chemistry *260*, 15840-15849.

Gupta, N., and Porter, T.D. (2001). Garlic and garlic-derived compounds inhibit human squalene monooxygenase. J Nutr *131*, 1662-1667.

Haberkant, P., Schmitt, O., Contreras, F.-X., Thiele, C., Hanada, K., Sprong, H., Reinhard, C., Wieland, F.T., and Br√ºgger, B. (2008). Protein-sphingolipid interactions within cellular membranes. Journal of Lipid Research *49*, 251-262.

Hampton, R.Y. (2002). ER-associated degradation in protein quality control and cellular regulation. Curr Opin Cell Biol *14*, 476-482.

Hampton, R.Y., and Bhakta, H. (1997). Ubiquitin-mediated regulation of 3-hydroxy-3-methylglutaryl-CoA‚ÄâreductaseProceedings of the National Academy of Sciences *94*, 12944-12948.

Hartman, I.Z., Liu, P., Zehmer, J.K., Luby-Phelps, K., Jo, Y., Anderson, R.G., and DeBose-Boyd, R.A. (2010). Sterol-induced dislocation of 3-hydroxy-3-methylglutaryl coenzyme A reductase from endoplasmic reticulum membranes into the cytosol through a subcellular compartment resembling lipid droplets. J Biol Chem *285*, 19288-19298.

Hebert, D.N., Zhang, J.X., Chen, W., Foellmer, B., and Helenius, A. (1997). The number and location of glycans on influenza hemagglutinin determine folding and association with calnexin and calreticulin. The Journal of cell biology *139*, 613-623.

Hellstrom, K.H., Siperstein, M.D., Bricker, L.A., and Luby, L.J. (1973). Studies of the In Vivo Metabolism of Mevalonic Acid in the Normal Rat. The Journal of Clinical Investigation *52*, 1303-1313.

Hidaka, Y., Hotta, H., Nagata, Y., Iwasawa, Y., Horie, M., and Kamei, T. (1991). Effect of a novel squalene epoxidase inhibitor, NB-598, on the regulation of cholesterol metabolism in Hep G2 cells. Journal of Biological Chemistry *266*, 13171-13177.

Hidaka, Y., Satoh, T., and Kamei, T. (1990). Regulation of squalene epoxidase in HepG2 cells. J Lipid Res *31*, 2087-2094.

Horie, M., Sawasaki, Y., Fukuzumi, H., Watanabe, K., Iizuka, Y., Tsuchiya, Y., and Kamei, T. (1991). Hypolipidemic effects of NB-598 in dogs. Atherosclerosis *88*, 183-192.

Horie, M., Tsuchiya, Y., Hayashi, M., Iida, Y., Iwasawa, Y., Nagata, Y., Sawasaki, Y., Fukuzumi, H., Kitani, K., and Kamei, T. (1990). NB-598: a potent competitive inhibitor of squalene epoxidase. Journal of Biological Chemistry *265*, 18075-18078.

Horton, J.D., Goldstein, J.L., and Brown, M.S. (2002a). SREBPs: activators of the complete program of cholesterol and fatty acid synthesis in the liver. The Journal of Clinical Investigation *109*, 1125-1131.

Horton, J.D., Goldstein, J.L., and Brown, M.S. (2002b). SREBPs: transcriptional mediators of lipid homeostasis. Cold Spring Harb Symp Quant Biol *67*, 491-498.

Horton, J.D., Shah, N.A., Warrington, J.A., Anderson, N.N., Park, S.W., Brown, M.S., and Goldstein, J.L. (2003). Combined analysis of oligonucleotide microarray data from transgenic and knockout mice identifies direct SREBP target genes. Proc Natl Acad Sci U S A *100*, 12027-12032.

Hsu, H.J., Hsu, N.C., Hu, M.C., and Chung, B.C. (2006). Steroidogenesis in zebrafish and mouse models. Molecular and cellular endocrinology *248*, 160-163.

Hua, X., Nohturfft, A., Goldstein, J.L., and Brown, M.S. (1996). Sterol resistance in CHO cells traced to point mutation in SREBP cleavage-activating protein. Cell *87*, 415-426.

Huff, M.W., and Telford, D.E. (2005). Lord of the rings - the mechanism for oxidosqualene:lanosterol cyclase becomes crystal clear. Trends in Pharmacological Sciences *26*, 335-340.

Istvan, E.S. (2002). Structural mechanism for statin inhibition of 3-hydroxy-3-methylglutaryl coenzyme A reductase. American Heart Journal *144*, S27-S32.

Istvan, E.S., and Deisenhofer, J. (2001). Structural Mechanism for Statin Inhibition of HMG-CoA Reductase. Science *292*, 1160-1164.

Jamin, N., Neumann, J.M., Ostuni, M.A., Vu, T.K.N., Yao, Z.X., Murail, S., Robert, J.C., Giatzakis, C., Papadopoulos, V., and Lacap√®re, J.J. (2005). Characterization of the cholesterol recognition amino acid consensus sequence of the peripheral-type benzodiazepine receptor. Molecular Endocrinology *19*, 588-594.

Janowski, B.A., Grogan, M.J., Jones, S.A., Wisely, G.B., Kliewer, S.A., Corey, E.J., and Mangelsdorf, D.J. (1999). Structural requirements of ligands for the oxysterol liver X receptors LXR-α and LXR-β. Proc Natl Acad Sci U S A *96*, 266-271.

Janowski, B.A., Shan, B., and Russell, D.W. (2001). The hypocholesterolemic agent LY295427 reverses suppression of sterol regulatory element-binding protein processing mediated by oxysterols. J Biol Chem *276*, 45408-45416.

Janowski, B.A., Willy, P.J., Devi, T.R., Falck, J.R., and Mangelsdorf, D.J. (1996). An oxysterol signalling pathway mediated by the nuclear receptor LXR[alpha]. Nature *383*, 728-731.

Javitt, N.B. (2002). 25R,26-Hydroxycholesterol revisited: synthesis, metabolism, and biologic roles. J Lipid Res *43*, 665-670.

Jentsch, S., and Rumpf, S. (2007). Cdc48 (p97): a molecular gearbox in the ubiquitin pathway? Trends in biochemical sciences *32*, 6-11.

Jo, Y., and DeBose-Boyd, R.A. (2010a). Control of cholesterol synthesis through regulated ER-associated degradation of HMG CoA reductase. Critical Reviews in Biochemistry and Molecular Biology *45*, 185-198.

Jo, Y., and DeBose-Boyd, R.A. (2010b). Control of Cholesterol Synthesis through Regulated ER-Associated Degradation of HMG CoA Reductase

. Crit Rev Biochem Mol Biol *45*, 185–198.

Kandutsch, A.A., and Chen, H.W. (1973). Inhibition of sterol synthesis in cultured mouse cells by 7α-hydroxycholesterol, 7β-hydroxycholesterol, and 7-ketocholesterol. J Biol Chem *248*, 8408-8417.

Kandutsch, A.A., Chen, H.W., and Heiniger, H.J. (1978). Biological activity of some oxygenated sterols. Science *201*, 498-501.

Kennedy, M.A., Barrera, G.C., Nakamura, K., Baldan, A., Tarr, P., Fishbein, M.C., Frank, J., Francone, O.L., and Edwards, P.A. (2005). ABCG1 has a critical role in mediating cholesterol efflux to HDL and preventing cellular lipid accumulation. Cell Metab *1*, 121-131.

Kielar, D., Dietmaier, W., Langmann, T., Aslanidis, C., Probst, M., Naruszewicz, M., and Schmitz, G. (2001). Rapid quantification of human ABCA1 mRNA in various cell types and tissues by real-time reverse transcription-PCR. Clin Chem *47*, 2089-2097.

Kikkert, M., Doolman, R., Dai, M., Avner, R., Hassink, G., van Voorden, S., Thanedar, S., Roitelman, J., Chau, V., and Wiertz, E. (2004). Human HRD1 Is an E3 Ubiquitin Ligase Involved in Degradation of Proteins from the Endoplasmic Reticulum. Journal of Biological Chemistry *279*, 3525-3534.

Kostova, Z., Tsai, Y.C., and Weissman, A.M. (2007). Ubiquitin ligases, critical mediators of endoplasmic reticulum-associated degradation. Seminars in Cell & Developmental Biology *18*, 770-779.

Kosuga, K., Hata, S., Osumi, T., Sakakibara, J., and Ono, T. (1995). Nucleotide sequence of a cDNA for mouse squalene epoxidase. Biochimica et Biophysica Acta (BBA) - Gene Structure and Expression *1260*, 345-348.

Kunjathoor, V.V., Febbraio, M., Podrez, E.A., Moore, K.J., Andersson, L., Koehn, S., Rhee, J.S., Silverstein, R., Hoff, H.F., and Freeman, M.W. (2002). Scavenger Receptors Class A-I/II and CD36 Are the Principal Receptors Responsible for the Uptake of Modified Low Density Lipoprotein Leading to Lipid Loading in Macrophages. Journal of Biological Chemistry *277*, 49982-49988.

Kuwabara, P.E., and Labouesse, M. (2002). The sterol-sensing domain: multiple families, a unique role? Trends in genetics : TIG *18*, 193-201.

Laden, B.P., and Porter, T.D. (2001). Resveratrol inhibits human squalene monooxygenase. Nutrition Research *21*, 747-753.

Laden, B.P., Tang, Y., and Porter, T.D. (2000). Cloning, Heterologous Expression, and Enzymological Characterization of Human Squalene Monooxygenase. Archives of Biochemistry and Biophysics *374*, 381-388.

Lange, Y., Ory, D.S., Ye, J., Lanier, M.H., Hsu, F.F., and Steck, T.L. (2008). Effectors of rapid homeostatic responses of endoplasmic reticulum cholesterol and 3-hydroxy-3-methylglutaryl-CoA reductase. J Biol Chem *283*, 1445-1455.

Langsjoen, P.H., and Langsjoen, A. (2003). The clinical use of HMG CoA-reductase inhibitors and the associated depletion of coenzyme Q_10. A review of animal and human publications. BioFactors *18*, 101-111.

Leber, R., Landl, K., Zinser, E., Ahorn, H., Spok, A., Kohlwein, S.D., Turnowsky, F., and Daum, G. (1998). Dual localization of squalene epoxidase, Erg1p, in yeast reflects a relationship between the endoplasmic reticulum and lipid particles. Mol Biol Cell *9*, 375-386.

Lee, J.P., Brauweiler, A., Rudolph, M., Hooper, J.E., Drabkin, H.A., and Gemmill, R.M. (2010). The TRC8 Ubiquitin Ligase Is Sterol Regulated and Interacts with Lipid and Protein Biosynthetic Pathways. Molecular Cancer Research *8*, 93-106.

Lee, J.W., Fuda, H., Javitt, N.B., Strott, C.A., and Rodriguez, I.R. (2006). Expression and localization of sterol 27-hydroxylase (CYP27A1) in monkey retina. Exp Eye Res *83*, 465-469.

Lee, P.C., Sever, N., and Debose-Boyd, R.A. (2005). Isolation of sterol-resistant Chinese hamster ovary cells with genetic deficiencies in both Insig-1 and Insig-2. J Biol Chem *280*, 25242-25249.

Lee, P.C.W., Nguyen, A.D., and DeBose-Boyd, R.A. (2007). Mutations within the membrane domain of HMG-CoA reductase confer resistance to sterol-accelerated degradation. Journal of Lipid Research *48*, 318-327.

Lehmann, J.M., Kliewer, S.A., Moore, L.B., Smith-Oliver, T.A., Oliver, B.B., Su, J.L., Sundseth, S.S., Winegar, D.A., Blanchard, D.E., Spencer, T.A., *et al.* (1997a). Activation of the nuclear receptor LXR by oxysterols defines a new hormone response pathway. J Biol Chem *272*, 3137-3140.

Lehmann, J.r.M., Kliewer, S.A., Moore, L.B., Smith-Oliver, T.A., Oliver, B.B., Su, J.-L., Sundseth, S.S., Winegar, D.A., Blanchard, D.E., Spencer, T.A., *et al.* (1997b). Activation of the Nuclear Receptor LXR by Oxysterols Defines a New Hormone Response Pathway. Journal of Biological Chemistry *272*, 3137-3140.

Liao, J.K., and Laufs, U. (2004). Pleiotropic Effects of Statins. Annu Rev Pharmacol Toxicol.

Liscum, L., Finer-Moore, J., Stroud, R.M., Luskey, K.L., Brown, M.S., and Goldstein, J.L. (1985). Domain structure of 3-hydroxy-3-methylglutaryl coenzyme A reductase, a glycoprotein of the endoplasmic reticulum. The Journal of biological chemistry *260*, 522-530.

Liu, R., Lu, P., Chu, J.W.K., and Sharom, F.J. (2009). Characterization of Fluorescent Sterol Binding to Purified Human NPC1. Journal of Biological Chemistry *284*, 1840-1852.

Loftus, S.K., Morris, J.A., Carstea, E.D., Gu, J.Z., Cummings, C., Brown, A., Ellison, J., Ohno, K., Rosenfeld, M.A., Tagle, D.A., *et al.* (1997). Murine Model of Niemann-Pick C Disease: Mutation in a Cholesterol Homeostasis Gene. Science *277*, 232-235.

Luskey, K.L., and Stevens, B. (1985). Human 3-hydroxy-3-methylglutaryl coenzyme A reductase. Conserved domains responsible for catalytic activity and sterol-regulated degradation. Journal of Biological Chemistry *260*, 10271-10277.

Lütjohann, D., Breuer, O., Ahlborg, G., Nennesmo, I., Siden, A., Diczfalusy, U., and Bjorkhem, I. (1996). Cholesterol homeostasis in human brain: Evidence for an age-dependent flux of 24S-hydroxycholesterol from the brain into the circulation. Proc Natl Acad Sci U S A *93*, 9799-9804.

Lyons, M.A., and Brown, A.J. (2001). Metabolism of an oxysterol, 7-ketocholesterol, by sterol 27-hydroxylase in HepG2 cells. Lipids *36*, 701-711.

Mark, M., Muller, P., Maier, R., and Eisele, B. (1996). Effects of a novel 2,3-oxidosqualene cyclase inhibitor on the regulation of cholesterol biosynthesis in HepG2 cells. J Lipid Res *37*, 148-158.

Maxfield, F.R., and Tabas, I. (2005). Role of cholesterol and lipid organization in disease. Nature *438*, 612-621.

McGinnis, B., Olson, K.L., Magid, D., Bayliss, E., Korner, E.J., Brand, D.W., and Steiner, J.F. (2007). Factors Related to Adherence to Statin Therapy. The Annals of Pharmacotherapy *41*, 1805-1811.

Meusser, B., Hirsch, C., Jarosch, E., and Sommer, T. (2005). ERAD: the long road to destruction. Nat Cell Biol *7*, 766-772.

Molinari, M., Galli, C., Piccaluga, V., Pieren, M., and Paganetti, P. (2002). Sequential assistance of molecular chaperones and transient formation of covalent complexes during protein degradation from the ER. The Journal of cell biology *158*, 247-257.

Moore, K.J., and Tabas, I. (2011). Macrophages in the Pathogenesis of Atherosclerosis. Cell *145*, 341-355.

Motamed, M., Zhang, Y., Wang, M.L., Seemann, J., Kwon, H.J., Goldstein, J.L., and Brown, M.S. (2011). Identification of luminal loop 1 of scap as the sterol sensor that maintains cholesterol homeostasis. Journal of Biological Chemistry.

Mukherjee, S., and Maxfield, F.R. (2004). Lipid and cholesterol trafficking in NPC. Biochimica et Biophysica Acta (BBA) - Molecular and Cell Biology of Lipids *1685*, 28-37.

Nakanishi, M., Goldstein, J.L., and Brown, M.S. (1988). Multivalent control of 3-hydroxy-3-methylglutaryl coenzyme A reductase. Mevalonate-derived product inhibits translation of mRNA and accelerates degradation of enzyme. J Biol Chem *263*, 8929-8937.

Nelson, J.A., Steckbeck, S.R., and Spencer, T.A. (1981a). Biosynthesis of 24,25-epoxycholesterol from squalene 2,3;22,23-dioxide. J Biol Chem *256*, 1067-1068.

Nelson, J.A., Steckbeck, S.R., and Spencer, T.A. (1981b). Biosynthesis of 24,25-epoxycholesterol from squalene 2,3;22,23-dioxide. J Biol Chem *256*, 1067-1068.

Nishimura, T., Inoue, T., Shibata, N., Sekine, A., Takabe, W., Noguchi, N., and Arai, H. (2005). Inhibition of cholesterol biosynthesis by 25-hydroxycholesterol is independent of OSBP. Genes Cells *10*, 793-801.

Ohsaki, Y., Cheng, J., Fujita, A., Tokumoto, T., and Fujimoto, T. (2006). Cytoplasmic Lipid Droplets Are Sites of Convergence of Proteasomal and Autophagic Degradation of Apolipoprotein B. Mol Biol Cell *17*, 2674-2683.

Ono, T. (2002). The first step of oxygenation in cholesterol biosynthesis. Biochem Biophys Res Commun *292*, 1283-1288.

Ono, T., and Bloch, K. (1975). Solubilization and partial characterization of rat liver squalene epoxidase. The Journal of biological chemistry *250*, 1571-1579.

Oram, J.F., Wolfbauer, G., Vaughan, A.M., Tang, C., and Albers, J.J. (2003). Phospholipid transfer protein interacts with and stabilizes ATP-binding cassette transporter A1 and enhances cholesterol efflux from cells. J Biol Chem *278*, 52379-52385.

Pennings, M., Meurs, I., Ye, D., Out, R., Hoekstra, M., Van Berkel, T.J.C., and Eck, M.V. (2006). Regulation of cholesterol homeostasis in macrophages and consequences for atherosclerotic lesion development. FEBS Letters *580*, 5588-5596.

Radhakrishnan, A., Ikeda, Y., Kwon, H.J., Brown, M.S., and Goldstein, J.L. (2007). Sterol-regulated transport of SREBPs from endoplasmic reticulum to golgi:

oxysterols block transport by binding to Insig. Proc Natl Acad Sci U S A *104*, 6511-6518.

Radhakrishnan, A., Sun, L.P., Kwon, H.J., Brown, M.S., and Goldstein, J.L. (2004). Direct binding of cholesterol to the purified membrane region of SCAP: mechanism for a sterol-sensing domain. Molecular cell *15*, 259-268.

Raskin, P., and Siperstein, M.D. (1974). Mevalonate metabolism by renal tissue in vitro. J Lipid Res *15*, 20-25.

Ravid, T., Doolman, R., Avner, R., Harats, D., and Roitelman, J. (2000). The ubiquitin-proteasome pathway mediates the regulated degradation of mammalian 3-hydroxy-3-methylglutaryl-coenzyme A reductase. The Journal of biological chemistry *275*, 35840-35847.

Rawson, R.B., DeBose-Boyd, R., Goldstein, J.L., and Brown, M.S. (1999). Failure to cleave sterol regulatory element-binding proteins (SREBPs) causes cholesterol auxotrophy in Chinese hamster ovary cells with genetic absence of SREBP cleavage-activating protein. J Biol Chem *274*, 28549-28556.

Rodwell, V.W., Nordstrom, J.L., and Mitschelen, J.J. (1976). Regulation of HMG-CoA reductase. Adv Lipid Res *14*, 1-74.

Roitelman, J., Olender, E.H., Bar-Nun, S., Dunn, W.A., Jr., and Simoni, R.D. (1992). Immunological evidence for eight spans in the membrane domain of 3-hydroxy-3-methylglutaryl coenzyme A reductase: implications for enzyme degradation in the endoplasmic reticulum. The Journal of cell biology *117*, 959-973.

Rowe, A.H., Argmann, C.A., Edwards, J.Y., Sawyez, C.G., Morand, O.H., Hegele, R.A., and Huff, M.W. (2003). Enhanced synthesis of the oxysterol 24(S),25-epoxycholesterol in macrophages by inhibitors of 2,3-oxidosqualene:lanosterol cyclase: a novel mechanism for the attenuation of foam cell formation. Circ Res *93*, 717-725.

Rundek, T., Naini, A., Sacco, R., Coates, K., and DiMauro, S. (2004). Atorvastatin Decreases the Coenzyme Q10 Level in the Blood of Patients at Risk for Cardiovascular Disease and Stroke. Arch Neurol *61*, 889-892.

Ryder, N.S. (1992). Terbinafine: mode of action and properties of the squalene epoxidase inhibition. Br J Dermatol *39*, 6.

Saat, Y.A., and Bloch, K.E. (1976). Effect of a supernatant protein on microsomal squalene epoxidase and 2,3-oxidosqualene-lanosterol cyclase. Journal of Biological Chemistry *251*, 5155-5160.

Sakai, J., Nohturfft, A., Cheng, D., Ho, Y.K., Brown, M.S., and Goldstein, J.L. (1997). Identification of complexes between the COOH-terminal domains of sterol regulatory element-binding proteins (SREBPs) and SREBP cleavage-activating protein. J Biol Chem *272*, 20213-20221.

Sakakibara, J., Watanabe, R., Kanai, Y., and Ono, T. (1995). Molecular cloning and expression of rat squalene epoxidase. J Biol Chem *270*, 17-20.

Sakakura, Y., Shimano, H., Sone, H., Takahashi, A., Inoue, N., Toyoshima, H., Suzuki, S., and Yamada, N. (2001). Sterol regulatory element-binding proteins induce an entire pathway of cholesterol synthesis. Biochem Biophys Res Commun *286*, 176-183.

Sawada, M., Matsuo, M., Hagihara, H., Seki, J., and Goto, T. (2001). Lipid-lowering effects of the squalene epoxidase inhibitor FR194738 in dogs, hamsters, and rats. Drug Development Research *54*, 202-208.

Schoenheimer, R., and Breusch, F. (1933). Synthesis and destruction of cholesterol in the organism. J Biol Chem *103*, 439-448.

Seabra, N., Mules, E., and Hume, A. (2002). Rab GTPases, intracellular traffic and disease. Trends Mol Med *8*, 7.

Sever, N., Lee, P.C.W., Song, B.-L., Rawson, R.B., and DeBose-Boyd, R.A. (2004). Isolation of Mutant Cells Lacking Insig-1 through Selection with SR-12813, an Agent That Stimulates Degradation of 3-Hydroxy-3-methylglutaryl-Coenzyme A Reductase. Journal of Biological Chemistry *279*, 43136-43147.

Sever, N., Song, B.L., Yabe, D., Goldstein, J.L., Brown, M.S., and DeBose-Boyd, R.A. (2003a). Insig-dependent ubiquitination and degradation of mammalian 3-hydroxy-3-methylglutaryl-CoA reductase stimulated by sterols and geranylgeraniol. J Biol Chem *278*, 52479-52490.

Sever, N., Yang, T., Brown, M.S., Goldstein, J.L., and DeBose-Boyd, R.A. (2003b). Accelerated Degradation of HMG CoA Reductase Mediated by Binding of Insig-1 to Its Sterol-Sensing Domain. Molecular Cell *11*, 25-33.

Sharipo, A., Imreh, M., Leonchiks, A., Imreh, S., and Masucci, M.G. (1998). A minimal glycine-alanine repeat prevents the interaction of ubiquitinated I kappaB alpha with the proteasome: a new mechanism for selective inhibition of proteolysis. Nat Med *4*, 939-944.

Simons, K., and Ikonen, E. (1997). Functional rafts in cell membranes. Nature *387*, 569-572.

Simons, K., and Ikonen, E. (2000). How cells handle cholesterol. Science *290*, 1721-1726.

Skalnik, D., Narita, H., Kent, C., and Simoni, R. (1988). The membrane domain of 3-hydroxy-3-methylglutaryl-coenzyme A reductase confers endoplasmic reticulum localization and sterol-regulated degradation onto beta-galactosidase. J Biol Chem *263*, 6836-6841.

Smith, L.L. (1981). Cholesterol Autoxidation (New York, Plenum Press).

Soleas, G., Diamandis, E., and Goldberg, D. (1997). Wine as a Biological Fluid: History, Production, and Role in Disease Prevention. J Clin Lab Anan *11*, 27.

Song, B.-L., and DeBose-Boyd, R.A. (2004a). Ubiquitination of 3-hydroxy-3-methylglutaryl CoA reductase in permeabilized cells mediated by cytosolic E1 and a putative membrane-bound ubiquitin ligase. J Biol Chem *279*, 28798-28806.

Song, B.-L., Sever, N., and DeBose-Boyd, R.A. (2005a). Gp78, a Membrane-Anchored Ubiquitin Ligase, Associates with Insig-1 and Couples Sterol-Regulated Ubiquitination to Degradation of HMG CoA Reductase. Molecular Cell *19*, 829-840.

Song, B.L., and DeBose-Boyd, R.A. (2004b). Ubiquitination of 3-hydroxy-3-methylglutaryl-CoA reductase in permeabilized cells mediated by cytosolic E1 and a putative membrane-bound ubiquitin ligase. J Biol Chem *279*, 28798-28806.

Song, B.L., Javitt, N.B., and DeBose-Boyd, R.A. (2005b). Insig-mediated degradation of HMG CoA reductase stimulated by lanosterol, an intermediate in the synthesis of cholesterol. Cell Metab *1*, 179-189.

Spencer, T.A., Gayen, A.K., Phirwa, S., Nelson, J.A., Taylor, F.R., Kandutsch, A.A., and Erickson, S.K. (1985). 24(S),25-Epoxycholesterol. Evidence consistent with a role in the regulation of hepatic cholesterogenesis. J Biol Chem *260*, 13391-13394.

Spencer, T.A., Li, D., Russel, J.S., Collins, J.L., Bledsoe, R.K., Consler, T.G., Moore, L.B., Galardi, C.M., McKee, D.D., Moore, J.T., *et al.* (2001). Pharmacophore analysis of the nuclear oxysterol receptor LXRalpha. J Med Chem *44*, 12.

Sposito, A.C., Carvalho, L.S.F., Cintra, R.M.R., Ara√∫jo, A.L.R., Ono, A.H., Andrade, J.M., Coelho, O.R., and Quinaglia e Silva, J.C. (2009). Rebound inflammatory response during the acute phase of myocardial infarction after simvastatin withdrawal. Atherosclerosis *207*, 191-194.

Stefkova, J., Poledne, R., and Hubacek, J.A. (2004). ATP-binding cassette (ABC) transporters in human metabolism and diseases. Physiol Res *53*, 235-243.

Stone, B.G., Evans, C.D., Prigge, W.F., Duane, W.C., and Gebhard, R.L. (1989). Lovastatin treatment inhibits sterol synthesis and induces HMG-CoA reductase activity in mononuclear leukocytes of normal subjects. Journal of Lipid Research *30*, 1943-1952.

Tai, H.H., and Bloch, K. (1972). Squalene epoxidase of rat liver. The Journal of biological chemistry *247*, 3767-3773.

Tam, S.-P., Mok, L., Chimini, G., Vasa, M., and Deeley, R.G. (2006). ABCA1 mediates high-affinity uptake of 25-hydroxycholesterol by membrane vesicles and rapid efflux of oxysterol by intact cells. Am J Physiol Cell Physiol *291*, 490-502.

Taylor, F.R., Saucier, S.E., Shown, E.P., Parish, E.J., and Kandutsch, A.A. (1984). Correlation between oxysterol binding to a cytosolic binding protein and potency in the repression of hydroxymethylglutaryl coenzyme A reductase. J Biol Chem *259*, 12382-12387.

Tchen, T.T., and Bloch, K. (1957). On the mechanism of enzymatic cyclization of squalene. The Journal of biological chemistry *226*, 931-939.

Terasaka, N., Wang, N., Yvan-Charvet, L., and Tall, A.R. (2007). High-density lipoprotein protects macrophages from oxidized low-density lipoprotein-induced apoptosis by promoting efflux of 7-ketocholesterol via ABCG1. Proceedings of the National Academy of Sciences *104*, 15093-15098.

Thiele, C., Hannah, M.J., Fahrenholz, F., and Huttner, W.B. (2000). Cholesterol binds to synaptophysin and is required for biogenesis of synaptic vesicles. Nat Cell Biol *2*, 42-49.

Thomas, S., and Fell, D.A. (1998). The role of multiple enzyme activation in metabolic flux control. Adv Enzyme Regul *38*, 65-85.

Tomkins, G.M., Sheppard, H., and Chaikoff, I.L. (1953). Cholesterol synthesis by liver. IV. Suppression by steroid administration. J Biol Chem *203*, 781-786.

Treier, M., Staszewski, L.M., and Bohmann, D. (1994). Ubiquitin-dependent c-Jun degradation in vivo is mediated by the delta domain. Cell *78*, 787-798.

Van Tamelen, E.E., Willet, J.D., Clayton, R.B., and Lord K.E. (1966). Enzymic conversion of squalene 2,3-oxide to lanosterol and cholesterol. J Am Chem Soc *88*, 3.

Vembar, S.S., and Brodsky, J.L. (2008). One step at a time: endoplasmic reticulum-associated degradation. Nat Rev Mol Cell Biol *9*, 944-957.

Wang, N., Lan, D., Chen, W., Matsuura, F., and Tall, A.R. (2004). ATP-binding cassette transporters G1 and G4 mediate cellular cholesterol efflux to high-density lipoproteins. Proc Natl Acad Sci U S A *101*, 9774-9779.

Wong, J., Quinn, C.M., and Brown, A.J. (2004). Statins inhibit synthesis of an oxysterol ligand for the liver x receptor in human macrophages with consequences for cholesterol flux. Arterioscler Thromb Vasc Biol *24*, 2365-2371.

Wong, J., Quinn, C.M., and Brown, A.J. (2006). SREBP-2 positively regulates transcription of the cholesterol efflux gene, ABCA1, by generating oxysterol ligands for LXR. Biochem J *400*, 485-491.

Wong, J., Quinn, C.M., and Brown, A.J. (2007a). Synthesis of the oxysterol, 24(S), 25-epoxycholesterol, parallels cholesterol production and may protect against cellular accumulation of newly-synthesized cholesterol. Lipids Health Dis *6*, 10.

Wong, J., Quinn, C.M., Gelissen, I.C., and Brown, A.J. (2008). Endogenous 24(S),25-epoxycholesterol fine-tunes acute control of cellular cholesterol homeostasis. J Biol Chem *283*, 700-707.

Wong, J., Quinn, C.M., Guillemin, G., and Brown, A.J. (2007b). Primary human astrocytes produce 24(S),25-epoxycholesterol with implications for brain cholesterol homeostasis. J Neurochem *103*, 1764-1773.

Yabe, D., Brown, M.S., and Goldstein, J.L. (2002). Insig-2, a second endoplasmic reticulum protein that binds SCAP and blocks export of sterol regulatory element-binding proteins. Proc Natl Acad Sci U S A *99*, 12753-12758.

Yamamoto, S., and Bloch, K. (1970). Studies on squalene epoxidase of rat liver. J Biol Chem *245*, 1670-1674.

Yang, C., McDonald, J.G., Patel, A., Zhang, Y., Umetani, M., Xu, F., Westover, E.J., Covey, D.F., Mangelsdorf, D.J., Cohen, J.C., *et al.* (2006). Sterol intermediates from cholesterol biosynthetic pathway as liver X receptor ligands. J Biol Chem *281*, 27816-27826.

Yang, J., Sato, R., Goldstein, J.L., and Brown, M.S. (1994). Sterol-resistant transcription in CHO cells caused by gene rearrangement that truncates SREBP-2. Genes Dev *8*, 1910-1919.

Yang, T., Espenshade, P.J., Wright, M.E., Yabe, D., Gong, Y., Aebersold, R., Goldstein, J.L., and Brown, M.S. (2002). Crucial step in cholesterol homeostasis:

sterols promote binding of SCAP to INSIG-1, a membrane protein that facilitates retention of SREBPs in ER. Cell *110*, 489-500.

Zelcer, N., Hong, C., Boyadjian, R., and Tontonoz, P. (2009). LXR Regulates Cholesterol Uptake Through Idol-Dependent Ubiquitination of the LDL Receptor. Science *325*, 100-104.

Zhang, M., and Coffino, P. (2004). Repeat sequence of Epstein-Barr virus-encoded nuclear antigen 1 protein interrupts proteasome substrate processing. The Journal of Biological Chemistry *279*, 8635-8641.